5-2015

Investigation Of The Role Of The Scaffold Protein Shc In Erk Signaling

kin man suen

INVESTIGATION OF THE ROLE OF THE SCAFFOLD PROTEIN SHC IN ERK SIGNALING

by

Kin Man Suen, B.Sc.

APPROVED:

_____
Dr. John E. Ladbury

_____
Dr. Swathi Arur

_____
Dr. Carmen W. Dessauer

_____
Dr. Jessica K. Tyler

_____
Dr. Naoto T. Ueno

APPROVED:

_____
Dean, The University of Texas
Graduate School of Biomedical Sciences at Houston

INVESTIGATION OF THE ROLE OF THE SCAFFOLD PROTEIN SHC IN ERK SIGNALING

A

DISSERTATION

Presented to the Faculty of

The University of Texas

Health Science Center at Houston

and

The University of Texas

MD Anderson Cancer Center

Graduate School of Biomedical Sciences

in Partial Fulfillment

of the Requirements

for the Degree of

DOCTOR OF PHILOSOPHY

by

Kin Man Suen, B.Sc.

Houston, Texas

May, 2015

Dedication

This work is dedicated to the Creator of this beautiful and harmonized world. Without His love and assurance that He will never leave me nor forsake me, I would not have pursued my passion in biomedical research.

ACKNOWLEDGEMENTS

I have always known that I am the most fortunate person on earth to be my parents' child. They have made enormous and numerous sacrifices in order to provide me with the best opportunity in life. Their strength and courage when faced with serious illnesses and financial difficulties taught me that all hardships can be overcome as long as you work hard, persevere and stay positive – which turn out to be life-saving qualities in scientific research. Therefore, even though my parents know nothing about science, my deepest gratitude and respect must go to them because they have helped me most in my study simply by living their lives. I would also like to thank Dr. Thomas Lin – without his companionship this journey would have been much harder both in life and in the laboratory. His steadfastness has been a much-needed anchor in the uncertain nature of biomedical research.

I would like to thank my advisor Professor John Ladbury for his trust in me and the freedom he has given me to be adventurous in my work. Even when my experiments failed, he never failed to encourage me to march on. I will never forget the warmth he and his family provided for those of us who were far away from home.

I would also like to thank my advisory committee members Dr. Swathi Arur, Dr. Carmen Dessauer, Dr. Jessica Tyler and Dr. Naoto Ueno. Without their gentle guidance, my study would have taken more wrong turns. In particular, I would like to express my gratitude towards Dr. Arur, who for some reasons has more faith in me than I have in myself. Her constant mentorship in the last few years has been inspiring. I am very much indebted to her generous help in the writing of this dissertation.

The necessity to work as part of a team in academic science has always been a major attraction to me. I have learnt so much throughout the years from my colleagues in the Ladbury and Arur laboratories. I will not mention everyone by name because the list is endless. However, I would like to express my gratitude towards a few Ladbury lab members specifically. Dr. Roger George patiently taught me about biochemistry, which I have come to love. Much of the work in this dissertation is based on his initial interesting finding. Dr. Zamal Ahmed and Dr. Paul Leonard have shown me the ropes in cell biology and structural biology, respectively. Dr. Ann-Marie Cimo went out of her way to help me with my candidacy examination.

I would like to thank the administrative staff at GSBS, which has been most efficient and kind.

I would like to thank the Rosalie B. Fellowship for their generous support of my research.

I would also like to thank my fellow graduate students Le and Mehrnoosh. Complaining about student life as a group was much more fun than doing it on your own.

Last but not least, I would like to thank my dear brothers and sisters in Christ for their love, understanding and support. The pride they have in me gives me great comfort and confidence as I move onto my postdoctoral training.

INVESTIGATION OF THE ROLE OF THE SCAFFOLD PROTEIN SHC IN ERK SIGNALING

Kin Man Suen, B.Sc.

Advisor Professor: John E. Ladbury, Ph. D.

Cells respond to environmental changes by converting extracellular signals into intracellular events. Scaffolding proteins play important roles in generating specificity in intracellular signaling through the combinatorial use of protein domains and posttranslational modifications. Using the scaffold protein Shc (Src-homology collagen-like) as a model system, we explored novel mechanisms whereby this class of protein shapes signaling output. In the present work, we focused on the role of Shc in the MAP kinase Erk signaling both prior to and post -growth factor stimulation. Prior to growth factor stimulation, we found Erk to be a direct interacting partner of Shc. The two proteins associate through a non-canonical interface. This interaction blocks the phosphorylation of Erk and restricts its nuclear translocation. Post -growth factor stimulation, Erk is released from Shc through an allosteric mechanism facilitated by the binding between Shc and the activated growth factor receptor. Furthermore, fully activated Erk phosphorylates Shc on three threonine residues. These phosphorylated residues on Shc subsequently serve as platforms to mediate both a positive feedforward loop in prolonging Erk activity and crosstalk with Akt signaling through protein recruitment.

Table of Contents

List of Figures

Chapter 1:

Chapter 2:

Chapter 3:

Chapter 4:

List of Tables

Chapter 4:

Chapter 1

Introduction

1.1 Signal Transduction

The ability for cells to respond to extracellular cues is critical to the normal development of an organism. Cells respond to environmental changes by converting extracellular events into intracellular signals. This process requires the detection of extracellular cues. When these extracellular ligands, for example growth factors and amino acids, cannot freely diffuse across the plasma membrane due to the membrane barrier, the signal reception is mediated by transmembrane proteins. A number of transmembrane protein families exist, for example receptor tyrosine kinases (RTKs), G-protein-coupled receptors (GPCRs), ion channels and transporters [1,2,3]. The interaction of the extracellular ligands with their cognate TM receptors in turn dictates specific cellular outcomes. However, how these interactions can be transmitted in the intracellular environment into specific cellular outcomes is not obvious. This is because different TM receptors often use the same downstream signaling cascades. Hence, although extracellular ligands are highly specific in which TM receptors they interact with, the protein-protein interactions that are mediated by the TM receptors within cells do not confer sufficient specificity in generating a particular biological outcome. For example, stimulation of the rat pheochromocytoma cell line PC12 with epidermal growth factor (EGF) leads to cell proliferation, whereas stimulation using nerve growth factor (NGF) leads to differentiation of the PC12 cells into neuron-like cells with neurites. Distinct

signaling outcomes from the two different ligand-receptor pairs suggest different downstream signaling components were used. Surprisingly, however, examination of the downstream signaling from these two receptors reveals that the same signaling cascade, the Erk (extracellular-regulated kinase) cascade, is responsible for the phenotypes and that the determining factor for these two very different outcomes is the duration of its activation [4,5]. How then is the activity of Erk, or other signaling enzyme, regulated temporally and how does this translate into phenotypic outcome?

Much progress has been made in the understanding of how specificity in intracellular signaling is conferred. It became apparent early-on that unidirectional linear pathways acting in isolation cannot support the diverse signaling output required in development. Rather, cells utilize feedback loops within a pathway and cross talks between pathways to build signaling networks in order to generate complex biological processes [6,7,8]. Two strategies are used to build these regulatory mechanisms. The first is the modular arrangement of folded domain structures in proteins. Each type of protein domain contains a certain polypeptide fold that enables it to recognize specific motifs. Some protein domains recognize covalently modified amino acids, such as the Src Homology 2 (SH2) domains binding to phosphorylated tyrosine residues. Others bind to unmodified motifs, as in the case of SH3 domains engaging Pro-X-X-Pro sequences [9]. The second strategy is posttranslational modifications (PTMs). PTMs provide stable and yet reversible effects on proteins such that they are ideal molecular switches [10,11,12,13,14,15,16]. A variety of PTMs have been described, each exploiting specific chemical properties on certain amino acids. For example, a phosphate moiety is added to the hydroxyl group on serine, threonine or tyrosine residues effectively changing its charge and size, binding interactions and thus function, such as activating / inactivating

protein function [17]. For example, Erk2 is inactive prior to phosphorylation on T183 and Y185. Phosphorylation on these two residues causes Erk2 to adopt an active conformation by rearranging both the ATP- and substrate-binding sites. Many proteins possess both multiple domains (strategy #1) and PTMs (strategy # 2), which lead to a combinatorial effect in protein recruitment and enable dynamic assembly of complexes that modulate biological outcomes [14,18,19].

Scaffolding/adaptor proteins, a term typically reserved for polypeptides that do not possess any enzymatic activity and whose major function is to facilitate the formation of protein complexes, utilize both of these strategies to direct the flow of signaling information (Figure 1) [20,21].

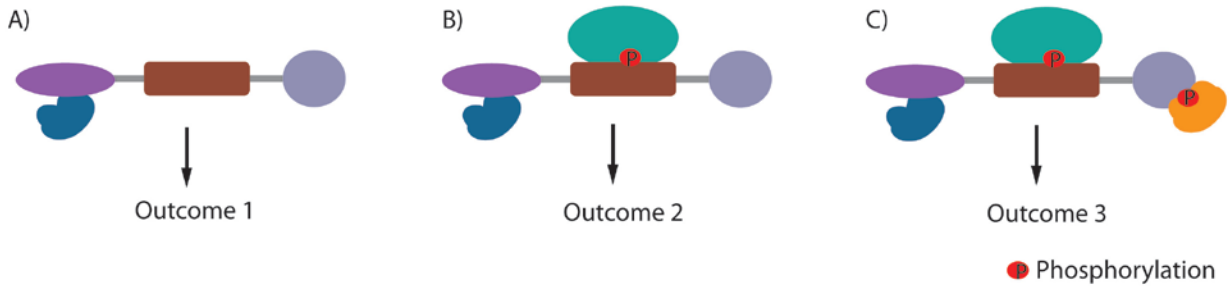

Figure 1. Scaffold proteins facilitate the formation of protein complexes to regulate signaling outcome. (A) and (B) Scaffold proteins usually contain multiple domains. Some domains bind to unmodified peptides, such as the SH3 domain binding to Pro-X-X-Pro motifs. Other domains interact with modified peptides, such as SH2 domain binding to motifs containing phosphorylated-tyrosine. (C) Scaffold proteins are post-translationally modified to form binding sites for other proteins. For example, a scaffold protein can be phosphorylated on a tyrosine residue, which recruits SH2 domain-containing proteins.

Recent advances in high-throughput techniques offer a glimpse into the complex role performed by scaffolding/adaptor proteins in signaling. For example, growth factor receptor bound protein 2 (Grb2) contains a Src-homology 2 (SH2) domain flanked by two Src-homology 3 (SH3) domains. By associating with son of sevenless (Sos) through its N-terminal SH3 domain and fibroblast growth factor (FGF) receptor via its SH2 domain, it drives embryonic stem cell into the primitive endoderm lineage. [22]. Furthermore, manipulation of the SH2 domain such that the affinity for phosphotyrosine-containing motifs leads is changed, which in turn leads to a change in its protein recruitment profile and consequently the expression of a pluripotency factor [23]. Another well-characterized example is kinase suppressor of Ras (KSR). By associating with the three kinases simultaneously in the Erk cascade, KSR enables efficient phosphorylation between the components by juxtaposing them close to each other and eliminating the need for diffusion. The final kinase of the Erk cascade, once activated by its kinase Mek, phosphorylates KSR to block its binding to Raf, the first member of the cascade, thereby terminating the signal [24].

This work focuses on the Src-homology collagen-like (Shc) scaffolding protein to explore novel mechanisms whereby scaffolding proteins regulate signaling events. Shc exemplifies how scaffold proteins shape signaling output. Shc has a large repertoire of protein binding partners, whose functions span diverse cellular processes [25,26]. Furthermore, in addition to its existing protein-protein interacting domains, Shc is also post-translationally modified at multiple sites. Post-translational modification of Shc creates transient binding motifs that in turn provide additional specificities in protein recruitment [27]. The many contributions of Shc in a large array of cellular processes are

discussed in the following sections, with emphasis on the molecular mechanisms involved where they are known.

1.2 Shc - General

The first member of the Shc family was identified in a cDNA library screen for SH2-domain-containing proteins in 1992 [28]. Since then, four *Shc* genes have been identified in mammals, which are classified according to their sequence of discovery as *ShcA, ShcB, ShcC* and *ShcD* [28,29,30,31,32]. The four *Shc* genes are differentially expressed in adult tissues: *ShcA* is ubiquitously expressed except in the nervous system; ShcB and ShcC are predominately expressed in the nervous system [29]; and ShcD is primarily expressed in the brain and skeletal muscle [31]. Despite difference in their primary sequences, all four of the Shc proteins consist of the core architecture of an N-terminal phosphotyrosine-binding (PTB) domain, a central collagen-homology 1 (CH1) domain and a C-terminal Src Homology 2 (SH2) domain. Additionally, some members of the family contain a collagen-homology 2 (CH2) domain N-terminal to the PTB domain (Figure 2). The PTB and SH2 domains are capable of binding to phosphorylated-tyrosines, whereas the CH1 and CH2 domains are phosphorylated on serine, threonine and tyrosine residues to form binding sites to recruit other proteins.

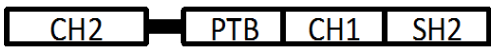

Figure 2. Shc protein architecture

1.3 ShcA

1.3.1 Isoforms

The *ShcA* gene produces three protein products. The p52 and p46 isoforms are generated by alternative start codons, while the p66 transcript is alternatively-spliced to contain an additional CH2 domain [33]. The p66 isoform was noted for its absence in hematopoietic cell lines [28] and was later found that its differential expression pattern is owed to epigenetic regulation through the use of an alternative promoter [34]. Although the core domains of the three ShcA isoforms share the same sequences, differences in downstream signaling involving these domains have been observed (discussed below), suggesting the N-terminal sequence interferes with the core domain functions.

1.3.2 Domain architecture

The phosphotyrosine-binding (PTB) and Src-homology 2 (SH2) domains form well-folded modules, whereas the collagen-homolgy 1 and 2 (CH1 and CH2) domains lack tertiary structures. Each domain is responsible for interacting with a distinct array of proteins, enabling Shc to coordinate multiple signaling events.

1.3.2.1 PTB domain

The PTB domain is composed of three α-helices, one of which at each N- and C-terminal ends, and two β-sheets that are placed orthogonally [35]. It is in a relatively disordered state which folds to form the phosphobinding pocket upon binding to phospho-

peptides [36]. Binding studies and structure of the PTB domain in complex with a phospho-peptide show that a β-turn on the peptide is critical to phosphotyrosine binding to the protein, conferring binding specificity of Asn-Pro-X-pTyr (NPXpY; where X is any reside), due to the ability of Asn-Pro to form a β-turn (Figure 3) [35,37,38]. The PTB domain has been shown to bind to a large array of receptor (See 1.4.1.1) and cytosolic kinases via their phosphorylated-tyrosine motifs [27]. While most of the binding partners for this domain are mediated by phosphorylated tyrosines, a few proteins have been reported to interact with the PTB domain independent of phosphorylation [39,40,41,42]. For example, the cytoskeletal protein IQGAP1 was found to interact with residues in the PTB domain outside of the phosphotyrosine-binding pocket [39]. The protein-tyrosine phosphatase-PEST (PTP-PEST) has also been shown to associate with the PTB domain via a Asn-Pro-Leu-His motif [40] and interestingly the PTP-PEST peptide was able to inhibit IQGAP1 binding, suggesting that the binding sites for these two proteins overlap to some extend but not completely. The tertiary structure of the PTB domain also resembles the Pleckstrin-homology (PH) domain [43], which prompted the characterization of the protein's phospholipid-binding ability. It was shown to bind to phosphatidylinositol 4,5-bisphosphate (PtdIns(4,5)P_2) using residues distinct from the ones utilized for phosphotyrosine-binding [35,44].

Figure 3. Structure of ShcPTB domain in complex with TrkA peptide (PDB: 1SHC). The PTB domain of Shc is in green. TrkA peptide is in wheat. The PTB domain is composed of three α-helices, one of which at each N- and C-terminal ends, and two β-sheets that are placed orthogonally. Asn-Pro forms a β-turn on the peptide, which is circled in black. This β-turn is important to the correct positioning of the peptide to the PTB domain.

1.3.2.2 CH1 domain

The CH1 domain contains an unusually high number of proline and glycine residues much like a collagen protein primary sequence [45]. However, it lacks the proline-glycine regular repeats that are required for the formation of helices and instead forms a disordered region in the Shc protein. The main function for this domain delineated thus

far is in the activation of mitogenic signaling to recruit the SH2 domain of Grb2. Recruitment of Grb2 is mediated by the phosphorylation of Y239, Y240 and Y317 on Shc [46,47]. Additional phosphorylation sites, T214 and S335 in this region have been identified recently via proteomic analysis of Rat1 cells that were trigged by EGF. However, the functions of this threonine/serine phosphorylation have not yet been characterized [26]. In addition to the phosphorylation sites, the CH domain contains multiple Pro-X-X-Pro motifs and it has been shown to associate with the Src, Fyn and Lyn SH3 domains [48]. However, physiological roles for these interactions have not been described.

1.3.2.3 SH2 domain

The SH2 domain of Shc consists mainly of a central anti-parallel β-sheet flanked by two α-helices (Figure 4) [49]. The SH2 domain recognizes tyrosyl phosphopeptides with a Ile/Leu/Met as the third residue C-terminal of the phosphotyrosine (pY+3) position is preferred [50]. A smaller set of binding partners have been reported for the SH2 domain compared with the PTB domain. Given the fact that SH2 domains in general are capable of interacting with a large number of proteins as in the case of PTB domains, it is likely that many of the ShcSH2 binding partners are still uncharacterized. The T-cell receptor zeta-chain interacts with the SH2 domain in a phosphotyrosine dependent manner [51], while SHCBP1 was shown to bind independent of tyrosine phosphorylation [52]. However, the physiological relevance of the Shc-SHCBP1 interaction has not been determined.

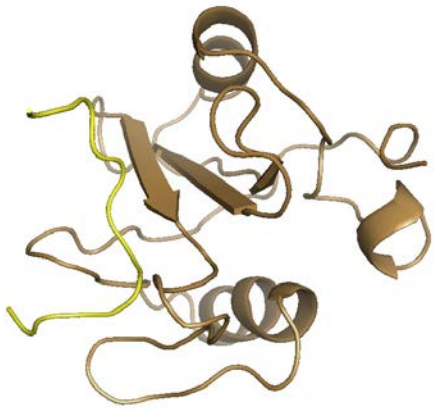

Figure 4. Structure of ShcSH2 domain in complex with TCR peptide (PDB: 1TCE). The SH2 domain consists of a central anti-parallel β-sheet flanked by two α-helices. A Leu in the pY+3 position on the TCR peptide confers specificity to the domain-peptide interaction.

1.3.2.4 CH2 domain

Only the $p66^{shc}$ isoform possesses a CH2 domain at its N-terminal. Similar to the CH1 domain, the CH2 domain is rich in proline and glycine residues. The best characterized feature of the CH2 domain is S36, which is phosphorylated under oxidative stress [53] by protein kinase C. Phosphorylation of S36 recruits the peptidyl-prolyl cis-trans isomerase NIMA interacting 1 protein (Pin1), which leads to apoptosis (see 1.4.4) [54].

1.3.2.5 Cytochrome C binding region

The linker region between the CH2 and PTB domains has been found to function as a redox center, by binding to and oxidizing cytochrome C via E132 and E133, and W134 (See 1.4.4) [55].

1.4 ShcA in signaling

1.4.1 Mitogen-activated protein kinase (MAPK) signaling

1.4.1.1 Extracellular signal-regulated kinase (Erk) pathway

The p52 and p46 isoforms of Shc act downstream of most RTKs to activate Erk signaling [27,56]. Upon activation of the receptor by a cognate ligand, the receptor undergoes autophosphorylation on its tyrosine residues [1]. Shc binds to the phoshotyrosine residues on the receptor via its PTB domain, which in turn leads to the phosphorylation on Y239, Y240 and Y317 in its CH1 domain [46,47,57]. These phosphorylated residues recruit Grb2, which is constitutively bound to the guanine nucleotide exchange factor, Sos [58,59]. Sos activates the small GTPase Ras by promoting GDP-GTP exchange. One of Ras' effectors is the MAPK-kinase-kinase Raf, whose activation leads to phosphorylation of Mek. Mek in turn phosphorylates and activates the terminal kinase Erk (Figure 5) [60]. Intriguingly, the p66 isoform has been reported to downregulate Erk signaling in EGF [33] and cytokine signaling [61], even though it is able to bind to the receptor and Grb2 [62]. How p66 Shc regulates Erk signaling differently from the p52 and p46 isoforms is unclear, although it is likely that the differences in their

N-terminal sequences may play a role. p52 Shc also leads to the activation of Erk downstream of T-cell receptor activation, although its phosphorylation is carried out by the cytosolic kinase Lck [63].

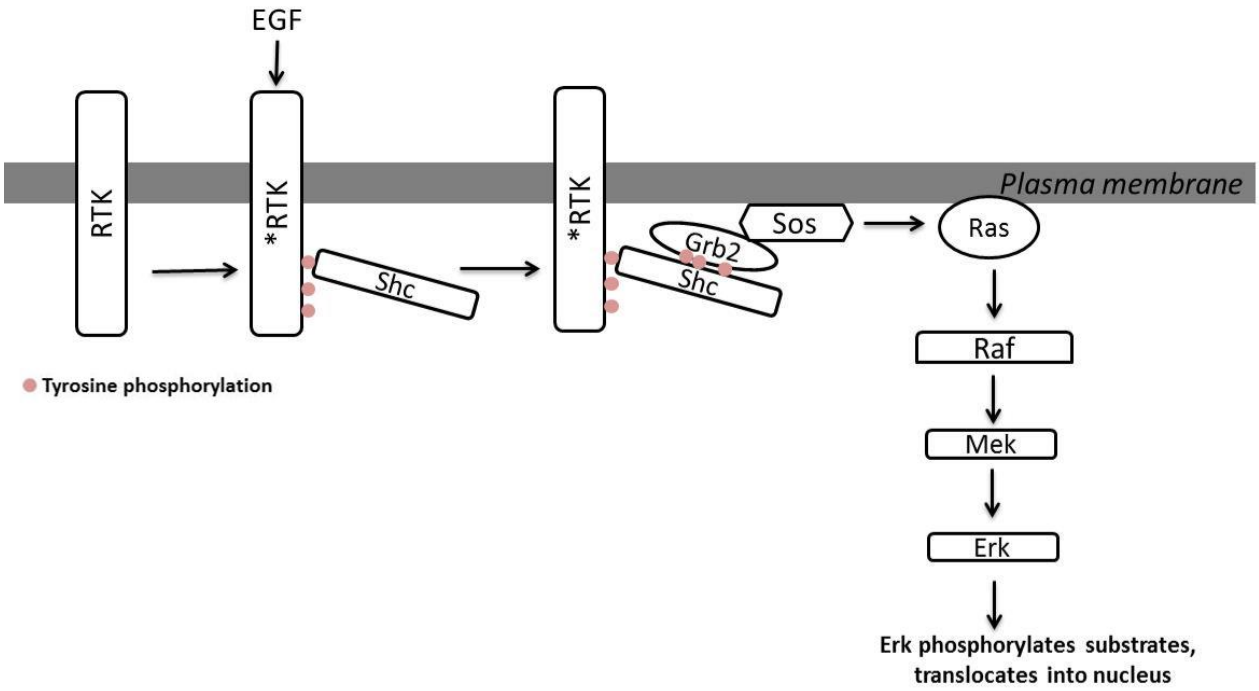

Figure 5. Canonical role of p52/p46 Shc in the activation of Erk pathway. RTK autophosphorylates on its tyrosine residues upon the binding of ligand. These phosphorylated tyrosines recruit Shc via the Shc PTB domain. Shc is subsequently phosphorylated by the receptor on Y239/240 and Y317. Phosphorylated Shc then recruits the Grb2/Sos complex. Sos activates the small GTPase Ras, which leads to the activation of the Erk cascade through the sequential phosphorylation of the three kinase members. Activated Erk phosphorylates a range of substrates which leads to various biological outcomes, such as proliferation and differentiation.

1.4.1.2 c-Jun N-terminal kinase pathway

Two studies in the *C. elegans* model system identified MEK-1, the MAPK kinase for the JNK pathway, to be a binding partner for SHC-1, the homolog of mammalian p52 Shc. While both studies showed that SHC-1 confers resistance to stress when the animals are exposed to heavy metal and that this response is MEK-1-dependent, Mizuno *et. al.* and Neumann-Haefelin *et. al.* attributed the phenotype to be mediated by KGB-1 (JNK-like kinase) and JNK-1, respectively [64,65]. These studies suggest that MEK-1 is able to activate multiple members of the JNK family. Although data showing conservation of the Shc-MEK-JNK pathway in higher vertebrates is lacking, a study in T-cell signaling found that tyrosine phosphorylation of p52 Shc augments JNK phosphorylation [66].

1.4.2 Phosphatidylinositol-4, 5-bisphosphate 3-kinase (PI3K) pathway

The Shc p52 isoform has been shown to activate PI3K signaling downstream of insulin-like growth factor stimulation in vascular smooth muscle cells by binding to Grb2, which then recruits the p85 subunit of PI3K. The over-expression of a Shc mutant that is defective in Grb2-binding leads to reduced phospho-AKT level and cell migration [67]. Two studies in cytokine signaling also support a direct role for Shc in the activation of the PI3K pathway, although achieved via different molecular mechanisms. Barry *et. al.* proposed that upon cytokine stimulation, the scaffolding protein 14-3-3 ζ is tyrosine phosphorylated, which then recruits Shc via its SH2 domain and this interaction is required for PI3K activation [68]. However, an earlier study by Gu *et. al.* carried out under similar conditions, reported that Shc activates PI3K signaling through the recruitment of

Gab2 and Grb2 [69], indicating that Shc is able to activate the PI3K pathway through the independent use of two of its domains via separate mechanisms.

1.4.3 Mammalian target of rapamycin (mTOR) signaling

A recent metabolomics analysis revealed p66 Shc to be a critical regulator in anabolic metabolism. Using p66 deficient mouse embryonic fibroblasts (MEFs), it was shown that the abundance of a number of intermediates, such as glucose-6-phosphate, in glycolysis is altered and that this trend can be partially reversed by inhibiting mTOR. Thus, p66Shc inhibits anabolic metabolism via mTOR signaling [70].

1.4.4 Redox signaling

Migliccio *et. al.* first reported a role for p66Shc in oxidation stress when *p66Shc* knockout mice exhibited resistance to oxidative stress and a prolonged life span. They also showed that the phosphorylation of S36 in the CH2 domain is critical to this process [53]. Subsequent studies established that p66Shc performs this task through multiple mechanisms. p66Shc was shown to regulate oxidative stress induced apoptosis involving the transcription factors Forkhead 1 and p53. It mediates the phosphorylation and inactivation of the Forkhead protein, whose activation in ROS-scavenger expression promotes oxidative stress resistance [71,72]. By contrast, p53 activity stabilizes the p66Shc protein level, thereby regulating cytochrome C release and apoptosis [73]. Giorgio *et. al.* made several important observations which led to the surprising discovery that p66Shc possesses oxidizing power. p66 Shc was shown to reside in the mitochondrial

intermembrance space and can induce swelling of the organelle. Further dissection of how this occurs reveals that residues 132-134 of p66Shc binds to and mediates the oxidation of cytochrome C. This leads to the generation of reactive oxidative species and triggers apoptosis [55]. Finer details for how p66Shc migrates in the mitochondria to carry out its redox function were established using Pin1 knockout MEFs. Pin1 is a phosphorylation-dependent prolyl isomerase. It was shown that when cells were challenged by oxidative stress, protein-kinase C β isoform (PKCβ) is specifically activated, which leads to the phosphorylation of S36 on p66Shc. Phosphorylated S36 recruits Pin1, which enables p66Shc to translocate to the mitochondria [54]. An earlier study also suggested that p66Shc is associated with the mitochondrial chaperone HSP70 such that when cells experience oxidative stress HSP70 releases p66Shc allowing it to trigger apoptosis [74]. Thus, p66Shc seems to exist in both the cytoplasm and mitochondria prior to oxidative stress. Upon oxidative stress, p66Shc is either transported to the mitochondria or released from the HSP70 inhibitory complex to induce apoptosis.

1.5 *ShcA* in Development

1.5.1 Cardiovascular system

Deletion of *ShcA* in mice is embryonically lethal and the animals die by E11.5. Investigation into the cause of death revealed that transcription of *ShcA* is detectable by E9 and predominately in the cardiovascular system. A number of defects in the vascular development were observed in Shc-deficient animals including reduced cell-to-cell contacts and complexity in vascular architecture. Shc-deficient MEFs provided insights

into the molecular pathway for these defects. While Shc is not required for Erk activity when cells were stimulated with growth factors, it sensitizes cells towards the presence low levels of growth factors. Also mutant MEFs exhibited abnormal distribution of actin bundles [75]. Although Shc is highly tyrosine phosphorylated in MEFs derived from E10 embryos and it potentiates Erk activity in these cells, it was however surprising that knock-in mice expressing the ShcA Y239/240/317F mutant were viable with grossly normal cardiovascular development. This was unexpected because the mutation of Y239 to F would prevent phosphorylation of the tyrosine residues, and this tyrosine phosphorylation is essential for the role of ShcA in Grb2-Sos recruitment. This reflects that not all ShcA signaling is channeled through the Grb2-Sos axis. This is also supported by the fact that in *Drosophila*, while DSHC acts downstream of RTKs Torso and DER, it lacks one of the mammalian Grb2 binding sites and that it acts in parallel to signaling transduced via DRK, the Drosophila Grb2 [76,77].

1.5.2 Muscular tissue

Hardy *et. al.* generated a series of mouse models to systematically study the contributions of the various phoshotyrosine binding modules in ShcA in development using the *cre-loxP* system to generate *ShcA* mutants specifically in muscles. Both ShcA-null and ShcPTB R175Q mutant (this mutation abolishes the phosphotyrosine-binding ability of the PTB domain) mice were non-viable. Unlike the ShcA-null or the ShcPTB R175Q mutant mice, animals harboring mutations in either the SH2 (R397K, this mutation prevents the SH2 domain from binding to phosphotyrosine motifs) or CH1 (Y239/240/313F; Y313 in mice is equivalent to Y317 in human) domains were viable.

However, these animals suffered from ataxia. Consistent with previous finding that p52 Shc associates with Grb2 upon ErbB3 activation in myotubes [78], the Y239/240/313F mutant mice possess a greatly reduced number of muscle spindles, which are derived from myotubes. This suggests that the Shc/Grb2-Sos axis is required for spindle development. While the SH2 mutant animals had comparable number of muscle spindles, the architecture was abnormal [79]. The differences in phenotypic outcomes among the mutants are consistent with the fact that the three Shc domains recruit distinct sets of proteins and can therefore mediate different biological processes.

1.5.3 Immune system

Zhang *et. al.* used two complementary mouse models to investigate the role of *ShcA* in T-cell development. Using the *lck*-cre-loxP system, expression of Shc Y239/240/317F mutant was only induced in early thymocytes. It was found that ShcA Y239/240/317F mutant mice have smaller thymi due to a decrease in thymocyte number. The reduction in thymocytes was caused by an arrest at the third phase of the double-negative stage (DN3) in which ShcA Y239/240/317F mutant specifically affects the proliferative, but not apoptotic, signaling from pre-TCR as revealed by cell cycle analysis. Similar observations were confirmed in *lck*-cre-*ShcA* conditional knockout mice [80]. Thus, ShcA functions in early T-cell development requires the phosphorylation of ShcCH1. Given the role of ShcA in the activation of Erk and the multiple functions of Erk in T-cell development including the promotion of DN3-DN4 transition in T-cells [81], a subsequent study was carried out using the same genetic strategy to overexpress ShcA Y239/240F mutant or ShcA Y317F mutant in early thymocytes, and the level of Erk phosphorylation was analyzed. The

overexpression of ShcA Y239/240F significantly diminishes phospho-Erk level to a comparable level when cells overexpressed ShcA Y239/240/317F. However, overexpression of ShcA Y317F led to a comparable phospho-Erk level as in ShcA WT animals. The same trend was observed for the total number of thymocytes. The study revealed that Y239/240 are primarily responsible for the reduction in thymocyte number and DN3 arrest as observed in the ShcA Y239/240/317F model. Furthermore, phospho-Erk level was severely reduced in these thymocytes [82]. Hence, while the only known function of Y239/240 and Y317is the recruitment of Grb2/Sos for the activation of Erk, this study suggests that in the context of T-cell signaling, Y317 is not necessary for this function. It is unclear how this differential effect of Y239/240 and Y317 occurs, or whether Y317 is phosphorylated endogenously in T-cells.

1.5.4 Neuronal tissue

ShcA is expressed at a high level during early embryonic development in the nervous system. Its expression declines gradually as the embryo develops, by postnatal stages, the expression of ShcA is undetectable. Culturing of isolated embryonic neuronal cells that were induced to differentiate show a concomitant reduction in *ShcA* expression. Furthermore, *ShcA* mRNA is detected mainly in the proliferative zones of the brain. Therefore, *ShcA* expression is highly temporally and spatially regulated during the development of the nervous system. The timing of ShcA expression suggests that it is required for neuroblast proliferation and downregulated for differentiation to proceed. Stimulating the cerebral ventricle system of mouse embryos with EGF injections showed that p46 and p52, but not p66 Shc, are tyrosine-phosphorylated and bind to EGFR as well

as Grb2 [83]. Again, this suggests that the N-terminal sequence in p66Shc interferes with functions of the other domains in the ShcA protein. Studies in mouse models show that ShcA acts through multiple signaling mechanisms to mediate nervous system development. For example, a mouse model with overexpression of the ShcA Y239/240/317F form specifically in neuronal cells using the nestin-cre-lox system exhibit microencephaly. Aside from being smaller in size, the gross architectures of the brain from the ShcA Y239/240/317F animals were similar to that of wild-type animals, with certain regions, such as the subventricular zone (SVZ), more severely affected. Quantification in proliferative index and differentiation markers did not reveal any alterations. However, there was an increase in cleaved-caspase 3 staining in the ShcA Y239/240/317F animals, indicating that microencephaly is the result of augmented apoptosis. Animals generated with *ShcA* deletion using the nestin-cre-lox strategy also resulted in animals with microencephaly, which was initially interpreted as to suggest that ShcA Y239/240/317F mimics ShcA deletion mutants, and thus lead to the same phenotype [84]. However, a subsequent study focused on the role of ShcA in the SVZ revealed that the effects of expressing ShcA Y239/240/317F and deleting ShcA are not completely the same. It was shown that the structure in SVZ is more severely disrupted in the ShcA deletion than the ShcA Y239/240/317F mutant animals. Deletion of *ShcA* resulted in enlarged blood vessels and appearance of unidentified cell types. In contrast to an increase in apoptosis in the ShcA Y239/240/317F mutant animal [84], ShcA deleted animals showed a marked decrease in cell proliferation but an unaltered level of apoptosis in the SVZ [85]. Taken together, these studies indicate that in the development of the nervous system, ShcA utilizes both Y239/240/317 phosphorylation-dependent and -independent mechanisms, and that other domains and/or PTMs of Shc are likely involved.

1.6 ShcA in human disease

1.6.1 Neurodegenerative disease

A role for ShcA has been implicated in Alzheimer's disease (AD). Comparison of AD and normal brains showed the ShcA is present at a higher level in the diseased tissue. The C-terminal fragments of amyloid precursor protein (APP) can be tyrosine phosphorylated [86] and recruit ShcA, which might lead to the elevated level of phospho-Erk through enhancing the interaction between Shc and Grb2 in AD tissues [87].

1.6.2 Cancer

ShcA has been associated with cellular transformation from the first report of its discovery, wherein ShcA overexpression led to a transformed morphology of mouse fibroblasts and enabled colony growth in soft-agar [28]. While it has since been shown that ShcA expression and post-translational modifications are altered in the cancer of a number of tissues [27,88], only the role of ShcA in breast cancers has been dissected to a great extent and hence will be discussed below.

1.6.2.1 Breast Cancer

As discussed in 1.4.1.1, tyrosine-phosphorylated p46/p52 Shc activates whereas p66Shc inhibits Erk activation. This led to the idea that the ratio between the levels of

Y317 phosphorylation on ShcA and p66Shc expression can serve as prognostic markers for breast cancer. Indeed, immunohistochemical analysis on archival primary breast tumor specimens showed that an increase in pY-Shc and decrease in p66Shc expression levels positively correlated with relapse of the disease, as well as with node-positive status [89]. Furthermore, this ratio was found to be a strong predictor for disease-relapse in patients who have undergone Tamoxifen [90].

A number of transgenic animal studies attest to the importance of ShcA in multiple processes required for breast cancer progression. Also, the different ShcA domains and phosphorylation sites have been found to be responsible for various oncogenic behaviors, including tumor initiation, cell growth, cell survival, angiogenesis and metastasis. Mice expressing activated ErbB2 in mammary epithelial cells completely failed to develop tumors when ShcA is deleted, indicating that ShcA is critical to the development of ErbB2 breast cancer [91]. Transgenic animals expressing mutated upstream activator of ShcA signaling also confirm its critical role in disease progression. In the Polyomavirus middle T antigen (MT) -driven mammary tumor model, a delay in tumor onset was observed in mice carrying the MT mutant in which the ShcA binding site is compromised. Even though tumors eventually developed and metastasis occurred, a reversion to the wild-type sequence on the MT gene was found in the metastatic tumors [92]. Furthermore, when the ShcA binding site is reconstituted in an ErbB2 tyrosine mutant, tumors developed earlier [93]. Finally, a study using a chimeric RTK composed of the extracellular domain of Met harboring either an EGFR or TrkA binding site for the ShcA PTB domain showed that the recruitment of ShcA via its PTB domain is required for both tumor onset and angiogenesis [94]. Hence, the oncogenic potential of active tyrosine kinases such as RTKs requires interaction between ShcA and the kinase.

Using the MT-driven mammary model, Urini-Siegel *et. al.* investigated the importance of phosphotyrosine signaling mediated by the CH1 domain in breast cancer. Mice homozygous for either Y239/240F or Y313F developed tumors much later than the WT animals, indicating that the phosphorylation of these tyrosine sites are required for tumor initiation. There were also a lower number of metastasized lesions in the lungs. Inspection of the mutant animal breast tissues showed retention of myoepithelial cells, which are known to suppress tumor cell invasion [95]. Hence, phosphorylation of Y239/240 and Y313 on ShcA is important in metastasis. As in the case of T-cell development (1.5.3), Y239/240 and Y313 elicited different biological effects. Y313 was found to promote cell survival, while Y239/240 is required for angiogenesis. Furthermore, injecting tumor cells expressing WT ShcA into the fat pads of Y313F animals led to a significantly reduced level of tumor outgrowth, whereas Y239/240F and WT animals had comparable levels of tumor outgrowth. This indicates a possible role for pY313 in stromal signaling, whereas pY239/240 are not important in this context [91].

It has been demonstrated that ShcA promotes angiogenesis by increasing vascular endothelial growth factor (VEGF) expression in a number of studies [91,94,96,97,98]. First, p52 Shc leads to an increase in the expression of α5 and β1 integrins. This in turn leads to the Src-dependent VEGF production as well as platelet derived growth factor (PDGF) receptor and hepatocyte growth factor (Met) receptor transactivation [98]. Second, in line with a role of Y239/240 in angiogenesis [91], p52 Shc activates Akt in a pY239/240/317-dependent manner. Activated Akt in turn inactivates 4EBP1 triggering the release of eIF4E and translation of VEGF [97].

ShcA also activates Akt via its SH2 domain to promote cell survival. Disabling the phosphotyrosine binding ability in the SH2 domain leads to a decrease in phospho-Akt

level and a significant increase in apoptosis. As it has been shown that Shc recruits tyrosine phosphorylated 14-3-3 via its SH2 domain for the activation of PI3 kinase (the upstream activator of Akt) [65], the association between Shc and 14-3-3 was investigated. Indeed, it was found that there was a reduction in the association between Shc and 14-3-3, as well as p85, suggesting that Shc activates Akt through the recruitment of the 14-3-3/p85 complex [96].

Transgenic animals expressing the ShcA R175Q mutant, which cannot bind to phosphotyrosine-motifs via the PTB domain, exhibited delayed tumor onset. However, these mice eventually developed tumors that grew to a large size with enhanced angiogenesis. In agreement with enhanced angiogenesis, profiling of tumors derived from these mice expressing ShcA R175Q mutant reveals a gene signature that associates with a higher microvessel density in breast cancer patients [98]. Since Y239/240 in the CH1 and SH2 domains are associated with angiogenesis, this suggests that abolishing PTB functions causes a bias towards CH1 and SH2 functions

These studies support the finding in mouse developmental models that the three ShcA core domains function non-redundantly as discussed in section 1.5. Intriguingly, no change in proliferative rate was found in most of the studies that investigated this aspect [91,96,98]. Cell proliferation is closely linked to Erk signaling, with which ShcA is most associated in cell culture transformation studies. Furthermore, in certain cases, Shc/Grb2 association and/or phospho-Erk level was not altered. Whether this is due to differences in signaling when experiments were carried out in a three-dimensional (i.e. in an organ) verses a two-dimensional environment (i.e. in monolayer cell culture) remains to be investigated.

1.7 Summary

The prototypical scaffold ShcA is involved in diverse cellular processes and the disruption of Shc-mediated signaling leads to disease states. Developmental and breast cancer mouse models have successfully assigned some of these cellular processes to certain domains/PTMs of ShcA. For example, in mouse breast cancer models, the phosphotyrosine-binding ability of ShcPTB is required for tumor initiation, whereas the SH2 domain is responsible for angiogenesis; also, phosphorylation of Y239/240, but not Y317, is important in DN3-DN4 transition of T- cells. However, these studies also reveal that the molecular mechanisms for some of the Shc-dependent functions are unclear. For example, deleting ShcA in the nervous system downregulates cell proliferation. It was shown that a pY239/240/317-independent mechanism was involved, however, the exact nature of this mechanism is currently unclear. Again, in the case of cardiovascular development, ShcA deletion led to lethality. Mutating tyrosine 239/240/317 to phenylalanine in mice led to grossly normal heart development and only affected Erk signaling moderately, indicating that the lethal effect of ShcA deletion is caused by mechanisms other than those mediated by the phosphorylation of Y239/240/317. Since it is known that Shc recruits a large array of protein factors, it is likely that these unknown mechanisms rely on the interaction between Shc and these protein factors. Hence, many questions remain as to how the interactions between Shc and each of its partners contribute towards biological outcomes at the molecular level.

1.8 Research objectives

To investigate novel mechanisms whereby intracellular signaling networks are regulated by scaffold proteins, we utilized Shc as a model system because it has been shown to lie at the intersection of a number of signaling pathways. I have previously identified the MAP kinase Erk as a potential interacting partner. In this thesis I investigate, 1) the molecular basis for the direct interaction between Shc and Erk, 2) the regulation of Erk signaling by Shc prior to growth factor stimulation and 3) the role of Erk-mediated phosphorylation of Shc in downstream signaling post- EGF stimulation.

Chapter 2

Materials and Methods

2.1 Materials

2.1.1 Chemicals

All chemicals were purchased from Sigma or Fisher, unless otherwise stated.

2.1.2 Enzymes and growth factor

Enzymes	**Supplier**
Vent DNA polymerase	NEB
Phusion DNA polymerase	NEB
T4 DNA polymerase	NEB
Restriction endonucleases	NEB
T4 DNA ligase	NEB
Recombinant EGF	R&D
Dpn1 demethylase	NEB

2.1.3 Kits and other materials

Kits and other materials	**Supplier**
Talon superflow resin	Clontech
Glutathiones agarose	Sigma or GE
Q Sepharose	GE
Sephadex G-75	GE
Sephadex G-200	GE
Protein A/G agarose	Santa Cruz
Complete Protease inhibitor Cocktail with EDTA	Roche
PhosphoSTOP phosphatase inhibitor cocktail	Roche
Metafectene transfection reagent	Biontex
Immobilon-P PVDF membrane	Millipore
QIAprep spin miniprep kit	Qiagen
QIAquick gel extraction kit	Qiagen
Enhanced chemiluminescence substrate	Pierce
Silver stain kit	Pierce

X-ray film	Denville

2.1.4 Bacterial cell culture reagents

Luria-Bertani (LB) broth

1.0% (w/v) tryptone

0.5% (W/V) yeast extract

0.5% (w/v) sodium chloride

Antibiotic working concentrations

All were 0.22µm filtered

Ampicillin: 50µg/ml (dissolved in H_2O)

Kanamycin: 50µg/ml (dissolved in H_2O)

Chloramphenical: 50µg/ml (dissolved in ethanol)

LB-Agar plates

1.0% (w/v) agar was added to LB broth followed by autoclaving. Antibiotics were added to cooled agar.

***E. coli.* glycerol stocks**

Glycerol stocks were prepared by mixing 700µl 50% autoclaved glycerol and 300µl E. coli overnight culture. Stocks were stored at -80°C.

2.1.5 Mammalian cell culture reagents

Reagent	Supplier
Dulbecco's Modified Eagle's Medium (DMEM)	**Lonza**
DMEM/F12	Invitrogen
RPMI	Lonza
Foetal Bovine Serum	Denville
Horse Serum	Sigma
Hydrocortisone	Sigma
Cholera Toxin	Sigma
EGF	Peprotech
Insulin	Sigma
Pen/Strep/Fungizone	Invitrogen

2.1.5 Composition of complete growth media

HEK293T, MCF7, MKN28, NIH3T3, MDA-MB-468, MDA-MB-231, A431: DMEM supplemented with 10% FBS and Pen/Strep/Fungizone.

PC12: DMEM supplemented with 10% HS, 5% FBS and Pen/Strep/Fungizone.

MDA-MB-361: DMEM/F12 supplemented with 10% FBS and Pen/Strep/Fungizone.

MCF10A: DMEM/F12 supplemented with 5% HS, 20ng/ml EGF, 0.5mg/ml hydrocortisone, 100ng/ml cholera toxin, 10μg/ml insulin and Pen/Strep/Fungizone.

Composition of starvation media:

HEK293T, MCF7, MKN28, NIH3T3, MDA-MB-468, MDA-MB-231, A431: DMEM supplemented with Pen/Strep/Fungizone.

PC12: DMEM supplemented with Pen/Strep/Fungizone.

MDA-MB-361: DMEM/F12 supplemented and Pen/Strep/Fungizone.

MCF10A: DMEM/F12 supplemented with 0.5mg/ml hydrocortisone, 100ng/ml cholera toxin and Pen/Strep/Fungizone.

Antibiotics for cell line selection

Antibiotic	**Cell line**	**Concentration**
Blasticidin	HEK293T	100µg/ml
Hygromycin	HEK293T	160µg/ml
Puromycin	MCF7	4 µg/ml

2.1.6 Antibodies

Antibody	**Cat. No.**	**Supplier**	**Use**
Erk1/2	4695	Cell Signaling Technology	Western Blot
Phospho-Erk1/2	4377	Cell Signaling Technology	Western Blot
EGFR	2646	Cell Signaling Technology	Western Blot
Tubulin	2125	Cell Signaling Technology	Western Blot
LaminA/C	4777	Cell Signaling Technology	Western Blot
Hsp90	4874	Cell Signaling Technology	Western Blot
GST	2625	Cell Signaling Technology	Western Blot
Shc	MAB0807	Abnova	Western blot/ Immunoprecipitation
Shc	sc-967	Santa Cruz	Western Blot
Shc	610879	BD Biosciences	Immunoprecipitation
Strep-tag	PAB-16601	Abnova	Western Blot
Phospho-Thr-Pro	9391	Cell Signaling Technology	Western Blot
Phospho-Akt (T308)	4056	Cell Signaling Technology	Western Blot
Akt	4691	Cell Signaling Technology	Western Blot
Phospho- Shc (T214)	Custom	Genscript	Western Blot / Immunoprecipitation
Grb2	sc-255	Santa Cruz	Western Blot
Phospho-Shc (Y239/240)	2434	Cell Signaling Technology	Western Blot
Phospho-Shc (Y317)	sc-23765R	Santa Cruz	Western Blot
GAPDH	sc-47724	Santa Cruz	Western Blot
HA-tag	sc-805	Santa Cruz	Immunoprecipitation

14-3-3 (pan)	8312	Cell Signaling Technology	Western Blot
GFP	sc-9996	Santa Cruz	Western Blot
Myc-tag	2278	Cell Signaling Technology	Western Blot
GFP-trap	gta-20	Chromotek	Immunoprecipitation
PIN1	sc-15340	Santa Cruz	Western Blot
GFP-trap	Gta-20	Chromotek	Immunoprecipitation

2.1.7 Plasmids

Plasmid	**Characteristics**	**Source**
pcDNA6 Myc/His C	Mammalian expression vector with a Myc and His tag at C-term driven by CMV promoter	Invitrogen
pcDNA6 Myc-His C-Erk WT	Mammalian expression of myc-tagged Erk WT	This study
pcDNA6 Myc-His C-Erk D20/100A	Mammalian expression of myc-tagged Erk D20/100A	This study
pGEX6P-Erk2 WT	Bacterial expression of Erk2 WT	This study
pGEX6P-Erk2 D20/100A	Bacterial expression of Erk2 D20/100A	This study
pET28 Erk2	Bacterial expression of Erk2	This study
pcDNA 3.1	Mammalian expression driven by CMV promoter	Invitrogen
pcDNA3.1 Strep-tagged Shc WT	Mammalian expression of strep-tagged Shc WT	This study
pcDNA3.1 Strep-tagged Shc R98Q	Mammalian expression of strep-tagged Shc R98Q	This study
pcDNA3.1 Strep-tagged Shc T214/276/407A	Mammalian expression of strep-tagged Shc T3A	This study
pcDNA3.1 Strep-tagged Shc T214/276/407E	Mammalian expression of strep-tagged Shc T3E	This study
pET28b	Bacterial expression vector of N-term His-tagged protein with T7 promoter	Novagen
pET28b p52Shc	Bacterial expression of p52Shc	This study
pET28b ShcPTB	Bacterial expression of p52Shc PTB domain	This study
pET28b p52Shc T214/276/407E	Bacterial expression of p52Shc T3E	This study
pGEX2T	Bacterial expression vector of GST-tagged protein	GE
pGEX2T ShcPTB	Bacterial expression of GST-tagged ShcPTB domain	George et. al.
pGEX2T ShcPTB R98Q	Bacterial expression of GST-tagged ShcPTB domain R98Q	This study
pGEX2T ShcPTB W24A	Bacterial expression of GST-tagged ShcPTB domain W24A	This study
pGEX2T ShcPTB R175Q	Bacterial expression of GST-tagged ShcPTB	This study

	domain R175Q	
pGEX2T ShcSH2	Bacterial expression of GST-tagged ShcSH2 domain	George et. al.
GST-Pin1	Bacterial expression of GST-tagged Pin1	Addgene #19027
GST-Pin1 C113A	Bacterial expression of GST-tagged Pin1 C113A mutant	This study
pMCSG7 Pin1	Bacterial expression of His-tagged Pin1	Addgene #40773
GFP-N 14-3-3 zeta	Mammalian expression of GFP-tagged 14-3-3 zeta	This study
pGEX4T2 14-3-3 Tau	Bacterial expression of GST-tagged 14-3-3 Tau	Addgene #13281
pGEX4T1 14-3-3 Epsilon	Bacterial expression of GST-tagged 14-3-3 Epsilon	Addgene #13279
pCI HA Nedd4	Mammalian expression of HA-tagged Nedd4	Addgene #27002

2.1.8 Stock solutions and buffers

Comassie blue stain solution

0.2% (w/v) Coomassie brilliant blue R

40% (w/v) Methanol

10% (w/v) Acetic acid

Comassie blue destain solution

40% (w/v) Methanol

10% (w/v) Acetic acid

Lysis buffer for mammalian cells

50mM HEPES, pH7.5

50mM NaCl

1mM EGTA

10% (w/v) Glycerol

1mM Sodium orthovanadate

10mM Sodium fluoride

0.1% NP-40

1x protease inhibitors

Ponceau S stain solution

0.1% (w/v) Ponceau S

5% (v/v) Acetic acid

Rapid screening buffer

5mM EDTA

10% (w/v) Sucrose

0.25% (w/v) SDS

100mM NaOH

60mM KCl

0.05(w/v) Bromophenol blue

SDS-PAGE running buffer (10X)

1.9M glycine

250mM Tris-base

10% (w/v) SDS

TBE buffer (10x)

890mM Tris-base

890mM Boric acid

20mM EDTA

TBS (10x)

63.04g Tric-HCl

12.11g Tris-base

87.99g NaCl

TBS-T (1x)

1x TBS

1mM EDTA pH8.0

0.1% Tween-20

Transfer buffer stock (10x)

30.3g Tris-base

144g Glycine

Transfer buffer (1x)

1X transfer buffer stock

20% Methanol

DNA loading dye (6x)

0.25% (w/v) Bromophenol blue

0.25% (w/v) Xylene cyanol

30% (v/v) glycerol

Laemmli loading buffer (6x)

300mM Tris-HCl pH6.8

60% (v/v) Glyerol

12% (w/v) SDS

0.6% (w/v) Bromophenol blue

30mM DTT (add before use)

Talon A

50mM Tris-base pH8.0

100mM NaCl

Talon B

50mM Tris-base pH8.0

100mM NaCl

200mM Imidazole

Talon resin regeneration

20mM MES pH5.0

300mM NaCl

GST A

20mM HEPES pH7.5

100mM NaCl

5mM BME

GST B

20mM HEPES pH7.5

100mM NaCl

10mM reduced glutathione

5mM BME

GST resin regeneration

100mM Sodium acetate

500mM NaCl

Anion exchange A

50mM Tris-base pH8.0

100mM NaCl

5mM BME

Anion exchange B

50mM Tris-base pH8.0

500mM NaCl

5mM BME

2.1.9 Peptides

Name	Sequence	Purpose
TrkA	HIIENPQpYFSDA	ITC studies
pT214	NPPKLVpTPHDRMAG	Antibody production

2.2 Molecular biology

2.2.1 Restriction cloning

To amplify a relevant segment of a gene, a set of primers with Tm between 58-64^{o}C were designed by the following equation:

no. of T or A bases x2 + no. of C or G bases x4 for the complementary bases

Corresponding restriction sites were added to the ends of the primers, with additional bases required for a particular enzyme.

Polymerase chain reaction (PCR)was set up as follows:

10ng DNA template

2uM of Each primer

2µl DMSO

1x Enzyme buffer

2µl DNTP

1µl Enzyme

Add sterile H_2O to 50µl

Thermal cycles:

1 x 95°C for 5min

30x 95 °C for 1min

56-62 °C for 1min (use 2 °C below the lowest Tm of the two primers)

72 °C for 30s for every 1kb

1x 72°C for 10min

∞ 4 °C

PCR products were run out on agarose gels at the indicated percentage. PCR products were then purified by gel extraction per manufacturer's instructions. Purified PCR products and vectors were digested by the appropriate restriction enzymes. Digested products were either cleaned or subjected to one more round of gel extraction. Digested PCR products and vectors were ligated as follows:

Vector: products at 1:3 ratio (at least 10ng of vector)

1x T4 ligase buffer

1µl of T4 ligase for every 10µl of ligation reaction

Add H_2O to the appropriate final volume

Ligation was carried out either overnight at room temperature or for 2 hrs at 37 °C.

Ligation products were transformed into DH5α. DNA from single colonies was subjected to further analysis.

2.2.2 Mutagenesis

Primers were designed using the online software Primer X. Briefly, 20-25bp on either side of mutation were included in the primers with C/G content between 30% to 60%.

PCR was set up as follows:

50ng DNA template

2µM of each primer

1x Enzyme buffer

2µM DMSO

1µl Enzyme

2µl DNTP

Add sterile H_2O to final volume of 50µl

Thermal cycles:

1 x 95^{o}C for 5min

30x 95 ^{o}C for 1min

55^{o}C for 1min

68 °C for 2min for every 1kb

1x 68°C for 10min

∞ 4 °C

1µl of Dpn1 was incubated with the mutagenesis products to digest DNA template for 1.5hrs at 37 °C. The product was then cleaned up and transformed into DH5α. DNA from single colonies was subjected to further analysis.

2.2.3 Transformation

Plasmids were incubated with DH5α or Rosetta 2 cells for 30min on ice. Cells were then incubated at 42°C for 1.5 min (routine plasmids production) to 2.5 min (cloning products). Cells were snap cooled on ice for 2min and allowed to recover in 1mL LB at 37 °C with shaking for 1hr. Cells were then pelleted, resuspended in 100µl LB and plated on agar plates containing appropriate antibiotics.

2.2.4 DNA extraction

5-10ml of LB was inoculated either with a single colony or glycerol stock. Cells were pelleted and DNA extraction was performed using the Qiagen miniprep kit.

2.2.5 Generation of competent cells

Inoculate 5ml of LB with bacterial cells for an overnight culture. Add overnight culture to fresh LB in a 1:100 dilution the next morning. Grow cells at 37°C until OD_{600} is 0.4-0.45.

Cool on ice for 15 min. Then pellet cells at 5000g for 15 min at 4°C. Remove supernatant and add 40% of the original volume of ice-cold 150mM $CaCl_2$ (freshly made). Resuspend cells gently and incubate on ice for 60min. Cells were then pelleted at 5000g for 15min. Supernatant was removed and cells were resuspended in 4% of the original volume of ice-cold 150mM $CaCl_2$. Cells were incubated on ice for 15 min. Cells were stored in 30% glycerol at -80 °C in small aliquots.

2.3 Cell biological methods

2.3.1 Maintenance of mammalian cell lines

Mammalian cells were maintained in their appropriate media as listed in 2.1.5 at 37°C with 5% CO_2. Cells were split at 1:5 ratio when they reach 80% confluency and replenished with fresh media every three-four days.

2.3.2 Transfection of mammalian cell lines

HEK293T Cells were seeded the day before for 80% confluency on the day of transfection. Manufacturer's instruction was followed for the ratio of DNA amount, cell numbers and transfection reagent. Cells were used for assays between 1 and 4 days after transfection.

2.3.3 Lentiviral infection of mammalian cell lines

Cells were seeded the day before infection for 50% confluency on the day of infection. 5µg/ml of Polybrene and lentiviral particles were added to the culture media at the end of the day. Cells were replenished with fresh culture media the next morning.

2.3.4 Generation of stable cell lines

24hrs after transfection or infection, cells were split in 1:5 ratio with fresh media

. The appropriate antibiotic was added to the culture media the next day and maintained until non-transduced cells died. Transduced cells were maintained and expanded for analysis.

2.3.5 Preparation and recovery of frozen stocks of mammalian cells

Cells were grown to 80% confluency, trypsinized and resuspended in 3-5ml of media (from a T75 flask), depending of cell types. Resuspended cells were then mixed at a 1:1 ratio with 20% DMSO and 80% FBS. Cells were frozen in 1.8ml aliquots. Each aliquot is sufficient for a T75 flask of cells. Cells were first frozen in an alcohol freezing carrier at -80^{o}C for 1-2 days before moving into long-term liquid N_2 storage. Cells were recovered by via a quick thaw in the water bath and placed into warm culture media.

2.3.6 Fluorescence lifetime imaging microscopy (FLIM)

The $EKAR_{nuclear}$ reporter was transfected into HEK293T cells in 12-well format with 1ug of the plasmid DNA. 24hrs after transfection, cells were seeded onto coverslips at $2.5x10^5$ to achieve 50% confluency the next day. Once the cells acquired the necessary confluency, they were starved for 18-24hrs. Starved cells were then washed with PBS and fixed in 4% paraformaldehyde for 20 minutes at room temperature. Samples were mounted in the presence of anti-fading agent. The FLIM measurements were performed on a Leica TCP SP5 confocal microscope system with internal PMT FLIM detector. Samples were excited

with a titanium-sapphire–pumped laser (Mai Tai BB, Spectral Physics) with SPC830 data and image-acquisition card for time-correlated single photon counting. Data processing and analysis were carried out with B&H SPC FLIM analysis software.

2.3.7 Immunoprecipitation

Cells were lysed in lysis buffer (typically 1ml of lysis buffer was used on a 10cm-dish) and cleared by centrifugation. One milligram of lysate was used per IP experiment. IP antibody was added to the lysate and incubated for overnight. 25 µl of Protein A/G slurry was added to the lysate for 2 h. The immunoprecipitants were washed three times with lysis buffer and boiled with 2× sample buffer (Bio-Rad) for 5 min to elute.

Antibody	**Dilution factor/Amount**
Shc (BD Bioscience, 610879)	5µg
Phospho Shc pT214 (Custom)	7.5µl
Shc (mouse)	10µg

2.4 Protein expression and purification

2.4.1 His-tagged full-length Shc proteins

pET28-Shc FL plasmids were transformed into Rosetta 2 cells. Either a single colony or glycerol stock was used to inoculate overnight culture supplemented with antibiotics. 1mL of overnight culture was then used to inoculate 1L of LB supplemented with antibiotics the next day. Bacterial culture was grown to OD_{600} 0.8 at 37°C and temperature

was reduced to 20°C. It was then induced with 0.1mM IPTG for overnight. Cells were pelleted and stored at -20°C until required.

To purify ShcFL proteins, cell pellets were lysed in Talon buffer A supplemented with protease inhibitors. Lysates were cleared by centrifugation at 20,000rpm for 1hr at 4°C. Cleared lysates were then applied to Talon resin using the AKTA chromatography system. Bound proteins were washed with 5 column volumes each of Talon buffer A and 7.5% Talon buffer B. Proteins were eluted in 100% Talon buffer B. Eluted proteins were then applied to the anion exchange column in anion exchange column A and subjected to a gradient from 0% to 100% anion exchange column B over 10 column volume. ShcFL proteins are eluted between 20-25% B. ShcFL fractions were pooled and concentrated to 5mL before being applied to size exclusion chromatography using a SD75 column (~120ml volume) in the appropriate buffer for subsequent assays.

2.4.2 His-tagged ShcPTB proteins

Growth conditions are as described in 2.4.1.

To purify ShcPTB proteins, the same protocol is used as in 2.4.1, except the anion exchange step is not necessary.

2.4.3 GST-tagged ShcPTB and ShcSH2 proteins

Growth conditions are as described in 2.4.1.

To purify GST-tagged ShcPTB and ShcSH2 proteins, cells were lysed and cleared as in 2.4.1. Lysates were incubated with Glutathione resin for at least 2hrs at 4°C. Resin was then

washed with 50mM Tris-base pH8.0, 200mM NaCl and 1% Triton-X100 5-10 times at 10x bead volumes. Proteins immobilized on beads were stored at 50% glycerol at -20^{o}C until required for assay.

2.4.4 His-tagged Erk2 protein

Growth conditions and purification procedures are as described in 2.4.2.

2.4.5 GST-tagged Erk2

Growth conditions and purification procedures are as described in 2.4.3.

2.4.6 GST-tagged Pin1 proteins

Growth conditions and purification procedures are as described in 2.4.3.

2.4.7 His-tagged Pin1

Growth conditions and purification procedures are as described in 2.4.2.

2.4.8 GFP-14-3-3 zeta

HEK293T cells were transfected with 20 μg of GFP-N-14-3-3 zeta plasmids on a 10cm-dish. Cells were harvested and lysed in 1ml of lysis buffer 48hrs after transfection. Cleared lysates was incubated with 50ul GFP-trap beads overnight. Beads were washed with 1ml lysis buffer 5-10 times.

2.4.9 GST-tagged 14-3-3 Tau and Epsilon proteins

Growth conditions and purification procedures are as described in 2.4.3.

2.4.10 HA-tagged Nedd4

HEK293T cells were transfected with 20ul of pCI-HA-Nedd4 plasmids in a 10cm dish. Cells were harvested and lysed in lysis buffer 48hrs after transfection. Cleared lysates was incubated with HA-tag antibody overnight and subsequently incubated with protein A/G for 2 hrs. Beads were washed with 1ml lysis buffer 5-10 times.

2.5 Biochemical methods

2.5.1 Western blotting

Samples separated by 10% or 4-15% SDS-PAGE and transferred to a PVDF membrane (0.45um) at 250mV for 2hrs or 25mV for 16hrs. Membranes were then blocked with 5% milk or 5% BSA for 30minutes for the detection of total and phospho-protein, respectively. Primary antibody was added at appropriate dilution for overnight at 4^{o}C. Excess antibody was washed with TBST three times before the addition of the secondary antibody in TBST. This was followed by three TBST washes. Signals were developed by the addition of ECL and membranes were exposed to X-ray films [99].

2.5.2 5,5'-Dithio-bis-(2-nitrobenzoic acid) (DTNB) assay

DTNB reacts with a free sulfhydryl group to yield TNB, which absorbs at 412nm with an extinction coefficient of 14,150$M^{-1}cm^{-1}$.

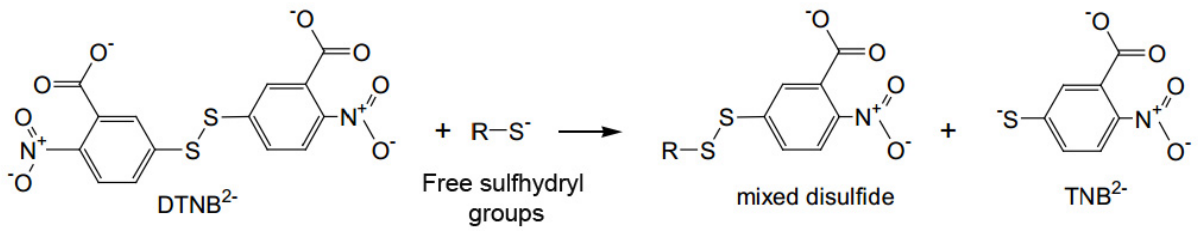

10µM purified ShcFL proteins in 0.1M sodium phosphate and 1mM EDTA was incubated with 80µg /mL DTNB for 15minutes at room temperature. Absorbance was measured at 412nm.

2.5.3 *In vitro* Erk2 phosphorylation of Shc

50 µl of 10µM purified ShcFL proteins in PBS were incubated with 1µl of active Erk2 (NEB, P6080) in the presence of 5mM buffered ATP and 10mM $MgCl_2$ overnight.

2.5.4 Two-dimensional gel electrophoresis

Samples were eluted in 200ul of rehydration buffer containing 7 M urea, 2 M thiourea, 1% ASB-14, 40mM Tris, 0.001% Bromophenol Blue (Biorad). 11cm pH5-8 ReadyStrips (Biorad) were then incubated with the eluents overnight. The Protean i12 system (Biorad) was used to separate samples according to their isoelectric points, using the

'gradient' program for the appropriate strip size and pH range. Samples were then separated by molecular weights using 10% SDS-PAGE gels.

2.5.5 Limited proteolysis

Chymotrypsin preferentially cleaves peptide amide bonds where the carboxyl side of the amide bond is either tyrosine, tryptophan or phenylalanine, thus causing proteolysis in a limited and targeted fashion. 100ng of ShcFL proteins were incubated with 0.5ng of chymotrypsin in PBS at 37^{o}C for each time point. Digestion process was terminated by the addition of 2X loading sample buffer and boiling for 5min.

2.6 Biophysical methods

2.6.1 Isothermal titration calorimetry (ITC)

ITC measures the change in heat (enthalpy) in a bimolecular interaction which leads to the determination of the full range of thermodynamic parameters of the bimolecular interaction. When two molecular species bind non-covalently, a number of bonds are formed or broken between the two molecular species, as well as between the molecular species and the solvent. These can be hydrogen bonds, van der Waals forces and hydrophobic interactions. The rearrangement of interactions thus produces a change in heat as one species is titrated into another, which is measured as the power per second required to maintain the same temperature between the reference and sample cells (Figure 1).

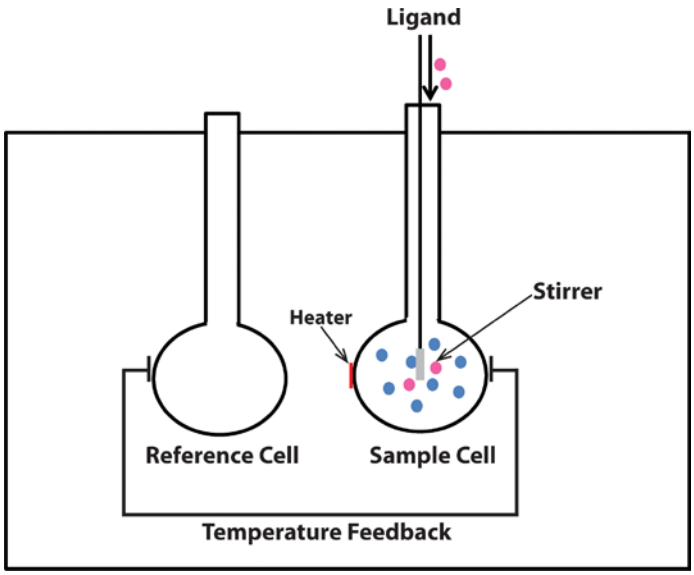

Figure 1. Schematic of the basic components of an ITC instrument. One of the protein binding partners is loaded into the sample cell and the ligand is titrated into the sample cell gradually with constant stirring to ensure the ligand and protein are mixed rapidly. The temperature in the sample cell is constantly monitored by a sensor and compared to the temperature in the reference cell. When there is a change in temperature in the sample cell as the ligand is titrated into the sample cell, the heater then alters the amount of heat that is applied to the sample cell to bring it to the same temperature as the reference cell.

The change in heat of each titration of the ligand is then used to determine the enthalpy, binding constant and stoichiometry of the interaction between the two binding partners using the following equations:

$$Q=nA_T\Delta H(V/2)\cdot\{X-[X^2-(4B_T/nA_T)]^{1/2}\}$$

and

$$X=\{1+B_T/nA_T)+ (1/nK_BA_T) \}$$

Where Q is the heat content of a particular titration (which is experimentally determined by the power required to maintain the same temperature between the reference and sample cells). A is the component in the sample cell and B is the ligand titrated into the sample cell. n is the stoichiometry of the interaction between A and B. T is the total amount of a particular component. H is the enthalpy of the interaction. V is the volume of the reaction. K_B is the binding constant for the interaction between A and B. It is converted into K_D as follows:

$$K_B=1/K_D$$

The molar calorimetric enthalpy and the equilibrium binding constant is determined directly by ITC. We then obtain the full range of thermodynamic parameters using the following equation:

$$-RTInK_B=\Delta G=\Delta H-T\Delta S$$

Where R is gas constant and T is the absolute temperature. S is the entropic term of the interaction.

Experiments were performed using either a VP or iTC200 instrument (GE). All experiments involve Erk2 binding interactions were carried out in 20 mM HEPES, pH 7.4, 50 mM NaCl, 3 mM EDTA and 5 mM βME. ShcPTB proteins binding to TrkA peptide were carried out in 50 mM Tris, pH8.0, 200 mM NaCl. All other experiments were carried out in PBS. ORIGIN7 software was used for data analysis using the single-site model.

2.6.2 Microscale thermophoresis (MST)

MST describes the flow of molecules induced by a temperature gradient. An infrared source heats up the sample at a specific spot, creating a thermal gradient of up to 5K between that specific point and its environment. The bound and unbound species move differently through the temperature gradient due to differences in their hydration shell (which is affected by size/conformation). To monitor the movement of the bimolecular complex in this study, the protein is fluorescently labeled, which is excited by the infrared-laser. The amount of fluorescence in the heated spot at a given time is determined by images taken of the heated spot (Figure 2A). Several steps in the MST process of a bimolecular complex can be monitored and used to determine the binding constant for the bimolecular interaction (Figure 2B).

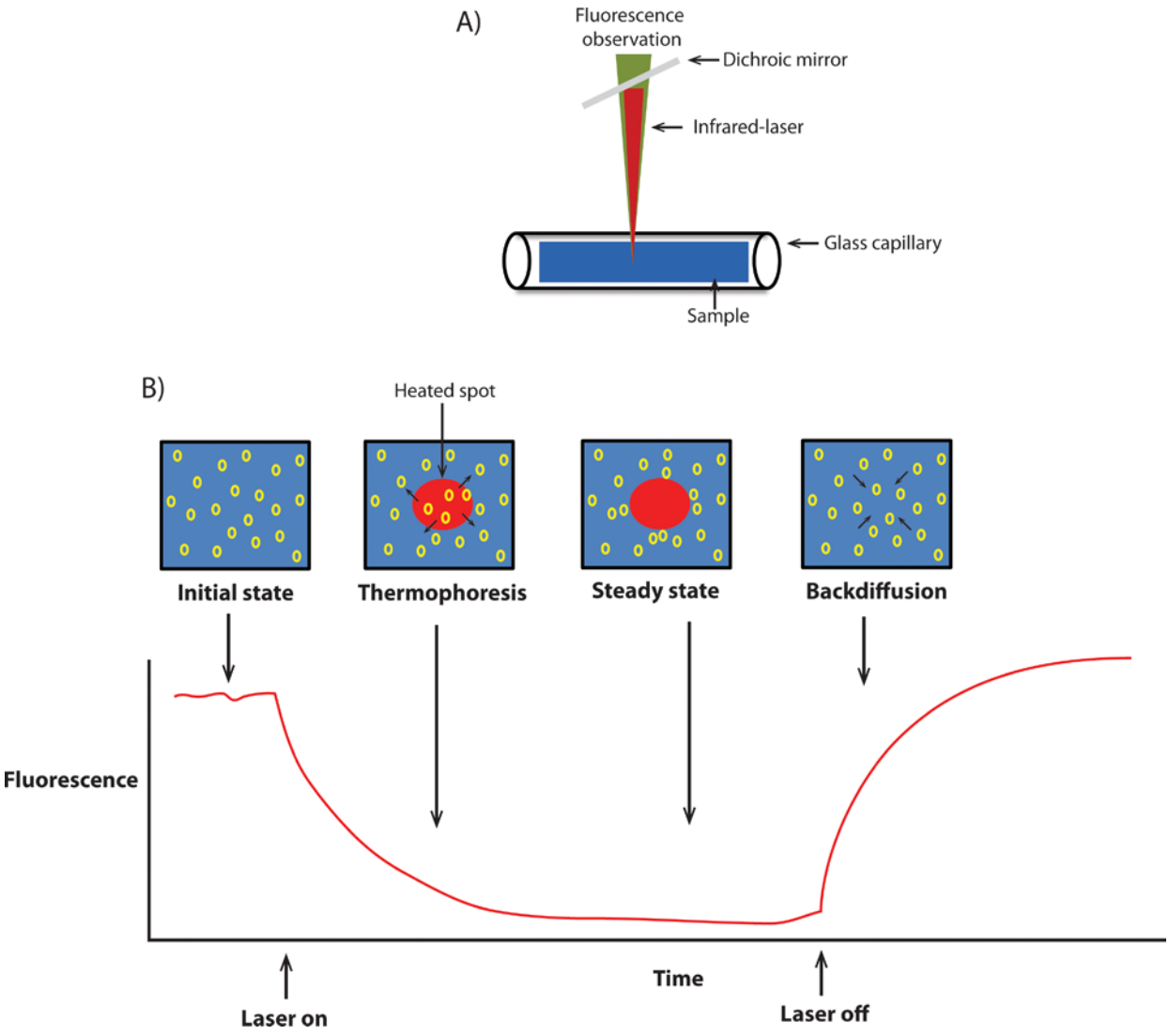

Figure 2. Basic principle for MST measurements. A) Protein samples are loaded into glass capillaries. An infrared source heats up the sample at a particular spot. The laser is turned on and off at specific times controlled by the user. The fluorescence at the heated spot is determined from images taken at that spot. B) Several steps in the MST process can be used to determine dissociation constant. Prior to the laser being switched on, the labeled molecules emit a certain level of fluorescence (initial state). At the early stage after the laser is switched on, molecules in the heated spot migrate into (or out of) the environment in the process of thermophoresis. Eventually, equilibrium of this movement

of molecules is reached (steady state). Finally, the laser is turned off, the molecules redistribute (backdiffusion).

In a bimolecular interaction in an MST experiment:

$$A+B \rightleftharpoons AB$$

Where A is the fluorescently labeled protein and B is the unlabeled binding partner.

To determine the dissociation constant for in this thesis, the following equation was used:

$$\mathbf{(F_{norm}[B]-F_{norm}[A])/(F_{norm}[AB]-F_{norm}[A])=\{1/(2[A])\}\{[A]+[B]+K_d-\{([A]+[B]+K_d)^2-4[A][B]\}^{1/2}}$$

Where F_{norm} is the normalized fluorescence. [ ] denotes concentration of the species in the brackets. K_d is the dissociation constant.

Protein was labeled using the NanotTemper labeling kit. Briefly, ShcPTB was diluted to 20μM in labeling buffer to the final volume of 100μl. 60μM of dye NT-647 was added to the diluted protein and incubated for 2-4hrs at room temperature. ShcPTB was then separated from the free dye using a G25-sephadex column in PBS. Labeling efficiency was calculated by determining the concentrations of the dye (molar extinction coefficient: 250,000$M^{-1}cm^{-1}$) and ShcPTB. To test binding between ShcPTB and ligands, a 1:2 dilution series of each ligand was prepared with a final volume of 10μl. 10μl of 25nM of labeled ShcPTB was added to the ligands and loaded into capillaries.

2.6.3 Circular dichroism (CD)

CD measures the differential absorption of circularly polarized light by chiral molecules. Circularly polarized light is either left-hand circular (LHC) or right-hand circular (RHC). Chirality of a molecule is generated when the molecule is placed in an asymmetric environment, as in the case of protein secondary structures. Secondary structures, such as α-helices and β-strands give rise to certain CD signatures [100,101], as shown below in Figure 3.

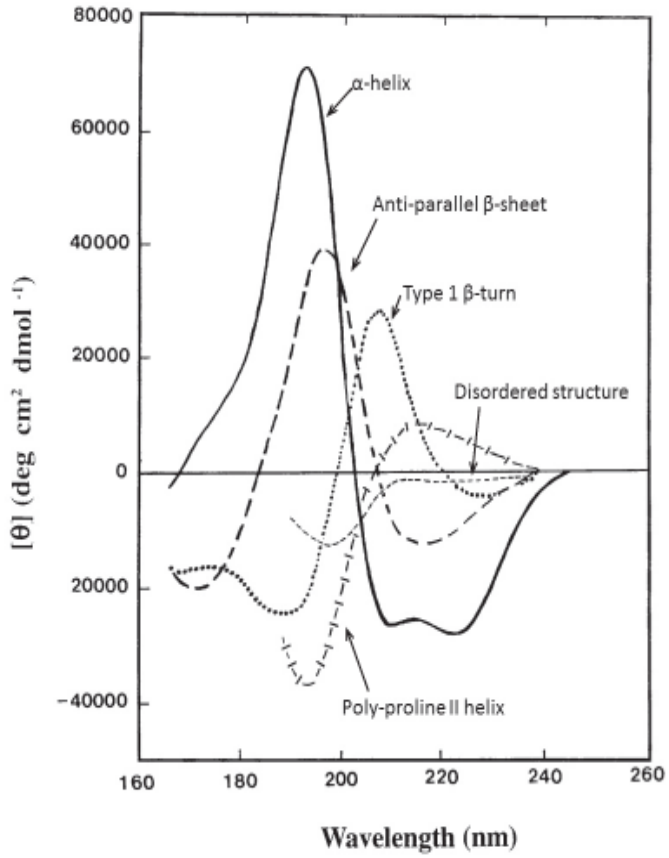

Figure 3. CD signatures of secondary structures. Secondary structures exhibit differential absorbance for LHC and RHC light at certain wavelengths. The overall CD

signal of a protein with multiple types of secondary structure is the sum of the CD signal from all secondary structures. θ is ellipticity.

Differential absorbance for LHC and RHC light is calculated as follows:

$$\Delta A = A_{LHC} - A_{RHC}$$

Where A is absorbance of a particular wavelength.

Absorbance is related to θ:

$$\theta = 32.98\ \Delta A$$

All CD spectra were recorded at room temperature a Jasco J-810 spectropolarimeter in PBS. Data was collected at 0.2nm intervals in triplicates. Data was plotted as molar ellipticity verses wavelength.

2.6.4 Differential scanning fluorimetry (DSF)

DSF monitors the unfolding of a protein by detecting the increase in fluorescence of a dye that interacts with hydrophobic patches of the protein (Figure 4).

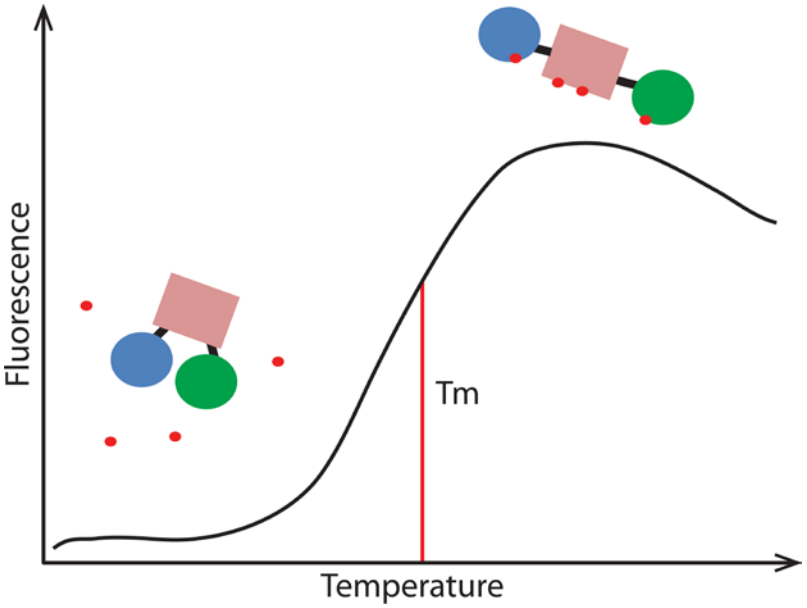

Figure 4. Principle of DSF for monitoring protein stability. Native protein is incubated with a dye that binds to hydrophobic patches on proteins and fluoresces. As the temperature increases, the native protein melts to become increasing denatured to expose hydrophobic patches. Tm is the temperature at which 50% of the protein is denatured.

5µM ShcFL proteins are incubated with 1X SYPRO Orange dye to a final volume of 10µl at 4°C for 20 minutes. Melting assay is performed on Roche LightCycler 480 instrument. Dye was excited at 483nm and emission was monitored at 568nm. Fluorescence is monitored between 20°C and 95°C. Fluorescence signals from the fully folded and unfolded states was then estimated manually and plotted as 0% (fully folded) to 100% (fully unfolded).

Chapter 3

Interaction with Shc inhibits Erk activity in the absence of extracellular stimuli

3.1 Introduction

The family of mitogen-activated protein kinases (MAPKs) plays important roles in diverse cellular processes. The best-characterized MAPK is the extracelluar signal-regulated kinase (Erk). It is the terminal member of a kinase cascade that can be activated by receptor tyrosine kinases (RTKs), which transduce and convert extracellular signals into intracellular events, in turn allowing cells to appropriately respond to the environment. Many steps of this process have been shown to be deregulated in human disease such as cancer. For example, gain-of-function mutations can be found in Ras in 90% of pancreatic cancer; 70% of melanoma patients possess B-Raf mutations. Therefore, members of the Erk cascade are targeted in cancer treatment [102].

Upon binding to their cognate ligands, RTKs are activated and autophosphorylates on their tyrosine residues. The phosphorylated receptors then recruit various adaptor proteins, resulting in the recruitment and activation of the GTPase Ras. One of the effectors of Ras is the serine kinase Raf, the first kinase in the Erk cascade. Raf in turn activates the dual-specificity kinase Mek, which then phosphorylates and activates Erk. Erk has two well-characterized functionally and structurally similar isoforms: Erk1 and Erk2 (85% sequence homology; henceforth communally referred to as Erk). Erk is a serine and threonine kinase that functions primarily by phosphorylating a wide range of substrates [60,103,104]. Activated Erk phosphorylates two proteins critical to cell-cycle entry, p90RSK and Elk [105,106]. p90RSK phosphorylates SRF, which, together with Elk

bind to the serum-response-element (SRE) [107]. SRE is the promoter for immediate-early gene such as *c-fos*, whose activation leads to cell-cycle entry and therefore cell proliferation [108,109].

Erk is tightly controlled by a number of mechanisms. As mentioned above, Erk requires phosphorylation by Mek to become activated upon stimulation of RTKs [110,111]. Erk is dephosphorylated and hence inactivated by a class of dual-specificity phosphatases, named MKPs [112]. Scaffolding proteins such as KSR are also responsible for maintaining the efficiency of the Erk cascade by binding to multiple members of the pathway [113]. It has also been demonstrated that Erk can be anchored in the cytoplasm by proteins such as PEA15 [114,115,116].

In this Chapter, I describe the mechanism whereby direct interaction of Shc with Erk inhibits Erk activity prior to extracellular factor stimulation. This interaction blocks the phosphorylation of Erk and restricts its nuclear translocation. The binding sites identified on both the PTB domain of Shc and the N-terminal lobe of Erk, have not been previously shown to take part in protein recognition. On epidermal growth factor stimulation, recruitment of Shc to phosphorylated RTKs through the PTB domain causes a conformational change in this domain which releases Erk, allowing it to take part in downstream signaling. Thus, Shc is revealed as a key negative regulator of MAP kinase signaling in non-stimulated cells and switches to a positive regulator on binding to activated RTKs through both release of Erk and recruitment of downstream effector proteins.

3.2 Results

3.2.1 Shc forms a complex with Erk prior to extracellular stimulation

Through a proteomics-based study work in the Ladbury lab have previously shown that Shc has many binding partners. Many of these protein binding partners have not been fully characterized [25]. This prompted us to search for other potential interacting partners for Shc. We found that several scaffold proteins with similar functions to Shc in early signaling complexes have been reported to be Erk substrates (see Section 4.1). Therefore, we investigated whether Shc and Erk are directly involved in RTK signaling.

To explore if Shc and Erk interact in mammalian cells, we immuno-precipitated Shc in three different cell lines and immunoblotted for Erk. In serum-starved NIH3T3, MKN28 and PC12 cells we observed the endogenous complex between Shc and Erk (Figure 1A-C). In all three cell lines the stimulation of endogenous epidermal growth factor receptor (EGFR) by EGF reduces the Shc association with Erk (Figure 1A-C). Since Shc is known to associate with EGFR, it appears that the activated, phosphorylated receptor disrupts the binding of Erk. In a reciprocal experiment, GST-tagged Erk immobilized on glutathione agarose beads was incubated with HEK293T lysates and immunoblotted for endogenous Shc. The formation of the Shc-Erk complex was again apparent and this dissociated on stimulation of endogenous EGFR (Figure 1D).

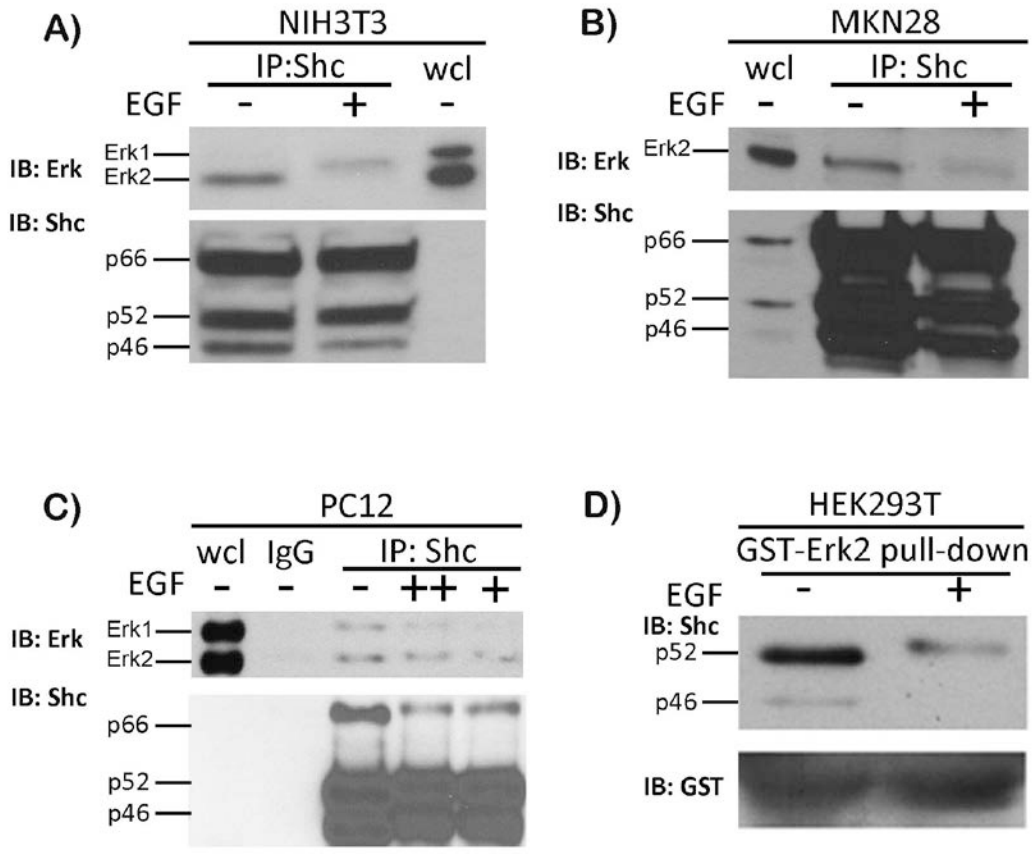

Figure 1. Shc forms a complex with Erk in the absence of extracellular stimulation. (A)-(C) After overnight serum starvation, cells were stimulated with 20ng/ml EGF (NIH3T3 and MKN28 cells), or 100ng/ml (++) and 50ng/ml (+) EGF (PC12 cells). 1 mg of whole cell lysate was incubated with anti-Shc antibody overnight prior to the addition of protein A agarose beads. Immunoprecipitants were washed with lysis buffer and separated by SDS-PAGE, followed by western blot analysis for the presence of Erk. (D) Purified and immobilized GST-Erk was incubated with 1mg of HEK293T cell lysate overnight. The presence of bound Shc was confirmed by western blotting.

3.2.2 Shc binds directly to Erk

To assess the strength of the interaction between Shc and Erk, we quantified the direct binding of full-length Shc and Erk *in vitro* using isothermal titration calorimetry (ITC). Both Shc and Erk were expressed recombinantly in *E. coli.* Shc was titrated into Erk. The equilibrium dissociation constant (K_D) was found to be 0.9μM (Figure 2) for the formation of a 1:1 complex between Shc and Erk.

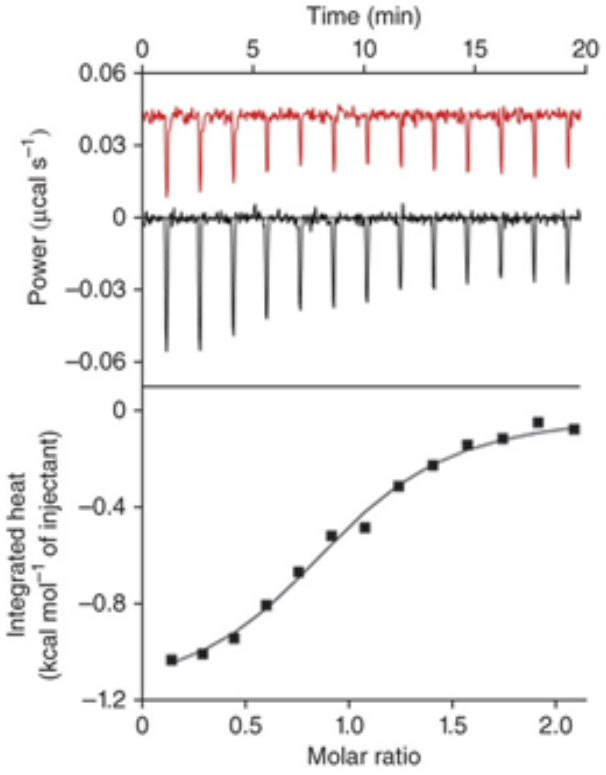

Figure 2. Shc binds directly to Erk. ITC measurement of the Shc and Erk interaction. Thirteen 3μl injections of Erk (60μM) were titrated into Shc (6μM) at 15ºC . Top panel: baseline-corrected power versus time plot for the titration (black) and the heat of dilution of Erk titrated into buffer (red; offset by −0.04 μcal/s). Bottom panel: the integrated heats

and the molar ratio of Erk binding to Shc. The data were corrected for the heats of dilution of Erk and fit to a one-site binding model.

3.2.3 Role of Shc in Erk phosphorylation in non-stimulated conditions

Having established that Shc and Erk form a complex under non-stimulated conditions, we investigated the effect of Shc on Erk phosphorylation. We depleted endogenous Shc in MCF7 cells by shRNA. To our surprise, the pErk level was up-regulated when Shc protein level is depleted (Figure 3A). Since activated Erk translocates into the nucleus [117], we performed nuclear extraction assays to assess the accumulation of Erk in the nucleus of the Shc knock-down cells. Analysis of MCF7 Shc knock-down and control cells fractionated into cytoplasmic and nuclear fraction, demonstrated an increased level of Erk was present in the nuclear fraction when endogenous Shc was diminished in MCF7 cells (Figure 3B). This suggests that Shc functions to inhibit Erk activity in the absence of growth factor stimulation.

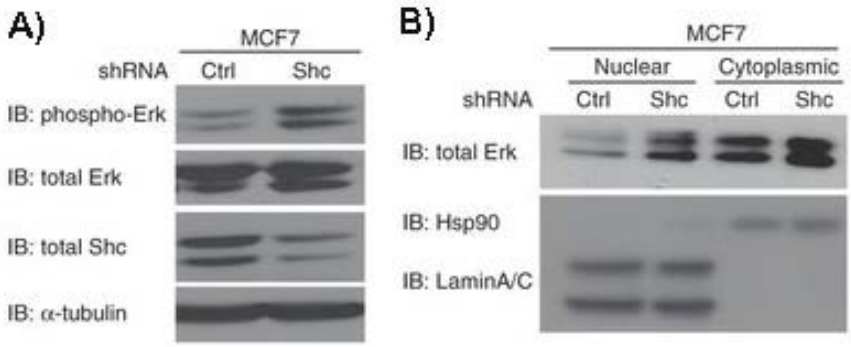

Figure 3. Shc downregulates Erk activation. (A) MCF7 cells were infected with either scrambled shRNA (control) or Shc shRNA and starved overnight. 50μg of total cell lysates were analyzed by western blotting for endogenous pErk. Shc-depleted cells exhibit a high level of pErk compared to those with the control shRNA. (B) Nuclear extraction was

performed on Shc-depleted MCF7 cells. Cells were obtained from 10cm-dishes for each sample. All of the nucleus extracts and 50μg of cytoplasmic fractions were analyzed by western blotting. More total Erk was found in the nucleus when the endogenous Shc level was reduced.

3.2.4 Shc-Erk interaction occurs through unique binding sites on both proteins.

To determine whether the inhibitory effect of Shc on Erk is mediated by the direct interaction of the two proteins, we next identified the molecular basis for the Shc-Erk complex. The CH1 domain of Shc has been shown to form complexes only upon Shc phosphorylation by active protein tyrosine kinases [118,119], therefore the binding site for Erk on Shc was assumed to involve either the N-terminal PTB domain or the C-terminal SH2 domain. ShcPTB and ShcSH2 fused with GST were recombinantly expressed in *E. coli.* and purified. Purified GST-ShcPTB and GST-ShcSH2 proteins were incubated with either HEK293T or PC12 lysates. Figures 4A and 4B indicate that the ShcPTB, and not the ShcSH2, forms the binding site for Erk.

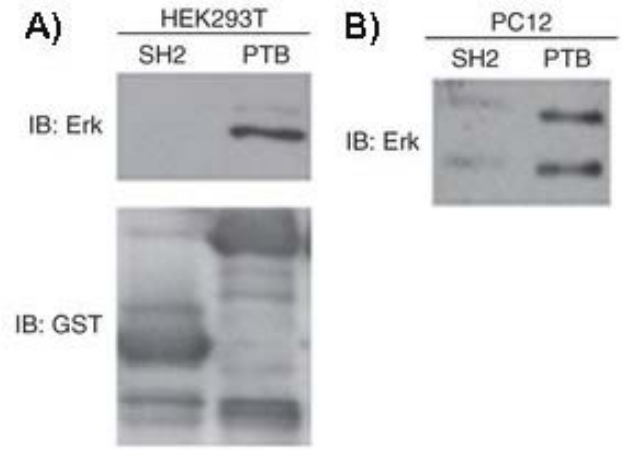

Figure 4. Identification of ShcPTB-Erk interaction. Purified GST-ShcSH2 or GST-ShcPTB were incubated with 500ug of (A) HEK293T or (B) PC12 total cell lysates. Cells were starved overnight. The ability of endogenous Erk to bind to the individual domains of Shc was analyzed by western blotting

To confirm that ShcPTB is responsible for directly interacting with Erk, the interaction of ShcPTB and Erk was measured by ITC. Erk was titrated into ShcPTB (K_D = 9.5μM; Figure 5). The affinity of the ShcPTB interaction with Erk with a K_D of 9.5μM is about an order of magnitude weaker than the interaction with the full length Shc protein with a of K_D of 0.9μM. Since the interaction between full-length Shc with Erk fitted well with a single-site model, the stronger affinity between the full length proteins is unlikely to be due to additional unidentified sites on the CH1 or SH2 domains. We have previously shown that the functions of ShcSH2 are affected by the CH1 domain [118], indicating that inter-domain interaction exists in the Shc molecule. Extending that rationale to this result, it is likely that the weaker affinity between Erk and ShcPTB compared with full length Shc is due to the CH1 and SH2 domains stabilizing the binding of the PTB domain with Erk through inter-domain interaction.

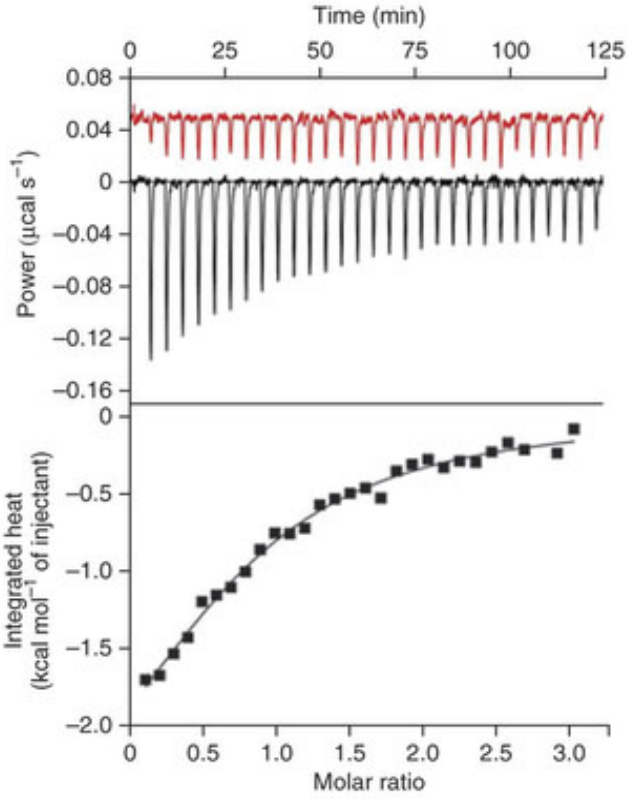

Figure 5. ITC measurement of the ShcPTB and Erk interaction. ShcPTB (203µM) was titrated into Erk (20µM) at 15ºC. Top panel: baseline-corrected power versus time plot for the titration (black) and the heat of dilution of buffer titrated into Erk (red; offset by −0.04 µcal/s). Bottom panel: the integrated heats and the molar ratio of ShcPTB binding to Erk. The data were corrected for the heats of dilution of Erk and fit to a one-site binding model.

Small angle X-ray scattering (SAXS) was employed to provide a model for the molecular juxtaposition of ShcPTB and Erk in the complex [120]. The SAXS-derived model for the complex between ShcPTB (purple) and Erk (green) revealed that the α2-β3 loop of Shc PTB binds to a groove in the N-terminal lobe of the Erk kinase domain (Figure 6A and B).

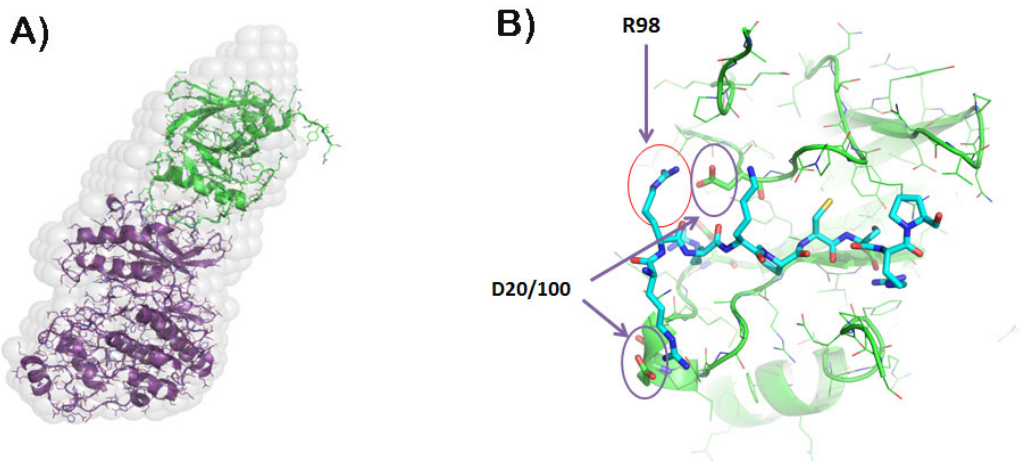

Figure 6. Determination of the binding interface between ShcPTB and Erk. (A) Atomic model of the Erk-ShcPTB complex (Erk, green; ShcPTB, magenta). (B) Close-up view of a structural model of the interaction between the ShcPTB peptide (cyan) and the Erk N-terminal lobe (green). Additionally highlighted are Shc R98, Erk D20 and D100.

The interaction of Erk on Shc is mediated through a previously unidentified binding site which is independent of both the canonical phosphotyrosine and phospholipid binding sites on ShcPTB [35,44]. To validate the binding site for Erk on Shc as seen in the SAXS analysis, a peptide based on the Shc sequence (Shc3R: RRRKPCSRPLS residues 97-107 of Shc) was synthesized and tested for binding to full length Erk. ITC data show that the Shc3R peptide binds to Erk with a K_D of 5.7μM (Figure 7). The binding affinities of Erk for ShcPTB and Shc3R peptide are in the same order of magnitude (9.5 μM verses 5.7μM), suggesting that the residues required for interacting with Erk on Shc are mostly contained within the Shc3R peptide.

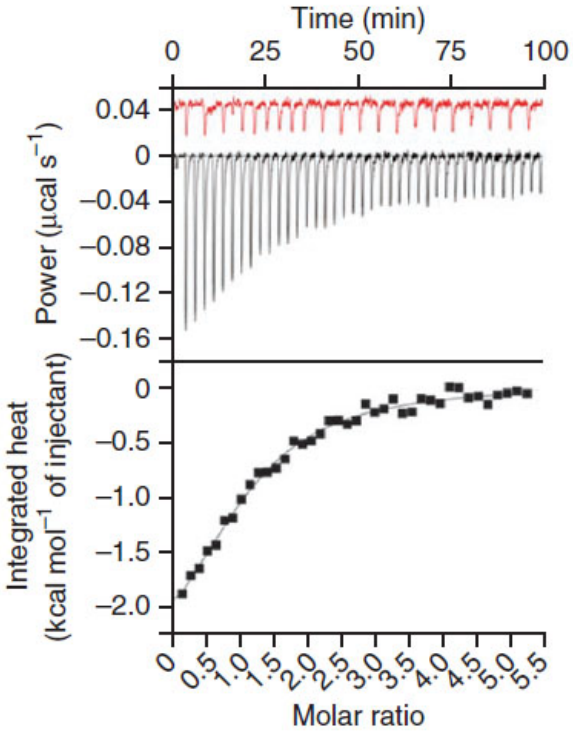

Figure 7. ITC measurement of the binding between Erk and ShcPTB 3R peptide. Thirty-nine 7µl injections of Shc3R peptide (250µM) were titrated into Erk (10µM) at 15ºC. Top panel: baseline-corrected power versus time plot for the titration (black) and the heat of dilution of buffer titrated into Erk (22 injections shown in red; offset by −0.04 µcal/s). Bottom panel: the integrated heats and the molar ratio of Shc3R peptide binding to Erk. The data were corrected for the heats of dilution of Erk and fit to a one-site binding model.

Mutants in the putative binding site for Erk on ShcPTB were generated to confirm the interaction suggested by the SAXS model. The model predicts that R98 in the α2-β3 loop of ShcPTB plays a major role in the recognition of Erk (Figure 6B). To test whether

this residue was necessary to mediate this binding, we mutated the arginine to a glutamine (R98Q; ^{R98Q}ShcPTB). We also made two other control mutant Shc variants (W24A and R175Q). A key residue in a potential consensus Erk substrate binding site, W24, was mutated to Ala (W24A; ^{W24A}ShcPTB), whilst R175, a critical residue in the phosphotyrosine binding pocket recognized by RTKs, was mutated to glutamine (R175Q; ^{R175Q}ShcPTB). These mutants were recombinantly expressed as GST-fusion proteins and purified. The data reveal that R98 is a direct binding residue to Erk, as shown in Figure 8A (upper panel), in which the ^{R98Q}ShcPTB fails to pull-down endogenous Erk from HEK293T cell lysates. This data also confirms that the location of the binding site on ShcPTB as that including the sequence incorporated in Shc3R and depicted in Figure 3B. The two other point-mutants ^{W24A}ShcPTB and ^{R175Q}ShcPTB retain the ability to interact with Erk. Furthermore, we tested the ability of the ^{R98Q}ShcPTB in binding to a tyrosyl phosphopeptide based on the TrkA receptor, a well-characterized ShcPTB binding partner [35]. ITC titrations show that there is no difference in the binding affinities of TrkA for ^{WT}ShcPTB and ^{R98Q}ShcPTB (Figure 8B and C, suggesting that the R98 residue is involved specifically in the interaction of Shc with Erk and not tyrosine-phosphorylated binding partners. Taken together, the location of the binding site for Erk on Shc does not include sites for other reported Shc interactions.

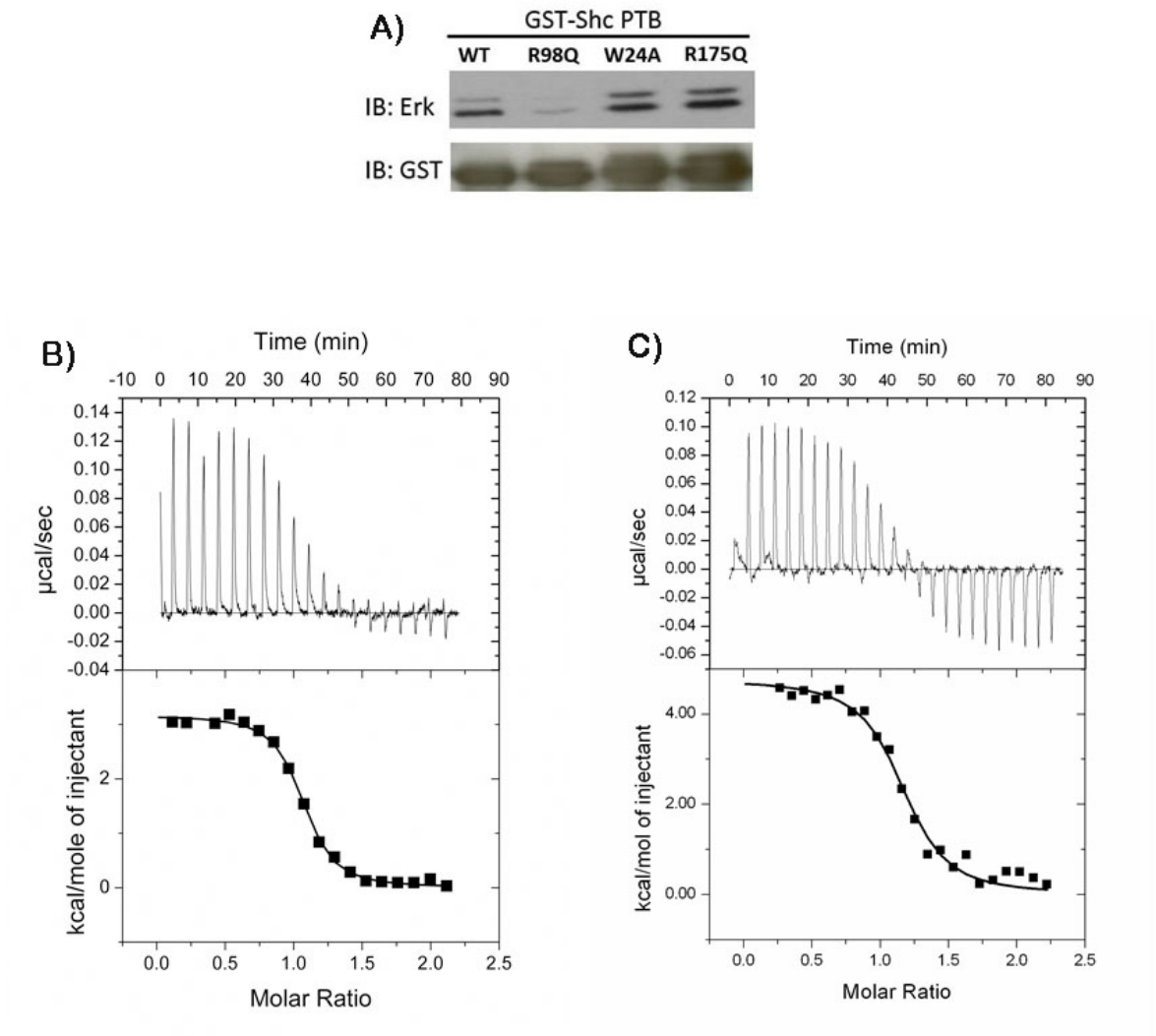

Figure 8. ShcPTB binds to Erk via a noncanonical site. (A) Top panel: GST-fusion of ShcPTB containing 3 different mutations (R98Q, W24A or R175Q) were immobilized on agarose beads and incubated with unstimulated HEK293T lysates. Erk from HEK293T lysates was pulled down by ^{WT}ShcPTB, ^{W24A}ShcPTB and ^{R175Q}ShcPTB. Only ^{R98Q}Shc disrupts the formation of the Shc-Erk complex. (B) ITC measurement of the binding between ^{WT}ShcPTB and TrkA peptide. Twenty 15µl injections of TrkA peptide (100µM) were titrated into ^{WT}ShcPTB (10µM) at 15ºC. The data were corrected for the heats of dilution of Erk and fit to a one-site binding model with a K_D of 140nM. (C) ITC measurement of the binding between ^{R98Q}ShcPTB and TrkA peptide. Twenty-five 12µl injections of TrkA

peptide (100μM) were titrated into ^{R98Q}ShcPTB (10μM) at 15ºC. The data were corrected for the heats of dilution of Erk and fit to a one-site binding model with a K_D of 250nM.

The modeled binding site for Shc on Erk also represents a novel mode of interaction not previously identified as a site of ligand binding on the kinase. To confirm the location of binding site two aspartic acids which were identified as being in the Erk binding site in the SAXS model (Figure 6B), D20 and D100, were mutated to alanines (D20A/D100A; $^{D20A/D100A}$Erk). This mutant form of Erk was unable to pull down Shc from HEK293T cell lysate (Figure 9).

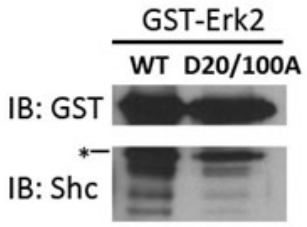

Figure 9. Erk binds to Shc via a novel site. GST-fusion with ^{WT}Erk or $^{D20/100A}$Erk were immobilized on agarose beads and incubated with unstimulated NIH3T3 cell lysates. The immunoblot shows that $^{D20/100A}$Erk diminishes the ability of Erk to bind to endogenous Shc. *Indicates non-specific protein bands.

3.2.5 Physiological role of Shc-Erk binding.

Having demonstrated the existence of the Shc-Erk complex in non-stimulated cells and identified the binding sites on the respective proteins, we investigated the physiological effects of the interaction. To test whether the Shc-Erk complex affects Erk

phosphorylation we established stable HEK293T cell lines over-expressing ^{WT}Shc and the mutant ^{R98Q}Shc. Under non-stimulated conditions, the overexpression of ^{WT}Shc reduces the level of pErk compared with cells transfected only with the control plasmids, whereas ^{R98Q}Shc overexpression does not influence Erk phosphorylation level (Figure 10A).

The above observations are supported by similar experiments in HEK293T cells stably expressing the $^{D20A/D100A}$Erk mutant in which the Shc-Erk interaction is abrogated. Again pErk levels increase in the mutant compared to wild type Erk-expressing cells (Figure 10B). These data demonstrate the inhibitory role that Shc has on Erk phosphorylation in the absence of extracellular RTK stimulation mediated by direct interaction between the two proteins.

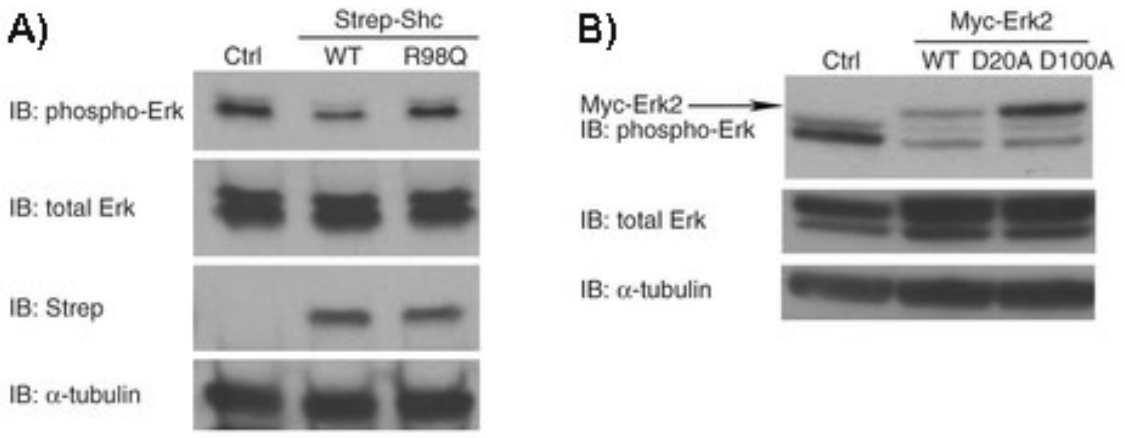

Figure 10. Shc binding has an inhibitory effect on Erk phosphorylation. (A) HEK293T cells stably over-expressing either strep-tagged ^{WT}Shc, ^{R98Q}Shc or strep-tag alone (control) were starved overnight. The phosphorylation level of endogenous Erk was analyzed by western blotting. Erk is more phosphorylated in cells over-expressing ^{R98Q}Shc than ^{WT}Shc under non-stimulatory conditions. (B) HEK293T cells stably over-expressing Myc-tagged ^{WT}Erk or $^{D20/100A}$Erk were starved overnight. $^{D20/100A}$Erk is more phosphorylated than ^{WT}Erk under non-stimulatory conditions.

Next, we used a specific Erk reporter system in a fluorescence lifetime imaging microscopy (FLIM)-based assay to test the levels of nuclear pErk [121]. The reporter $EKAR_{nuclear}$ contains an N-terminal GFP, followed by a WW phospho-binding domain, a substrate peptide, an Erk-docking domain and RFP at its C-terminus (Figure 11A). Activated Erk binds to this reporter through the Erk docking-domain and then phosphorylates the substrate peptide, which subsequently serves as a docking site for the WW phospho-binding domain. This binding event causes a conformational change in the reporter such that the GFP is in close proximity to the RFP and allows for fluorescence resonance energy transfer between the two fluorophores. This results in a shortening of the lifetime of GFP emission. We co-transfected HEK293T cells with the nuclear-localized form of EKAR ($EKAR_{nuclear}$) and either ^{WT}Erk or $^{D20/100A}$Erk. We then measured the lifetime of the GFP fused to $EKAR_{nuclear}$. We observe a clear shortening of the $EKAR_{nuclear}$ GFP lifetime in the presence of $^{D20/100A}$ Erk compared to in the presence of ^{WT}Erk (right panels). This demonstrates the presence of a greater concentration of phospho-Erk in the nucleus of the $^{D20/100A}$Erk-overexpressing cells compared to ^{WT}Erk-overexpressing cells in the non-stimulated state (Figure 11B).

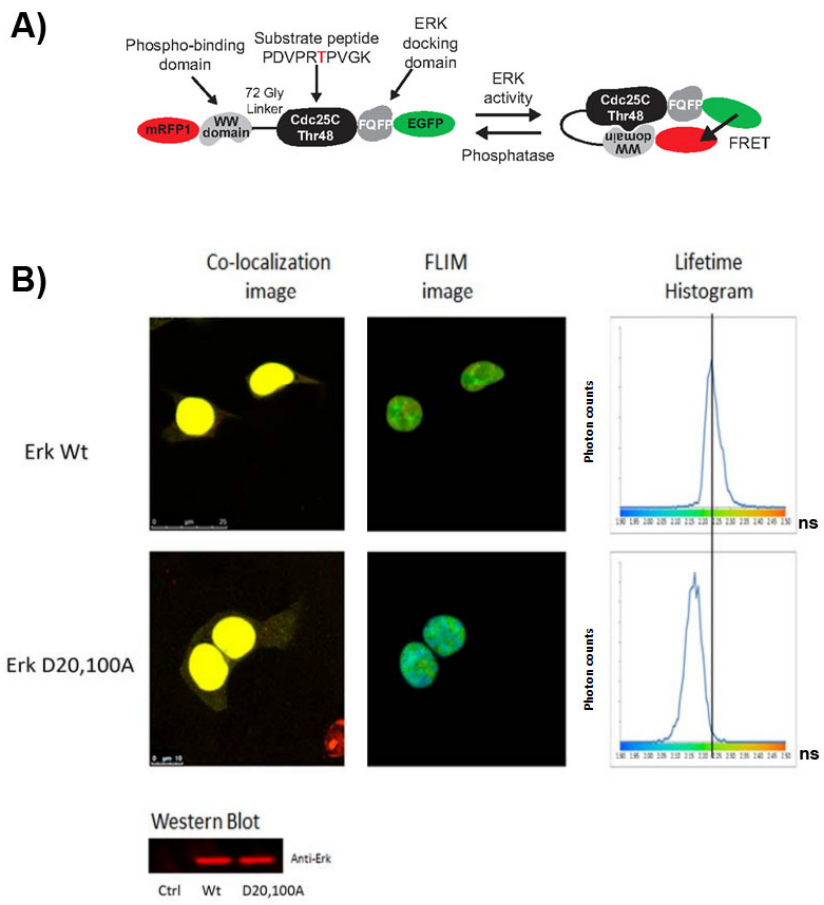

Figure 11. Erk activity in the nucleus. (A) Schematic of the structure of the Erk activity reporter structure. The reporter $EKAR_{nuclear}$ contains an N-terminal GFP, followed by a WW phospho-binding domain, a substrate peptide, an Erk-docking domain and RFP at its C-terminus. (B) HEK293T cells were transiently co-transfected with $EKAR_{nuclear}$ and either vector, Myc-tagged ^{WT}Erk or Myc-tagged $^{D20/100A}$Erk. 24hrs after transfection, cells were starved for 18-24hrs. Overexpression of the $^{D20/100A}$Erk mutant results in a left-shift of $EKAR_{nuclear}$ fluorescence lifetime (histogram), indicating higher Erk activity in the nucleus compared with cells overexpressing ^{WT}Erk. Western blot shows equal overexpression of ^{WT}Erk and $^{D20/100A}$Erk.

3.2.6 Binding of tyrosyl phosphopeptide to ShcPTB promotes dissociation of Erk.

The above characterization of the interaction and the functional consequences of the Shc-Erk complex relate to conditions in the absence of extracellular stimulation. Since the endogenous Shc-Erk complex is present at a reduced level upon growth factor stimulation (Figure 1A-E), we investigated the mechanism by which Erk escapes the inhibitory regulation of Shc. The dissociation of the Shc-Erk complex does not appear to be associated with tyrosyl phosphorylation of Shc by activated RTKs, since ITC data shows that Erk can still bind to phosphorylated Shc (K_D=0.8μM. Figure 12).

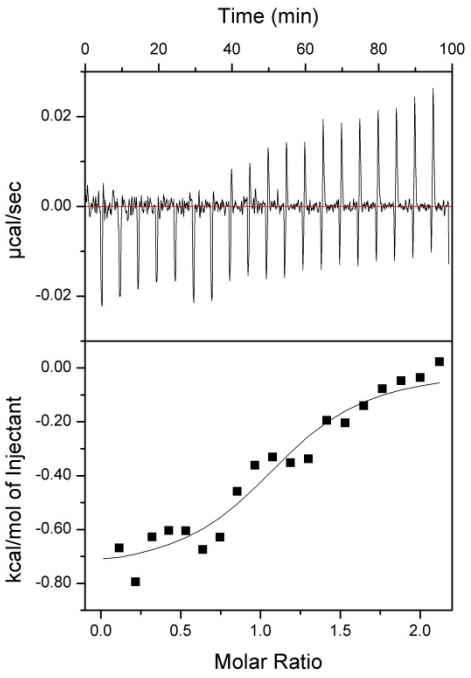

Figure 12. ITC measurement of tyrosine phosphorylated Shc with Erk. Twenty 15ul injections of Erk (96μM) were titrated into tyrosine-phosphorylated full-length Shc (10μM) at 15°C. Integrated heats of the titration were corrected for heats of dilution and fitted to a one-site binding model. The K_D for the Erk-Shc interaction was 0.84μM.

Comparison of NMR spectroscopic structural data on the apo- and TrkA-bound forms of ShcPTB revealed that the apo-form is partially disordered [36]. Regions associated with the binding of TrkA peptide are particularly dynamic. The binding of TrkA peptide results in reorganization of the binding site through local folding events which appear to trigger a conformational switch between free and complex states [35,36]. Large changes in chemical shifts were observed in the region in direct contact with TrkA peptide (the β2-α2 loop region), as well as in part of α2. Q76, R79 and E80 point toward the α2-β3 loop that contains the Erk-binding Shc3R motif (Figure 13). Residues from the α2-β3 loop region also experience significant change in chemical shifts, especially S103 which is facing Q76, R79 and E80 of the α2- β3 loop. Based on these data we hypothesize that the dissociation of the Shc-Erk complex results from an allosteric mechanism, whereby tyrosyl phosphopeptide binding induces structural changes onto the β2-α2 loop which are propagated via helix α2 to the Erk-binding motif.

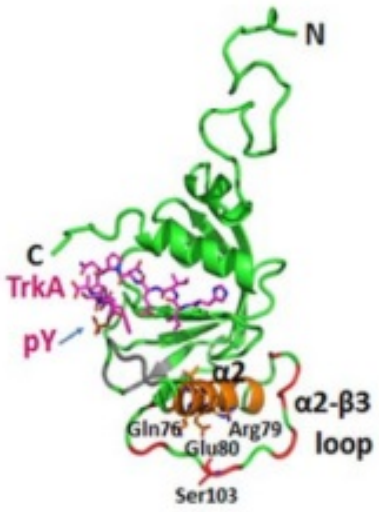

Figure 13. Proposed allosteric changes in ShcPTB responsible for Erk dissociation. Selected NMR chemical shift changes highlighted onto ShcPTB structure (PDB: 1SHC).

TrkA peptide is shown as stick model (magenta). The phosphate group of the phosphotyrosine is indicated by an arrow. Grey: chemical shift changes, cluster1, β2-α2 loop region residues 61-70; orange: cluster 2, α2 (residues 72-87). Residues 75-80 within α2 display the largest chemical shift changes of all ShcPTB residues and are shown as stick models; red: cluster3, residues from the α2- β3 loop which also experience significant chemical shift changes, especially S103.

To confirm this allosteric model we tested if the presence of a known tyrosyl phosphopeptide ligand could provoke the abrogation of the Shc-Erk complex. ShcPTB was titrated into Erk in the presence of TrkA peptide in an ITC experiment. No binding between Shc and Erk was observed. This suggests that TrkA abrogates the Shc-Erk complex formation (Figure 14A).

In addition we demonstrated that the Shc-Erk interaction was inhibited by tyrosyl phosphorylated ligand binding in a pull-down experiment (Figure 14B). HEK293T cells over-expressing strep-tagged WT Shc were starved overnight and the exogenous Shc was precipitated by strep-tactin agarose beads and washed under non-stringent conditions. TrkA peptide was incubated with the precipitants. In the presence of the peptide the interaction between Erk and Shc was abrogated as shown by the absence of Erk from the eluted fractions. These data support a mechanism for tyrosyl phosphorylated ligand-stimulated dissociation of Shc and Erk.

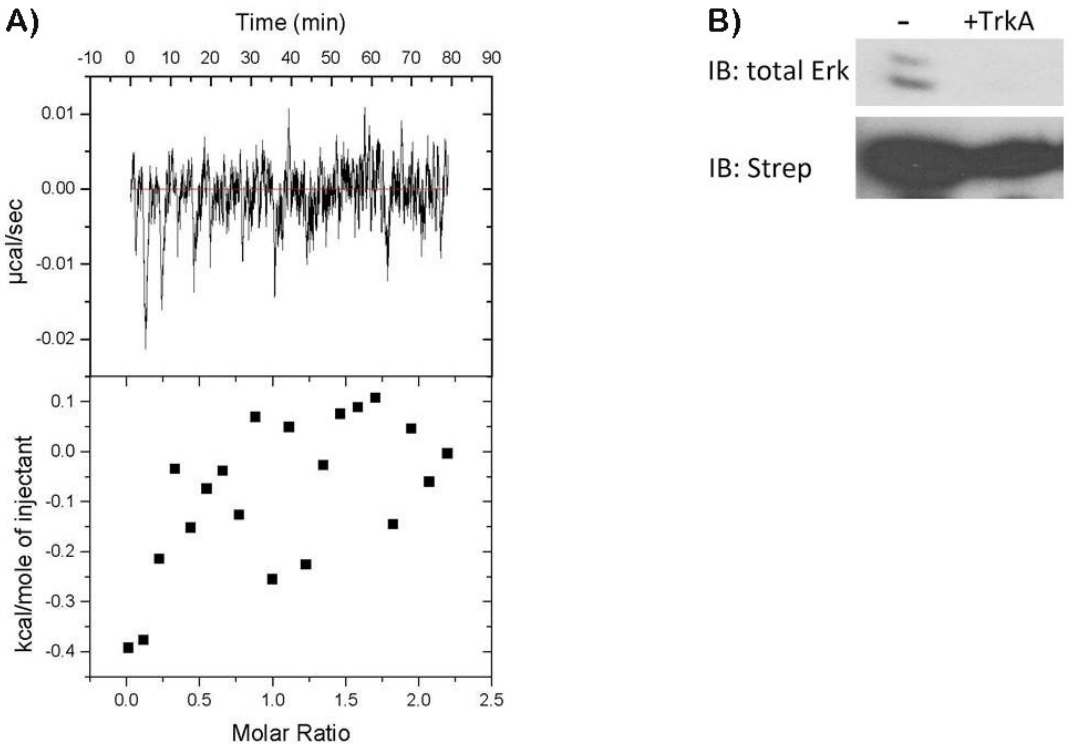

Figure 14. Binding of tyrosine-phosphorylated proteins/peptides to the ShcPTB domain inhibits Shc-Erk interaction (A) ITC measurement of ShcPTB and Erk in the presence of TrkA peptide. 200µM of ShcPTB was pre-incubate with 275µM of TrkA peptide. Twenty 10ul injection of ShcPTB/TrkA complex were titrated into 20µM of Erk at 15°C. No interaction between Erk and Shc was detected. (B) HEK293T cells over-expressing strep-tagged ^{WT}Shc were starved overnight. Total cell lysates were incubated with agarose beads coated with strep-Tactin for 2 hours. Beads were washed and incubated with buffer or 900µM pTrkA peptide for an additional 1hr. Beads were then washed and precipitants were analyzed by western blotting for the presence of Erk. In the presence of the tyrosyl phosphopeptides no interaction of Shc and Erk was detected.

3.2.7 Screening for small molecules to stabilize the Shc-Erk complex

A recent breast cancer study using a mouse model shows that abrogating the tyrosyl phosphopeptide binding ability of the ShcPTB domain delays tumor development [98]. In light of our present finding, we reasoned that a molecule that can block Shc binding to activated RTKs without introducing a conformational change in the Erk-binding site could be beneficial to the treatment of ErbB2-driven breast cancer.

An *in silico* screen (Dr. C. Montanari, personal communication) revealed several potential hits for molecules that could inhibit the binding of Shc with activated RTKs. One such molecule was the nonsteroidal anti-inflammatory drug indomethacin. It has been reported that indomethacin possesses anti-tumor properties, however its mode of action has not been identified. To establish whether this compound can inhibit Shc and activated RTKs, we tested for indomethacin binding to ShcPTB. However, we were unable to observe interaction between the two molecules as monitored by microscale thermophoresis (MST).

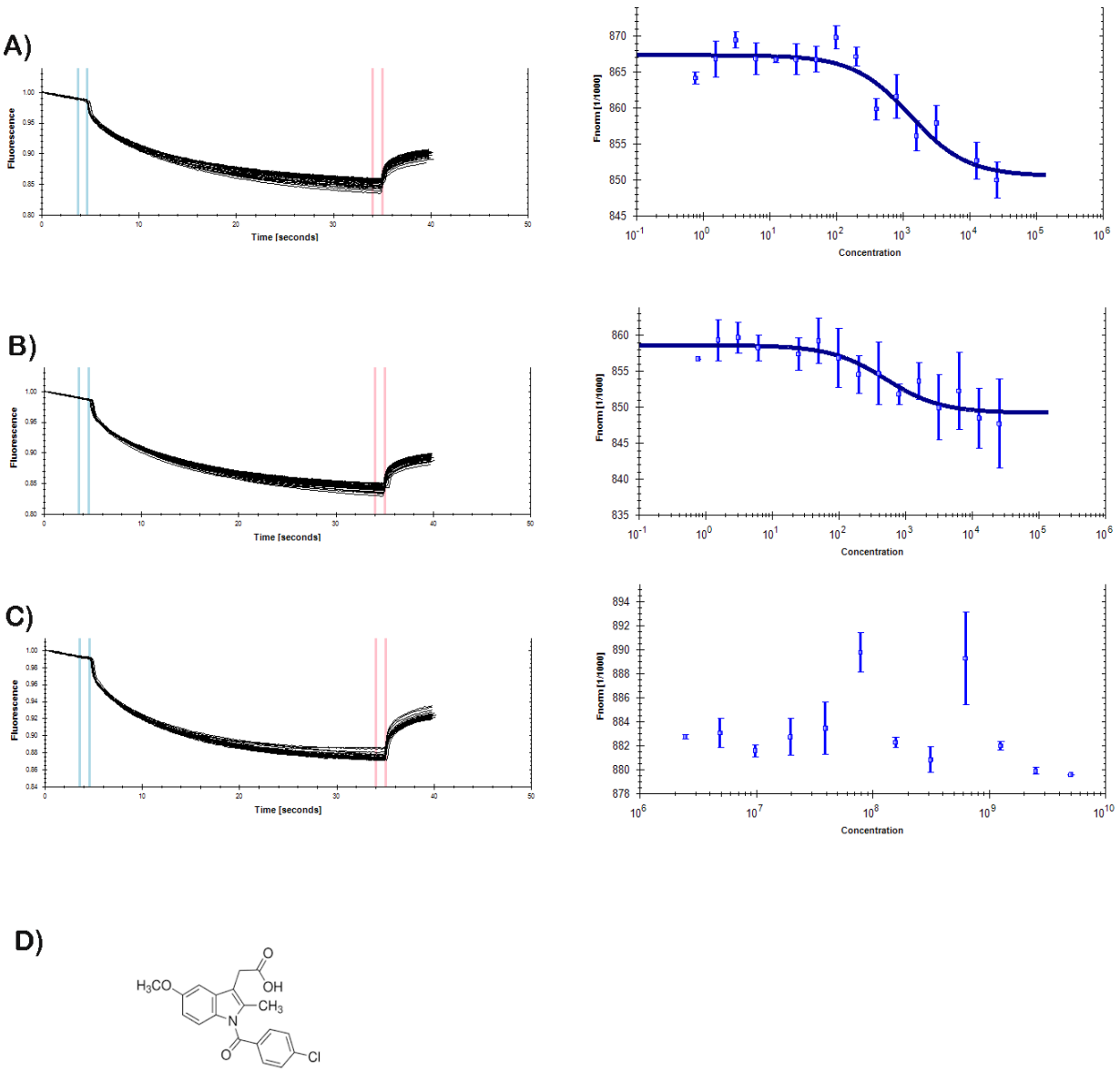

Figure 15. MST measurement of binding between ShcPTB to Indomethacin. 95nM of fluorescently-labeled ShcPTB was incubated with the ligands in a 1:2 dilution series at 25°C. The movement of ShcPTB was monitored by fluorescence measured at 647nm. Left panels: normalized thermophoresis traces. Right panels: Data fitted to one site model. Thermophoresis with temperature jump measurements were made at 90% LED power and 20% IR power. (A) ShcPTB binding to TrkA peptide with K_D=1.2±0.219 μM. Top concentration of TrkA dilution series was 15 μM. (B) ShcPTB binding to TrkA peptide in the presence of 1mM Indomethacin; K_D=452±176nM. Top concentration of TrkA dilution

series was 15 μM. (C) ShcPTB does not bind to indomethacin. Top concentration of indomethacin dilution was 5M. (D) Chemical structure of Indomethacin.

In an attempt to identify potential inhibitors for the Shc PTB-RTK interaction an initial screen of a library of tyrosyl phosphomimetics using differential scanning fluorescence (DSF) was adopted. This resulted in one potential binder for the Shc PTB domain (Dr. G. Poncet-montange, personal communication; Figure 16A). To determine a dissociation constant (K_D) for this interaction, we performed a MST experiment. As shown in Figure 16B, the K_D is ~100μM, which is two orders of magnitude weaker than the binding between ShcPTB and the TrkA peptide.

A short peptide was designed based on the known PTB-phospho-peptide structure (NPQpYFS). This peptide lacks the residues that might be responsible for triggering the conformational change in the PTB domain that leads to Erk dissociation while retaining the residues that are important in phosphotyrosyl binding. The K_D for this interaction is again ~100μM (Figure 16C). Although the binding affinities of Shc PTB domain for these two peptides are considerably lower than its affinity for its intracellular target RTKs (Figure 16E), these peptides serve as good templates for further chemical modifications to yield more suitable compounds.

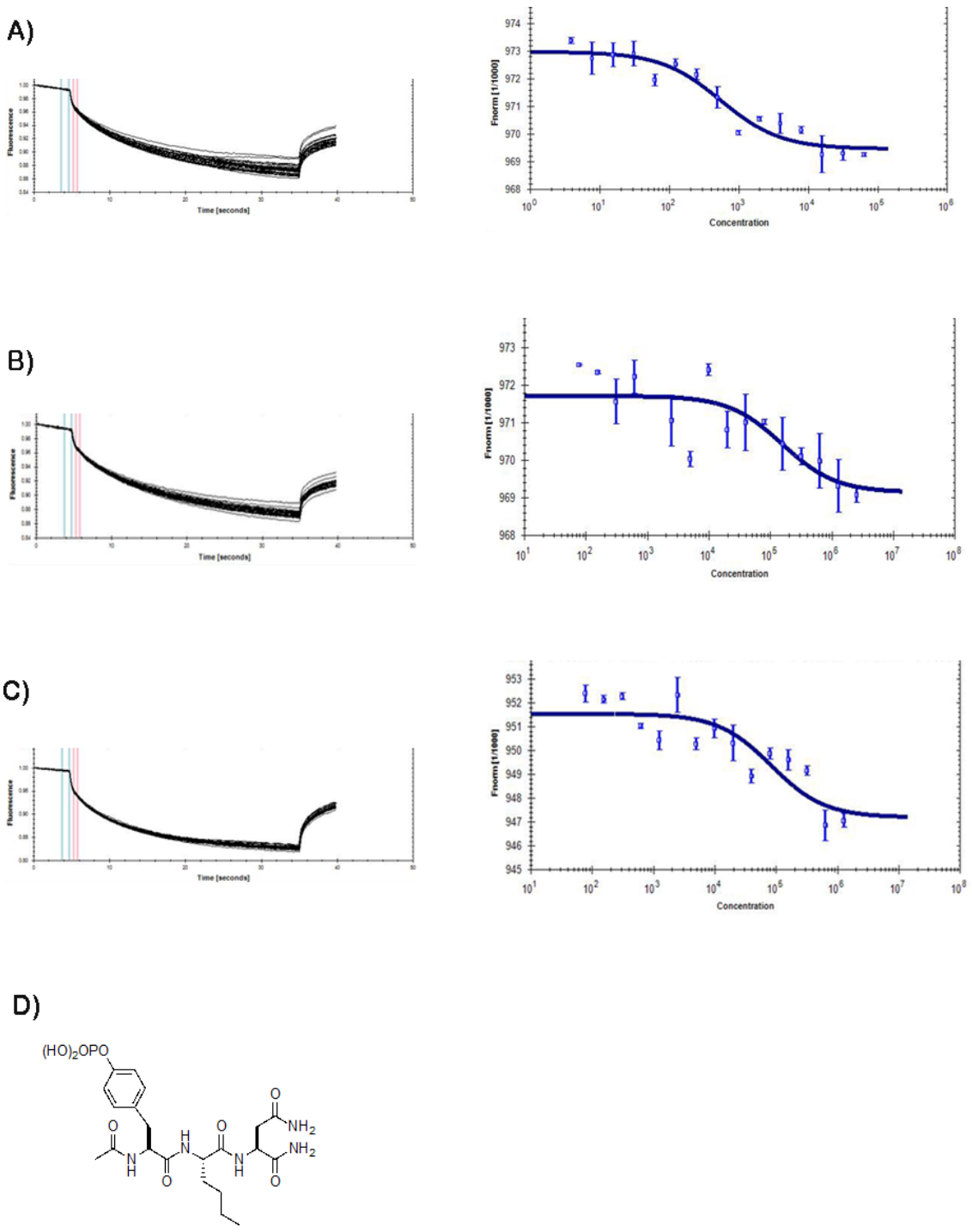

Figure 16. MST measurement of binding between ShcPTB to short peptides. 25nM of fluorescently-labeled ShcPTB was incubated with peptides in a 1:2 dilution series at 25°C. The movement of ShcPTB was monitored by fluorescence measured at 647nm. Left panels: normalized thermophoresis traces. Right panels: Data fitted to one site model.

Temperature jump measurements were made at 70% LED power and 20% IR power. (A) ShcPTB binds to TrkA peptide with K_D=535±74nM. Top concentration of TrkA peptide dilution series was 80μM. (B) ShcPTB binds to tyrosyl mimetic no. 18 with K_D=155±41μM. Top concentration of no. 18 dilution series was 1mM. (C) ShcPTB binds to short TrkA peptide with K_D=83±17μM. Top concentration of short TrkA peptide dilution series was 200μM. (D) Chemical structure of tyrosyl mimetic no. 18.

3.3 Discussion

Many elegant mechanisms for the roles of kinases [122], phosphatases [123] and scaffolding proteins [115,124] have been discovered in the regulation of kinase activity post-extracellular stimulation. However, significant basal kinase activity occurs in cells even in the absence of extracellular stimulation [125,126,127], for which requires control mechanisms to prevent aberrant cellular response. Here we report a novel mechanism in which Shc prevents aberrant signal transduction by Erk in cells prior to extracellular stimulation. We show that prior to growth factor stimulation, Shc and Erk interact directly in a non-canonical manner through the N-terminal lobe on Erk and the α2-β3 loop on the ShcPTB domain. These regions are independent of the previously reported binding-motifs on both proteins. By forming a complex with Shc, Erk phosphorylation level is downregulated and nuclear translocation is restricted. This is in contrast to the well-established role of Shc as an activator of the Erk cascade post-stimulation of growth factor in which through the recruitment of Grb-Sos complex.

This report adds to the growing list of other discoveries we have made in the regulation of background signaling. We previously identified a role for the adaptor protein

Grb2 in inhibiting FGFR2 signaling by forming a heterotetrameric complex with the receptor [127]. Furthermore, Timsah *et. al.* described a mechanism whereby Grb2 competes with Plc-gamma in the absence of extracellular stimulation to inhibit cell motility [125].

Since Shc contributes towards various aspects of ErbB2-driven breast cancer, we investigated if there is any evidence that the Shc-Erk interaction may play some part in disease progression. Based on our finding, we reasoned that if the inhibition of Erk by Shc was important in cancer, we might find 1) mutations on either of the protein at the binding interface and 2) downregulation of Shc expression through either gene disruption or micro-RNA action. However, having examined various public databases available, we did not observe any of the above. However, in line with our observation in mammalian cell lines, work in *Caenorhabditis elegans* shows that disrupting the *Shc1* gene leads to Erk/MPK-1 activation [120]. Alignment of the *C. elegans* and human Shc1 gene reveals that while the Erk-binding site is conserved, the two Grb2 binding sites are not [79]. Therefore, it is possible that we do not observe any downregulation of Shc expression in cancer because it is more advantageous for cancerous cells to upregulate the Shc-Grb2 axis than to disengage Erk from Shc. In fact, it has been shown that Shc sensitizes cells towards growth factor stimulation. This is particularly true in diseases that are driven by active tyrosine kinases, in which ShcPTB is likely to be recruited to phosphotyrosine motifs such that Shc-Erk would be dissociated 'permanently'. Thus, the Shc-Erk direct interaction is likely to be important *in vivo*, as highlighted by the finding in *C. elegans*, under certain circumstances.

Both Shc and Erk possess numerous known intracellular binding partners. The distinct domains of Shc provide docking sites for a diverse array of signaling molecules

[25,26]. Erk also has several consensus sites for docking substrates and scaffold proteins [128,129]. However, the ShcPTB-Erk binding site is independent of these reported sites. The closest reported site to the one we observe for the ShcPTB-Erk interaction, involves the scaffold protein Ste5 binding to a site on the N-terminal lobe of Fus3 MAPK from the yeast mating cascade [132]. However the corresponding site on the N-terminal lobe of Erk is obstructed by Erk's own N-terminus and hence preventing ligand binding. Furthermore, the kinase suppressor of Ras (KSR) protein which serves a similar function as Ste5 in mammals but evolved separately, does not contain a similar sequence as Shc (i.e. rich in positive charges) in the cysteine-rich 4 domain, where it interacts with Erk [133].

While the Erk-binding site is specific to ShcPTB, it is conserved among the Shc family members (Figure 17a). This suggests that this mode of Erk regulation is also mediated by ShcB, ShcC and ShcD. Since ShcB/C/D are expressed in tissue-specific manners, it would be interesting to see if and how the Shc-Erk interaction is involved in these tissues. Furthermore, while *ShcA* expression is not downregulated in cancers, ShcB/C/D genes are deleted in certain cancers. What the implications are for the Shc-Erk complex in these diseases require further investigation. Alignment of members of the MAPK family shows that the Shc-binding site is conserved, suggesting that other MAPKs may also directly interact with Shc. This would have important implication in signaling outcome as the various members of the MAPK family mediate different phenotypic responses (Figure 17b) [130,131].

The role of Shc as an adaptor protein in stimulated cells forming a docking platform for enzymes in signaling pathways is well established. The involvement of Shc in signal transduction in response to growth factor stimulation is contrasted by its function in the absence of cellular stimulation. One notable interaction in this context is the binding of Shc

to protein phosphatase 2A (PP2A) under basal conditions [41]. Similar to Erk, PP2A is released on stimulation by EGF or insulin-like growth factor 1 (IGF-1). Furthermore, the Shc-PP2 complex is believed to negatively regulate growth factor signaling by preventing phosphorylation of Shc and the subsequent recruitment of Grb2-Sos complex. While PP2A also associates with ShcPTB, dissociation of the two proteins require the presence of Y317. Thus, it seems unlikely that PP2A binds to ShcPTB in the same manner as Erk.

Erk has been shown to be anchored in the cytosol by proteins other than Shc. For example, the phosphoprotein protein enriched in astrocytes 15 (Pea-15) has been demonstrated to bind to Erk regardless of its phosphorylation state and depletion of Pea-15 show leads to increased levels of Erk in the nucleus [115]. The similar expression to FGF (Sef) protein also regulates Erk cellular localization. This is achieved by Sef binding to activated forms of Mek and preventing the dissociation of Erk from the Mek-Erk complex [134]. Again knock down of Sef results in nuclear accumulation of Erk in stimulated cells. However, although Pea-15 and Sef exert control of spatial distribution of Erk (the latter in stimulated cells only), neither are involved in induction of MAPK signaling as in the case of Shc.

Finally, we attempted to identify small molecules that can inhibit Shc-RTK binding in order to sequester Erk activity. Such compounds could be useful in diseases driven by Erk activity with an overexpression of Shc. Taking short-listed 'hits' from *in silico* and DSF screens, we identified two chemicals that can bind to ShcPTB. However, the affinities of these two chemicals for ShcPTB are too weak to compete with RTK-binding. Therefore, further chemical modifications are required.

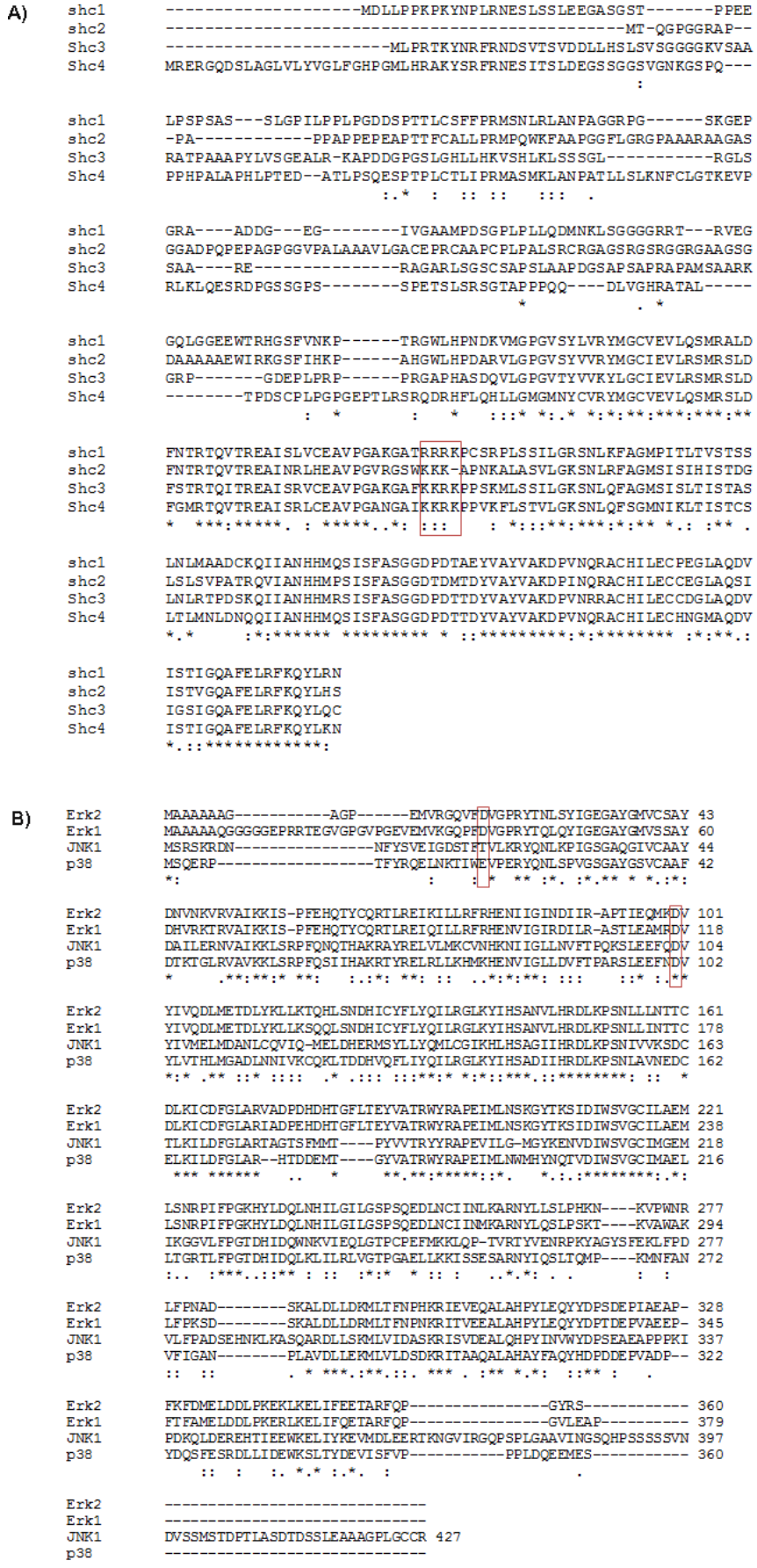

Figure 17. Sequence alignment of (A) PTB domain of Shc family members and (B) MAPK family members. Sequence alignment was performed by ClustalW2.

Chapter 4

Shc phosphorylation mediates crosstalk between MAPK and AKT pathways through protein recruitment

4.1 Introduction

Posttranslational modifications are important in signal transduction due to their inducibility and reversibility which enables the signaling cascades to be regulated in a context dependent and transient manner as discussed in Chapter 1. Specialized protein domains recognize most PTMs, conferring specificity when relaying intracellular signals [10,135,136,137]. Of the numerous PTMs identified to date, phosphorylation remains to be the best characterized modification in RTK signaling [138]. At the physiological pH, the attachment of a phosphate group adds a double-negative charge to the modified amino acid. This relatively dramatic change in the polypeptide enables it to regulate protein function by altering protein conformation and protein-protein interactions [17].

Upon ligand binding to RTKs, intracellular signal transduction is initiated by the autophosphorylation of the receptors on tyrosine residues. These phosphorylated tyrosines, together with their flanking amino acids, then recruit downstream tyrosine-binding proteins which lead to the activation of downstream signaling cascades. One of the downstream effectors of RTK signaling is the proline-directed serine/threonine kinase Erk. While activated Erk phosphorylates various downstream effectors as discussed in Section 3.1, it also phosphorylates scaffolding proteins involved in early signaling as feedback mechanisms (Figure 1). For example, the scaffolds Grb2-associated binding protein (Gab1) [139,140,141,142], fibroblast growth factor substrate 2 alpha (Frs2α) [143,144] and insulin receptor substrate 1 (IRS1) [104,145], which are tyrosine

phosphorylated by the receptors upon growth factor stimulation as part of early signal transduction, are also Erk substrates. It has been shown that serine/threonine and tyrosine phosphorylation are inversely correlated events, suggesting a negative feedback mechanism whereby phosphorylation on serine/threonine residues of Gab1 and Frs2α leads to a reduced level of tyrosine phosphorylation. Since tyrosine phosphorylation is the event that is required to initiate downstream signaling, reduction in signaling through this phosphorylation results in negative feedback mechanism for pathway control. [142,143]. Interestingly, a positive feedback role for serine/threonine phosphorylation on scaffold proteins has also been shown. For example, Erk phosphorylation of Gab leads to an enhancement of p85 subunit recruitment to Gab and increases PI3K and Erk signaling, indicating a positive feedback mechanism. While the molecular details for how these phosphorylation events mediate feedback in signaling requires further characterization, it was noted that one of the phosphothreonine sites on Gab are in close proximity to the phosphotyrosine site responsible for p85 recruitment and increases Gab and p85 binding. Since p85 has not been shown to bind to phosphoserine/threonine motifs, this suggests that these phosphothreonine events on Gab induces local conformational changes that enable Gab to recruit p85 more efficiently [146]. Hence, RTK signaling is initiated by tyrosine kinases but terminated or amplified by serine/threonine kinases, such as Erk. This raises the possibility that by juxtaposing tyrosine and serine/threonine residues on the same scaffold protein, scaffold proteins can fine-tune RTK signal transduction through altering protein-protein interactions.

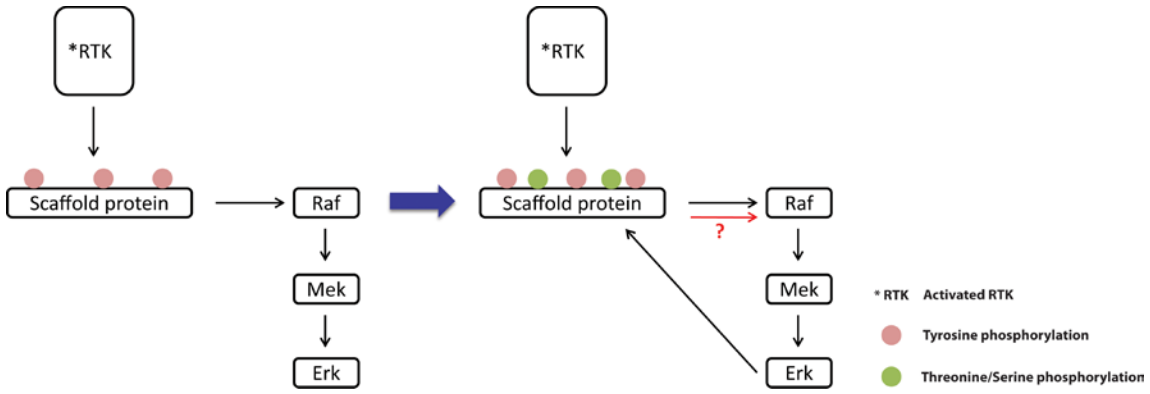

Figure 1. Erk phosphorylates scaffold proteins to fine-tune RTK signaling. Activated receptor tyrosine phosphorylates scaffold proteins to activate downstream effectors, such as the Erk cascade. Activated Erk then phosphorylates scaffold proteins on their threonine/serine residues. The threonine/serine-phosphorylated scaffold proteins subsequently down- or up-regulate the activity of the Erk cascade as feedback mechanisms, possibly through protein recruitment.

Several novel phosphorylation and a neddylation sites have been identified recently. The timing of phosphorylation on S29, T214 and S335 suggests that these events are mediated by downstream effectors, such as AKT for S29. An increase in cell proliferation when Shc -/- MEFs were reconstituted with the triple phospho-deficient mutant ($^{S29/T214/S335A}$Shc) indicates a negative feedback loop is mediated by these sites [26]. Lys3 on Shc has been identified as a site which is neddylated by NEDD8 in T-cell signaling [147].

Having established that Shc and Erk interact directly prior to growth factor stimulation in Chapter 3, we describe the identification of three Erk-mediated phosphothreonine sites on Shc both *in vitro* and in breast cancer cell lines post-EGF stimulation. We show that phosphorylation on these residues leads to elevated Erk and

Akt phosphorylation post-EGF stimulation. To investigate how these effects are mediated we examined whether phosphorylation induces changes in Shc conformation and protein recruitment. We identified a number of proteins whose association with Shc is phosphothreonine-dependent.

4.2 Results

4.2.1 Shc is an Erk substrate

Erk mediates numerous biological functions as a threonine/serine kinase [103,104]. Moreover, other scaffolding proteins have been identified as Erk substrates [140,143,145]. Having discovered a direct interaction between Shc and Erk, we investigated whether Shc is also a substrate for Erk. This would have important implications in feedback mechanisms whereby Erk regulates the functions of Shc in downstream signaling. Three threonine residues on Shc are contained within the Erk consensus substrate sequence (S/T-P). To test if Shc is an Erk substrate, we incubated purified Shc with active Erk2 in the presence of ATP and $MgCl_2$. The phosphorylation state of the putative Erk substrate sites on Shc was then analyzed by immunoblotting using an antibody specific for phosphorylated threonine followed by a proline (Figure 2A).

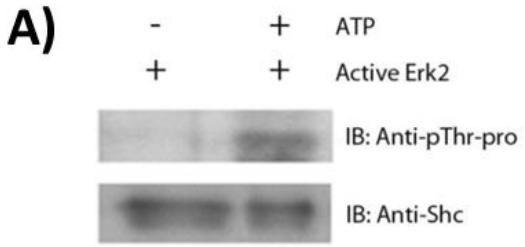

Figure 2. Phosphorylation of Shc on Erk substrate motifs (TP) (A) 10μM of 50μl purified Shc protein was incubated with 1μl of active Erk2 in the presence or absence of ATP and $MgCl_2$ overnight. Phosphorylation of T-P motifs on Shc was analyzed by western blotting using an antibody specific to pTP motifs.

Since the anti-Thr-Pro antibody can be detecting any one of the three phosphorylation sites on Shc, we wanted to confirm whether all three sites on Shc are accessible for Erk phosphorylation. Therefore, Erk-phosphorylated Shc was analyzed by mass spectrometry and all three T-P motifs were found to be phosphorylated (Figure 2B-D). This confirms the recent observation of T214 as an Erk substrate site [26], whereas phosphorylation of threonines 276 and 407 on p52Shc has not been previously reported. T214 and T276 are found in the CH1 domain, whilst T407 is in the SH2 domain (Figure 3).

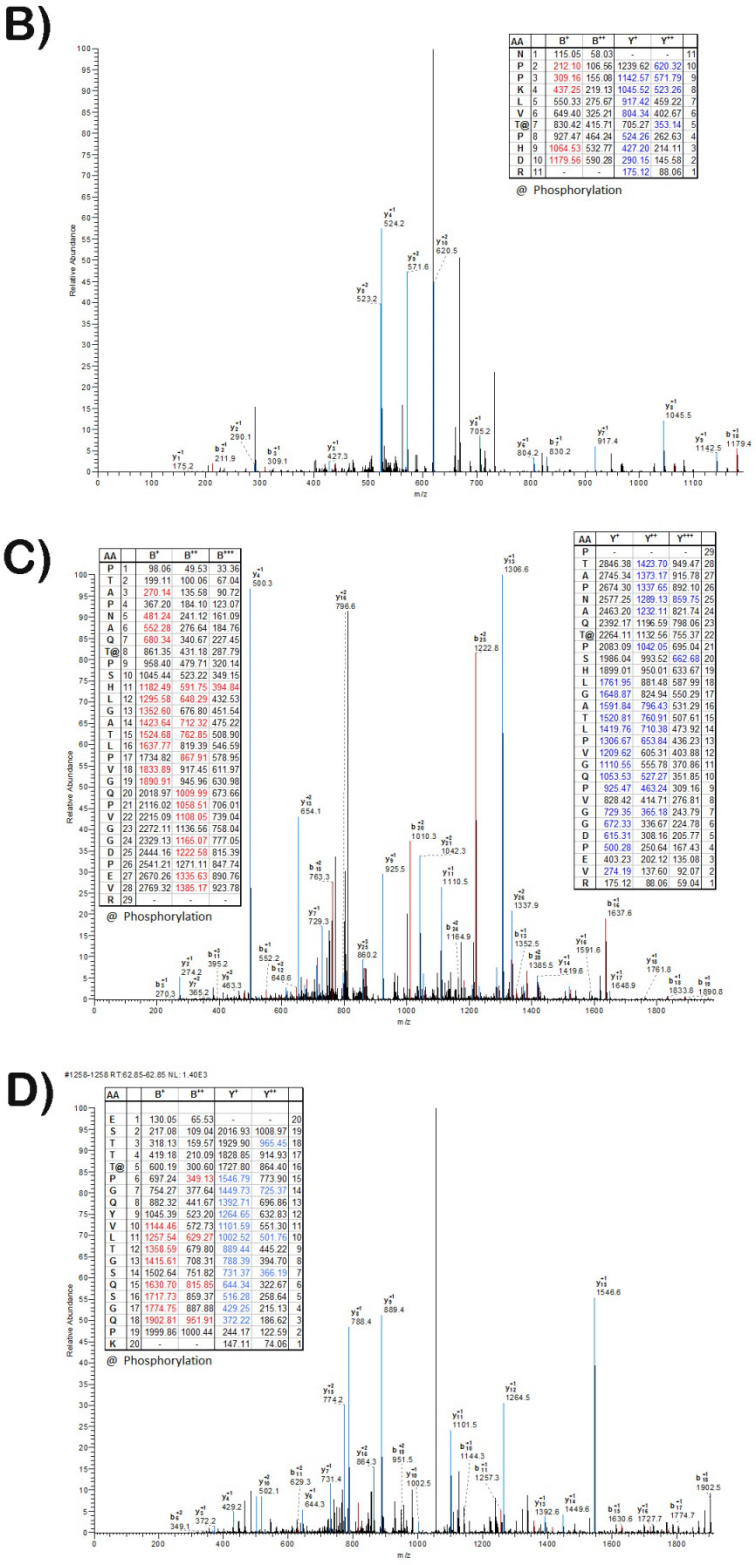

Figure 2. Mass Spectrometry analysis of phosphorylation status of Shc TP motifs.

50µl of purified Shc at 100µM and incubated with 10µl of active Erk2 in the presence of

$MgCl_2$ and ATP for 16h at 20 °C. The mass spectrum for (B) T214 (C) T276 and (D) T417. Mass spectrometry measurements and analysis were performed by the MDACC core.

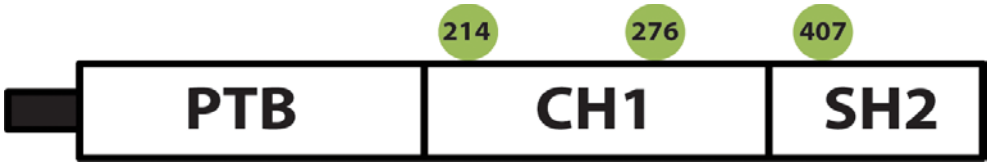

Figure 3. Location of the threonine residues on Shc phosphorylated by Erk. Three threonine residues on Shc are phosphorylated by Erk: T214 and T276 are in the CH1 domain; T407 is in the SH2 domain.

4.2.2 Shc threonine phosphorylation upregulates Erk and Akt phosphorylation

To investigate the importance of threonine phosphorylation in Shc function in the cellular environment, we mutated all three threonine residues either to alanines (^{TA}Shc phospho-deficient mutant) or glutamic acids (^{TE}Shc phospho-mimic mutant) and stably overexpressed these constructs in HEK293T cells. We first assayed Erk phosphorylation in response to EGF stimulation, to test the hypothesis that Erk and Shc function in a feedback loop post-growth factor stimulation, as has been reported for other scaffold proteins including Gab and Frs2. We found that overexpressing ^{TE}Shc in HEK293T cells leads to higher Erk phosphorylation upon either a 2 min or a longer 15 min EGF stimulation when compared with ^{WT}Shc and ^{TA}Shc overexpressing cells (Figure 3, top panels). This indicates that the phosphorylation of these three threonine sites on Shc amplifies the level of Erk phosphorylation post-EGF stimulation.

Next, we examined the level of Akt phosphorylation because Shc is also involved in PI3K signaling (see Section 1.4.2). We observed an increase in Akt phosphorylation from 2

minutes up until 30 minutes post-EGF stimulation in cells overexpressing ^{TE}Shc compared with cells overexpressing ^{WT}Shc and ^{TA}Shc (Figure 4, middle panels). This suggests that post-EGF stimulation, threonine-phosphorylated Shc amplifies the phosphorylation level of Akt. It also suggests that a cross-talk mechanism exists between the Erk and Akt signaling whereby Erk-mediated phosphorylation of Shc upregulates Akt activity. This is an unexpected result as expressing the T214A phospho-deficient Shc mutant led to a moderate increase in cell numbers when compared with wild-type Shc in Zheng *et. al.* [26], which would be indicative of a downregulation of downstream signaling when Shc is threonine phosphorylated. This difference in our data could be due to a number of factors. First, among the three sites in the present study, Zheng *et al.* only investigated the role of T214, whereas here all three sites were simultaneously mutated. Hence, the differences in the effects of Shc threonine phosphorylation could be due to a cooperative effect of phosphorylation on all three threonine sites on Shc. Second, HEK293T cells were used in this study, whereas Zheng *et. al.* used MCF10A cells. Different cell lines are likely to respond to Shc threonine phosphorylation in distinct manner through a number of mechanisms. For example, the interacting partner of threonine phosphorylated Shc that is responsible for the upregulation in downstream signaling may not be overexpressed in the MCF10A cells (see below) Third, since Shc is a scaffold protein, the amount of Shc overexpressed would also affect signaling outcome due to a titration effect of protein binding partners [24] resulting in a different outcome in our study from that of Zheng *et. al*.

Another observation is that overexpressing ^{WT}Shc downregulated Akt and Erk phosphorylation (compare HEK293T control and ^{WT}Shc cells (Figure 4). This could be due to the mechanism described in Chapter 3, or that multi-protein complexes are not formed because of the high concentration of Shc titrates proteins into separate complexes.

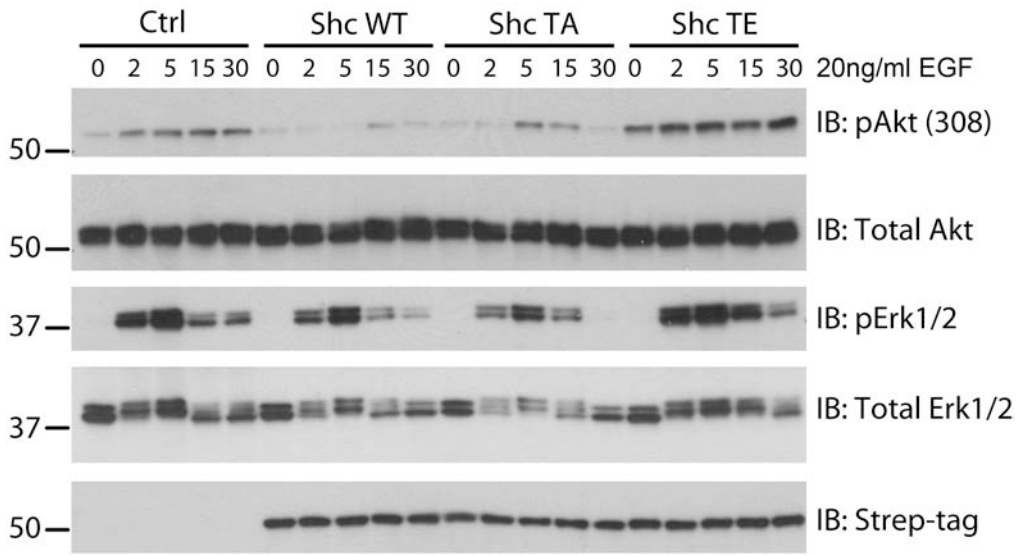

Figure 4. Shc threonine phospho-mimic mutant leads to elevated pAkt and pErk levels. HEK293T cells stably overexpressing either empty vector, strep-tagged ^{WT}Shc, ^{TA}Shc or ^{TE}Shc were starved overnight and then stimulated with 20ng/ml EGF for the indicated time periods. 25μg of total cell lysates were analyzed by western blotting for the phosphorylation states of Akt T308 (upper panels) and Erk (middle panels). Equal expression of the Shc constructs were confirmed by blotting for strep-tag (bottom panel).

4.2.3 Shc threonine phosphorylation level in non-transformed and transformed cell lines

Both Erk and Akt signaling play important roles in tumorigenesis [102,148]. We hypothesize that Shc is threonine phosphorylated endogenously in cancer cells because Erk and Akt are more phosphorylated in the presence of the Shc phospho-mimetic mutant (^{TE}Shc) compared with ^{WT}Shc and ^{TA}Shc in HEK293T cells. To test this hypothesis, we generated a specific antibody against the pT214 motif (Figure 5).

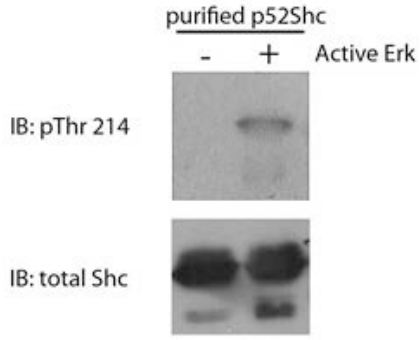

Figure 5. Specificity test for anti-pT214 antibody. Purified recombinant Shc was phosphorylated by active Erk2 as in Figure 1. A western blot signal is only present when Shc was phosphorylated by Erk2. This confirms that the anti-pT214 antibody is specific for phosphorylated Shc.

We first screened for the presence of phosphorylation on T214 in a number of transformed/cancer cell lines, with a particular interest in breast cancer cell lines due to the critical role of Shc in this disease as discussed in Chapter 1 [149]. The non-transformed mammary epithelial cell line MCF10A was used for comparison. Cells were stimulated with EGF for between 2 to 30 minutes to investigate the temporal pattern of Shc threonine phosphorylation. Cells were also pre-incubated with the Mek inhibitor U0126 to abolish Erk activity, in order to confirm that the phosphorylation event is

mediated by Erk. Since the antibody is not sensitive enough to detect the endogenous level of pT214 (data not shown), we first immunoprecipitated total Shc and then probed for pT214. To our surprise, even though all cell lines exhibited Erk activity upon EGF stimulation, only the triple negative cell lines MDA-MB-468 and MDA-MB-231 exhibited a significant level of phosphorylation on T214 (Figure 6). Two of the known binding partners for Shc in EGF signaling, EGF receptor and Grb2, were probed for to confirm that the immunoprecipitation experiments were successful. It is interesting to note that even though Shc does not pull-down a significant amount of EGF receptor in some cell lines, it is still tyrosine phosphorylated and hence was able to recruit Grb2. This could be because Shc can be phosphorylated by cytosolic kinases such as Src, which is also activated by EGF-stimulation [48,63,150]. It has been reported that serine/threonine phosphorylation affects tyrosine phosphorylation in scaffold proteins, so we examined the phosphorylation levels on the three known Shc tyrosine sites, 239, 240 and 317. If Shc threonine phosphorylation affects its tyrosine phosphorylation level, we should observe a difference in Shc tyrosine phosphorylation when the cells are treated with the Mek inhibitor. However, we observed variable differences in phosphotyrosine levels when cells were treated with the Mek inhibitor U0126, independent of pT214 level. For example, we observed phosphorylation on T214 in both MDA-MB-468 and MDA-MB-231 cells. When Shc threonine phosphorylation is indirectly abolished by the inhibition of Erk, a decrease in the level of pY239/240 was detected in MDA-MB-468 cells and not in MDA-MB-231 cells. The reverse is true for pY317 level in these two cell lines where pY317 level is reduced in MDA-MB-231 upon treatment with U0126, while pY317 level is unaffected in MDA-MB-468 cells. Also, in other cell lines such as MCF10A and MCF7, while there is no significant phosphorylation on T214, the level of pY317 is affected when cells were treated

with the Mek inhibitor suggesting that pY317 level in these two cell lines are not affected by the phosphorylation of T214 on Shc.

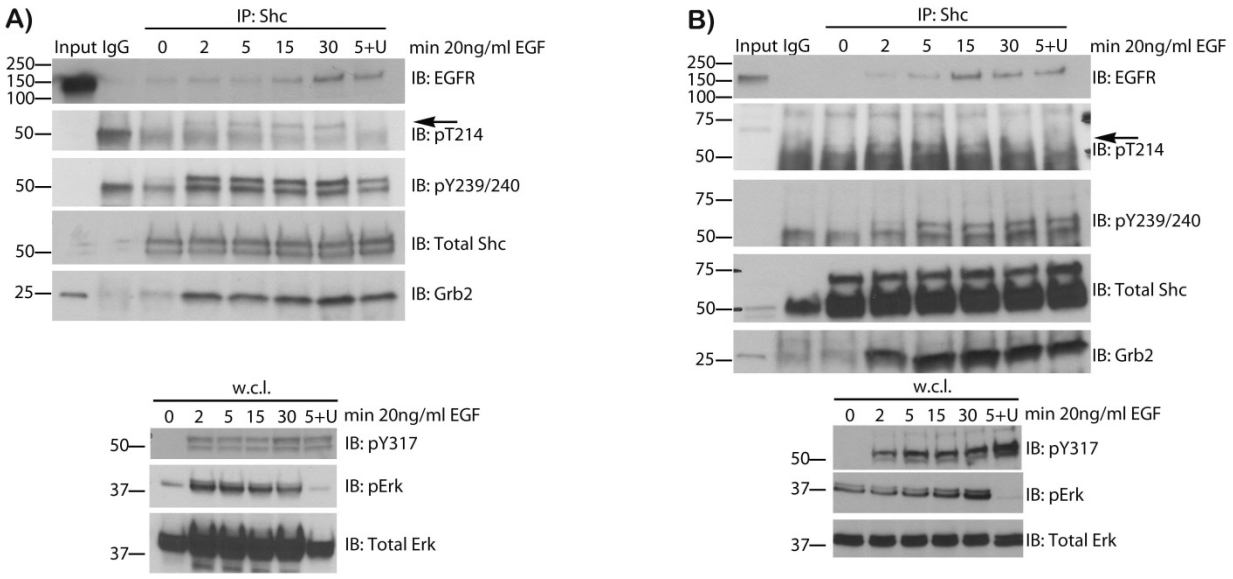

Figure 6. Phosphorylation of T214 in endogenous Shc in mammalian cell lines. Cell lines (A)MDA-MB-468 (B)MDA-MB-231 were starved overnight and then stimulated with 20ng/ml EGF for the indicated time periods. The Mek inhibitor U0126 was applied at 10μM for 45 minutes prior to EGF stimulation in '5+U' samples. Shc was immunoprecipitated from 1mg of lysates. Immunoprecipitants (IP) were probed for pT214 and pY239/240 levels of Shc, the presence of EGFR and Grb2. Whole cell lysates (w.c.l.) of the same samples were also analyzed for pErk level and pY317 of Shc.

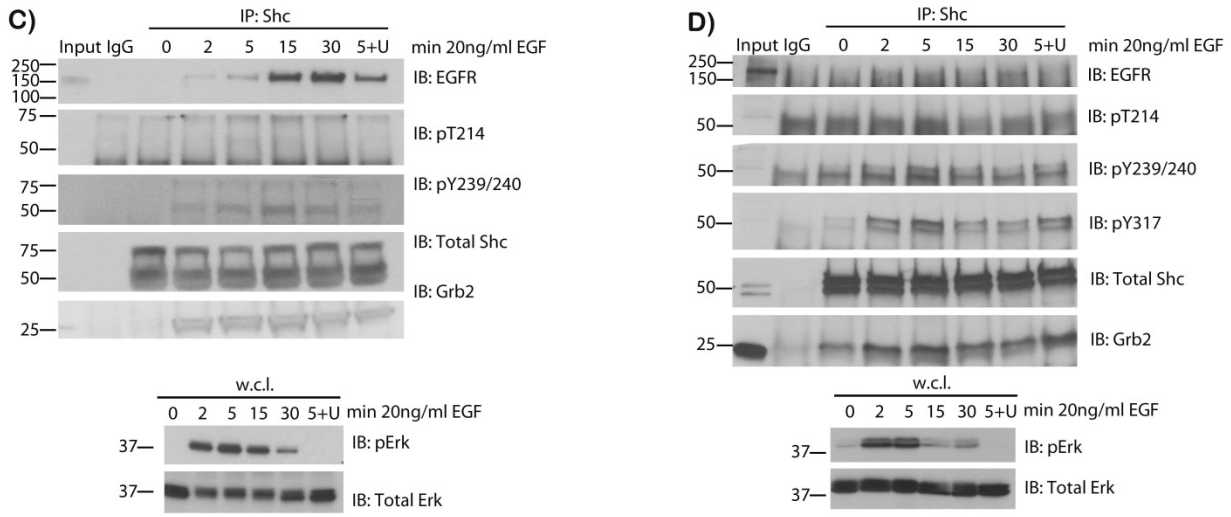

Figure 6. Phosphorylation of T214 in endogenous Shc in mammalian cell lines. Cell lines (C)MCF10A (D)MDA-MB-361 were starved overnight and then stimulated with 20ng/ml EGF for the indicated time periods. The Mek inhibitor U0126 was applied at 10μM for 45 minutes prior to EGF stimulation in '5+U' samples. Shc was immunoprecipitated from 1mg of lysates. Immunoprecipitants (IP) were probed for pT214 and pY239/240 levels of Shc, the presence of EGFR and Grb2. Whole cell lysates (w.c.l.) of the same samples were also analyzed for pErk level and pY317 of Shc.

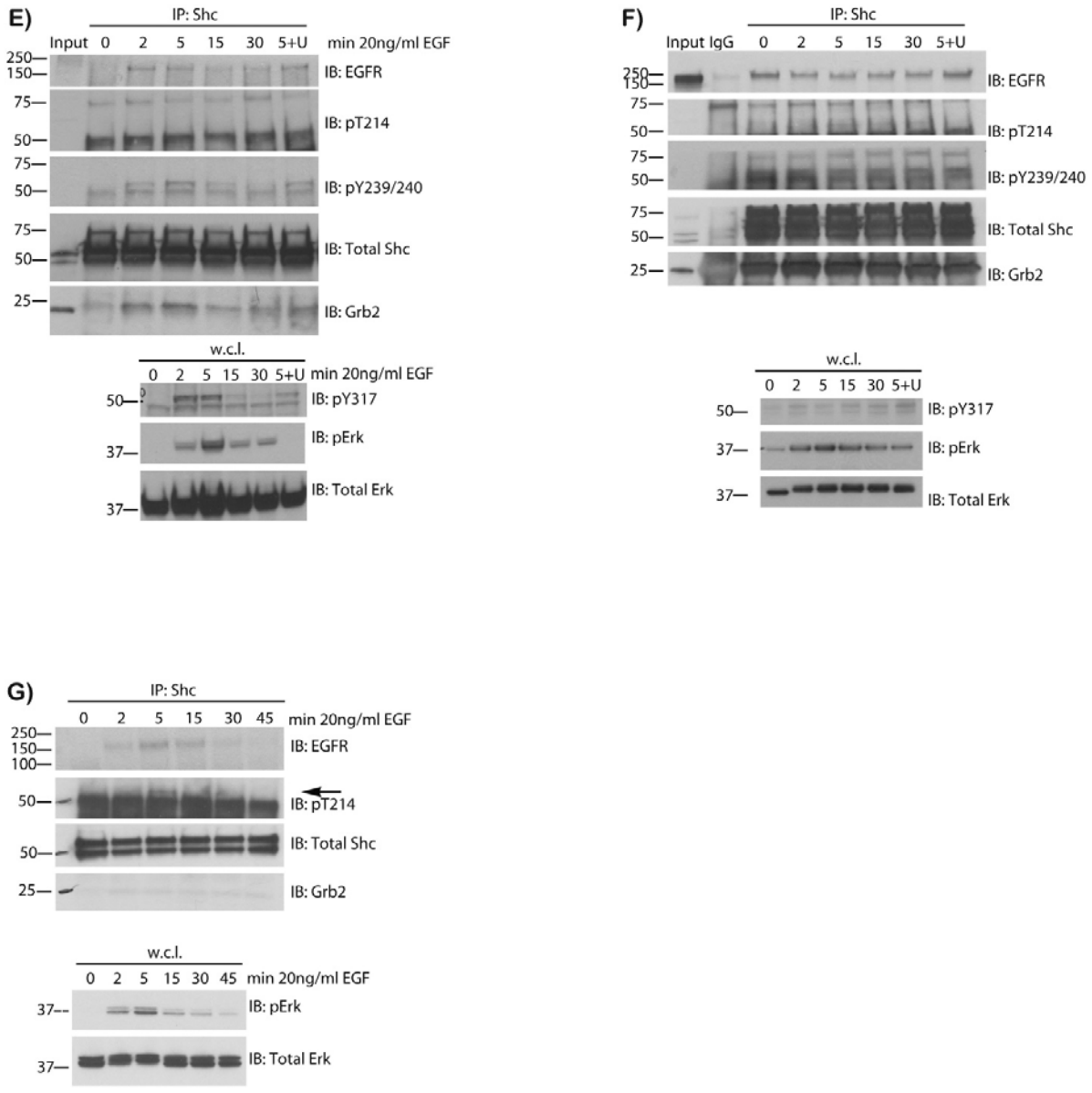

Figure 6. Phosphorylation of T214 in endogenous Shc in mammalian cell lines. Cell lines (E)MCF7 (F) A431 (G)HEK293T were starved overnight and then stimulated with 20ng/ml EGF for the indicated time periods. The Mek inhibitor U0126 was applied at 10μM for 45 minutes prior to EGF stimulation in '5+U' samples. Shc was immunoprecipitated from 1mg of lysates. Immunoprecipitants (IP) were probed for

pT214 and pY239/240 levels of Shc, the presence of EGFR and Grb2. Whole cell lysates (w.c.l.) of the same samples were also analyzed for pErk level and pY317 of Shc.

In addition to analysis of pAkt and pErk, we also observed that the level of pY239/240 or pY317 does not result in a reduction in Grb2 recruitment. This is probably because the pY239/240 or pY317 level is not completely abolished by Erk inhibition. If so, it would suggest that a certain degree of variance in signal transduction can be tolerated by the system. Therefore, we cannot conclude whether threonine phosphorylation is sufficient to impact tyrosine phosphosphorylation as has been shown in other scaffolding proteins. Another observation is that in certain cell lines, Shc-EGFR interaction is increased when the Mek inhibitor is applied. Although it occurs in cell lines with, or without Shc T214 phosphorylation, we tested the binding of the TrkA peptide and Shc phosphorylation mutants to confirm that modifications on T276 and T407 do not alter phosphotyrosine binding of ShcPTB, the domain responsible for EGFR binding. ITC experiments show that, as expected, there is no difference in the phosphotyrosine binding ability of ShcPTB within the context of full length ^{WT}Shc or ^{TE}Shc (Figure 7). Hence, the increased binding between Shc and EGFR upon Erk inhibition is not due to a direct effect of Shc threonine phosphorylation on Shc-EGFR interaction. EGFR has been reported to be phosphorylated on T669 by Erk [151] and that phosphorylated T669 mediates internalization of EGFR [152]. It is therefore possible that abrogating Erk activity by the use of Mek inhibitor in turn inhibits EGFR T669 phosphorylation and thus receptor internalization. This might then lead to the retention of EGFR on plasma membrane and Shc-EGFR association.

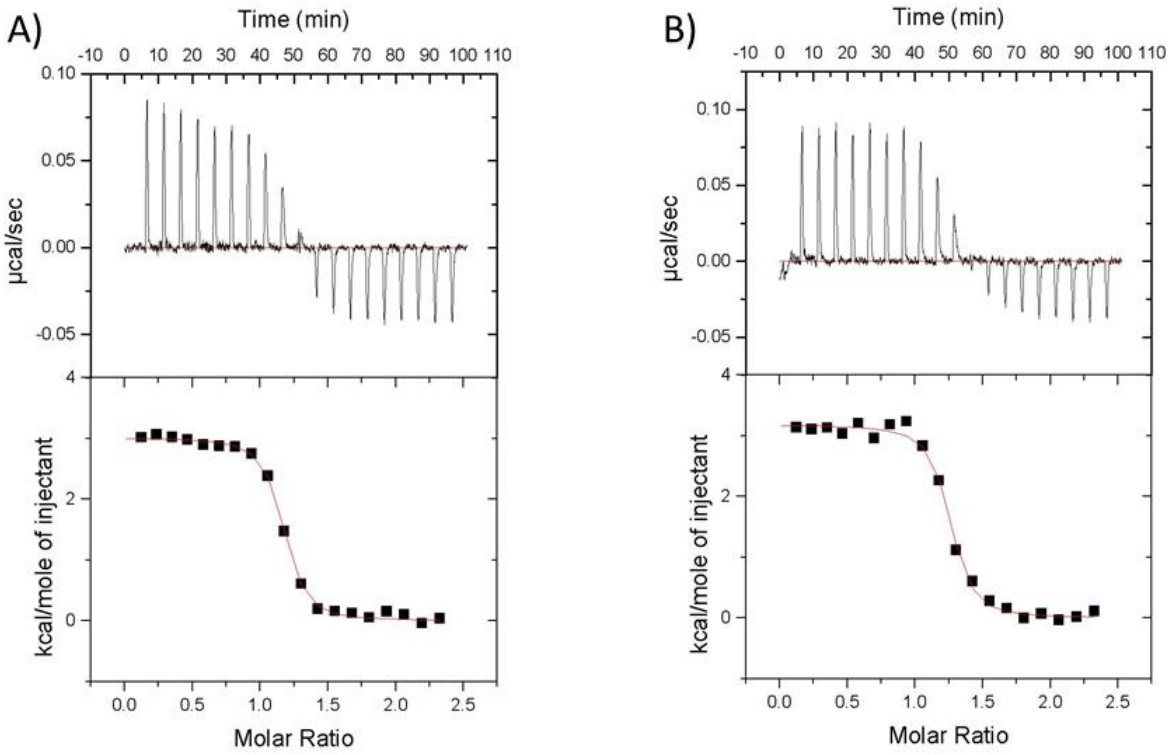

Figure 7. ITC measurement of the ^{WT}ShcFL and ^{TE}ShcFL. Twenty 10µl injections of TrkA peptide (100µM) were titrated into ShcFL (10µM) at 13ºC. Top panel: baseline-corrected power versus time plot for the titration. Bottom panel: the integrated heats and the molar ratio of TrkA binding to ShcFL. The data were corrected for the heats of dilution of TrkA and fit to a one-site binding model. (A) ^{WT}ShcFL (B) ^{TE}ShcFL. Titrations were fitted into a one-site model. K_D for ^{WT}Shc and ^{TE}Shc are 53nM±435nM and 38nM±427nM, respectively.

To confirm that Shc is threonine phosphorylated in MDA-MB-468 cells, we immunoprecipitated Shc using the pT214 antibody and then probed for Shc (Figure 8). MCF10A cells were used as comparison. In agreement with the previous immunoprecipitation experiments, Shc is phosphorylated on T214 only in MDA-MB-468 and MDA-MB-231 cells and not significantly in MCF10A, nor MCF7 cells. Furthermore, the

phosphorylation of T214 is sustained throughout the time-points tested which corresponds to the sustained activation of Erk1/2. This supports the finding that when Shc is overexpressed in Rat-1 cells, Shc pT214 and pErk levels temporally coincide [26].

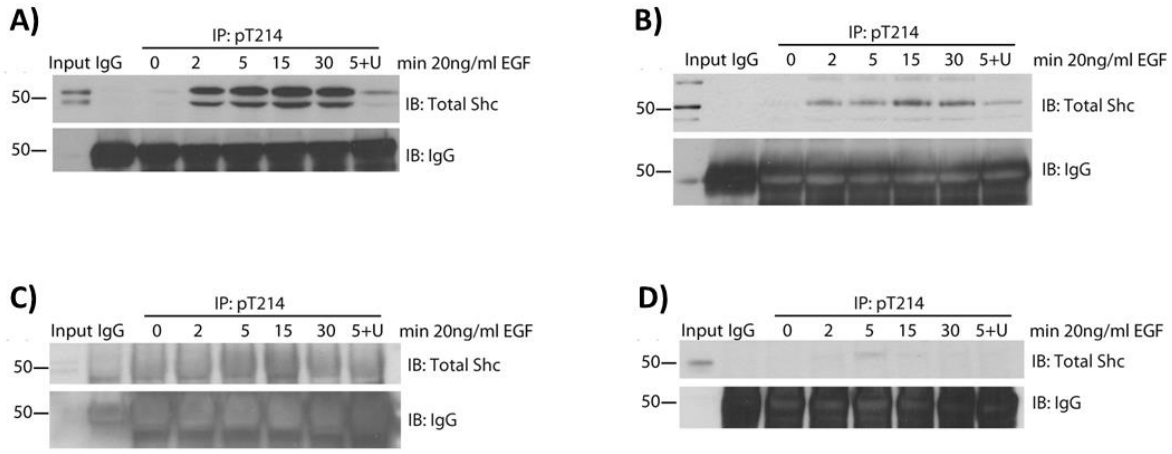

Figure 8. Phosphorylation of T214 in endogenous Shc in mammalian cell lines. Cells were starved overnight and then stimulated with 20ng/ml EGF for the indicated time periods. The Mek inhibitor U0126 was applied at 10μM for 45 minutes prior to EGF stimulation in '5+U' samples. Anti-pT214 antibody was used to immunoprecipitate Shc from 1mg of lysates. Immunoprecipitants (IP) were probed total Shc. (A) MDA-MB-468 (B) MDA-MB-231 (C) MCF10A (D) MCF7

4.2.4 Shc threonine phosphorylation does not induce significant conformational change

We previously reported a gating mechanism driven by tyrosine phosphorylation on Shc, whereby the SH2 domain is only available for ligand-binding when the CH1 domain is phosphorylated on its tyrosine residues [118]. It has also been proposed that phosphorylation on Y317 introduces rigidity to the protein and limits the dynamic motions of the PTB and SH2 domains in molecular dynamics simulations studies [153,154]. While these studies differ in their conclusions on whether phosphorylation leads to an activating or inhibiting conformation in Shc, they agree on the existence of regulation mechanisms imposed by inter-domain interactions. We therefore explored the possibility that threonine phosphorylation induces a conformational change in Shc that might contribute towards the upregulation of Erk and Akt signaling.

Circular dichroism (CD) measures the differential absorption of circularly polarized light by chiral molecules. Chirality can be generated when molecules are placed in an asymmetric environment, as in the case of protein secondary structures. Secondary structures, such as α-helices and β-strands, as well as disordered segments give rise to certain CD signatures [100,101]. The structural model of the full length Shc protein suggests that T214 and T276 reside on helices (PDB 1WCP) [154]. We therefore employed CD to investigate the effect of threonine phosphorylation on the secondary structures of Shc. We compared the CD signals from the full length unphosphorylated, threonine-phosphorylated and ^{TE}Shc. As expected, the CD signal of the full length Shc protein contains a mixture of α-helical, β-strand and disorder signals (Table 1). However, we failed to observe any significant changes in the secondary structures using this technique as shown by the overlapping signals from the various Shc proteins (Figure 9).

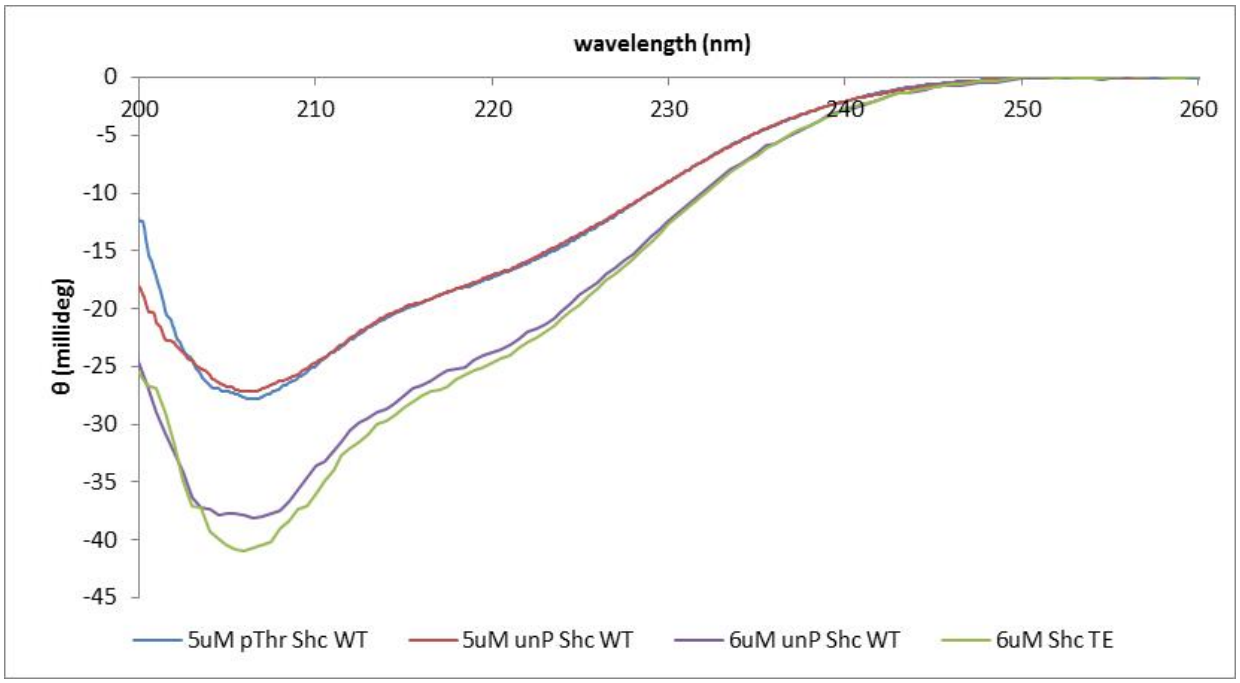

Figure 9. CD spectral analysis of ShcFL proteins. The average of three scans at 0.5nm intervals for each sample is plotted. Experiments were carried out at room temperature in PBS. Blue: 5μM threonine phosphorylated Shc; Red: 5μM unphosphorylated Shc; Purple: 6μM unphosphorylated ^{WT}Shc; Green: 6μM ^{TE}Shc. Data was subtracted from the buffer signal and plotted on Excel.

ShcFL	Helix	Strand	Turns	Unordered
Unphosporylated	0.345	0.117	0.238	0.317
T-phosphorylated	0.365	0.133	0.274	0.338

Table 1. Composition of Shc proteins secondary structures derived from CD spectra. Analysis of the CD signals from ShcFL proteins was analyzed by the CDSSTR software [155]. ShcFL proteins are composed of α-helices, β-strand, turns and disordered regions. Both ^{WT}Shc and ^{TE}Shc have similar compositions.

Shc contains nine cysteine residues with seven in the ShcPTB and one in each of the CH1 and SH2 domains. To test if there is a change in the overall conformation of Shc such that the accessibility of cysteine residues to solvent is altered, we incubated either ^{WT}Shc or ^{TE}Shc with 5,5'-Dithio-bis-(2-nitrobenzoic acid) (Ellman's reagent; DTNB) [156]. DTNB is reduced by free sulfhydryl groups, such as the SH-group from cysteine, and the reduced product TNB absorbs at 412nm. Both the wild-type and mutant proteins reacted with DTNB to the same extent (Table 2). Since two of the phosphothreonine residues are in ShcCH1, it is possible the conformational changes were not detected because most of the cysteine residues are located in the PTB domain. We generated a cysteine-null mutant of Shc and a series of single cysteine constructs. We individually mutated Ser225 and Ser344 into cysteine residues, as well as mutated in Cys316. However, all of the constructs were expressed in inclusion bodies. Attempts at refolding the proteins were unsuccessful (data not shown). This is probably because Shc consists of three domains and each requires different refolding dynamic [157].

Shc	normalized abs 412
WT	0.338
TE	0.336

Table 2. DTNB assay of ShcFL proteins. 5μM of ^{WT}Shc and ^{TE}Shc were incubated with 80μg /mL of DTNB reagent. Absorbance was measured at 412nm.

Next, we investigated if the thermostability of Shc is affected by threonine phosphorylation, which could also serve as an indication of conformational changes in protein. To monitor protein stability, we turned to the technique DSF [158]. Either ^{WT}Shc

or ^{TE}Shc was heated up in the presence of Sypro Orange, a dye that fluoresces when bound to hydrophobic surfaces which are exposed as the protein is melted. Again, no difference in the stability of the ^{WT}Shc and ^{TE}Shc proteins was detected as reflected by the lack of Tm shift between the melt-profile of the two proteins (Figure 10).

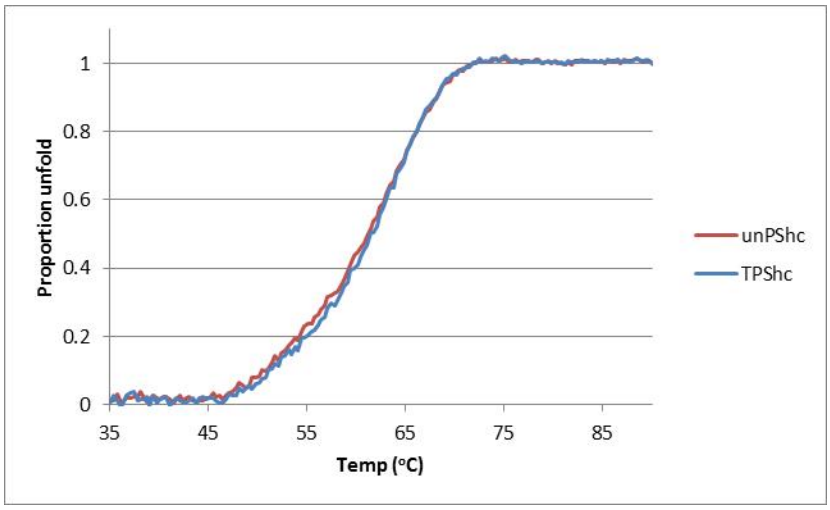

Figure 10. DSF analysis of the thermostability of ShcFL proteins. 5μM of ^{WT}ShcFL and ^{TE}ShcFL in PBS were incubated with 1x Sypro orange dye and heated from room temperature to 95°C. Unfolding of proteins was monitored by increase in fluorescence and is plotted as proportion unfolded. Red: 5μM ^{WT}ShcFL; Blue: 5μM ^{TE}ShcFL

Finally, we compared the pattern of chymotrypsin digestion of the Shc proteins as conformational changes may affect its accessibility to protease digestion [159]. Chymotrypsin is predicted to cleave the CH1 domain at regular intervals. ^{WT}Shc and ^{TE}Shc were incubated with the protease for various time periods and the digestion patterns were analyzed by SDS-PAGE. We failed to detect any major differences in the digestion pattern

of the two proteins (Figure 11).

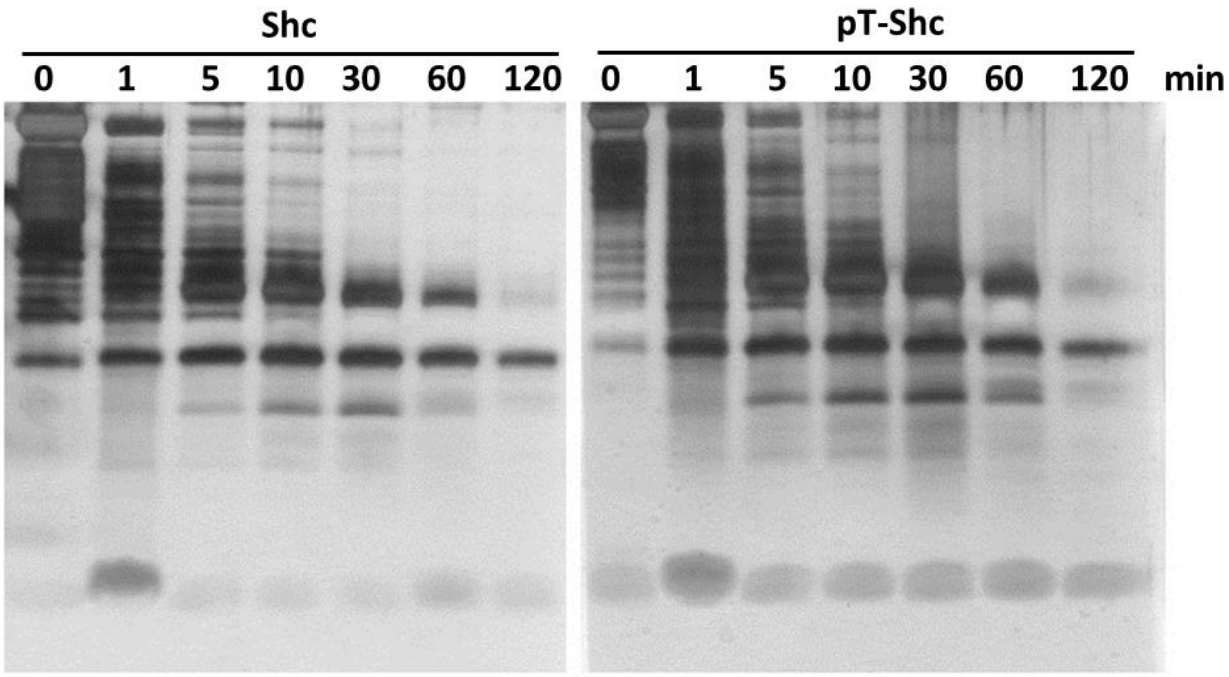

Figure 11. Limited proteolysis analysis of ShcFL proteins. 100ng of ^{WT}Shc or ^{TE}Shc was incubated with 1ng of chymotrypsin at 37^{o}C for various periods of time as indicated. Samples were analyzed by SDS-PAGE, followed by silver staining.

4.2.5 Protein recruitment dependent on threonine phosphorylation of Shc

We tested the hypothesis that Erk-mediated phosphorylation regulates protein recruitment on Shc by creating phosphothreonine-motifs. A large array of proteins bind to phosphorylated threonine or serine residues, such as the 14-3-3 family and WW-domain containing proteins [135,160]. We took two different approaches to examine if Shc threonine phosphorylation affects protein recruitment. Using the HEK293T Shc-overexpressing cell lines we performed a two-dimensional gel electrophoresis analysis on the proteins that bind to Shc. Cells were serum-starved overnight and then stimulated

with EGF for 2 minutes. The 2-minute time point was chosen because the difference in phospho-Erk level was most significant in the 293T Shc overexpressing cell lines at this time point (Figure 4). Strep-tagged Shc and its associated proteins were pulled-down using strep-tactin beads. These proteins were separated by their isoelectric points and then by their molecular weights. The protein spots were then visualized by silver-stain. ^{TE}Shc mutant exhibits increased protein recruitment compared with ^{WT}Shc and ^{TA}Shc mutant (Figure 12, right panel).

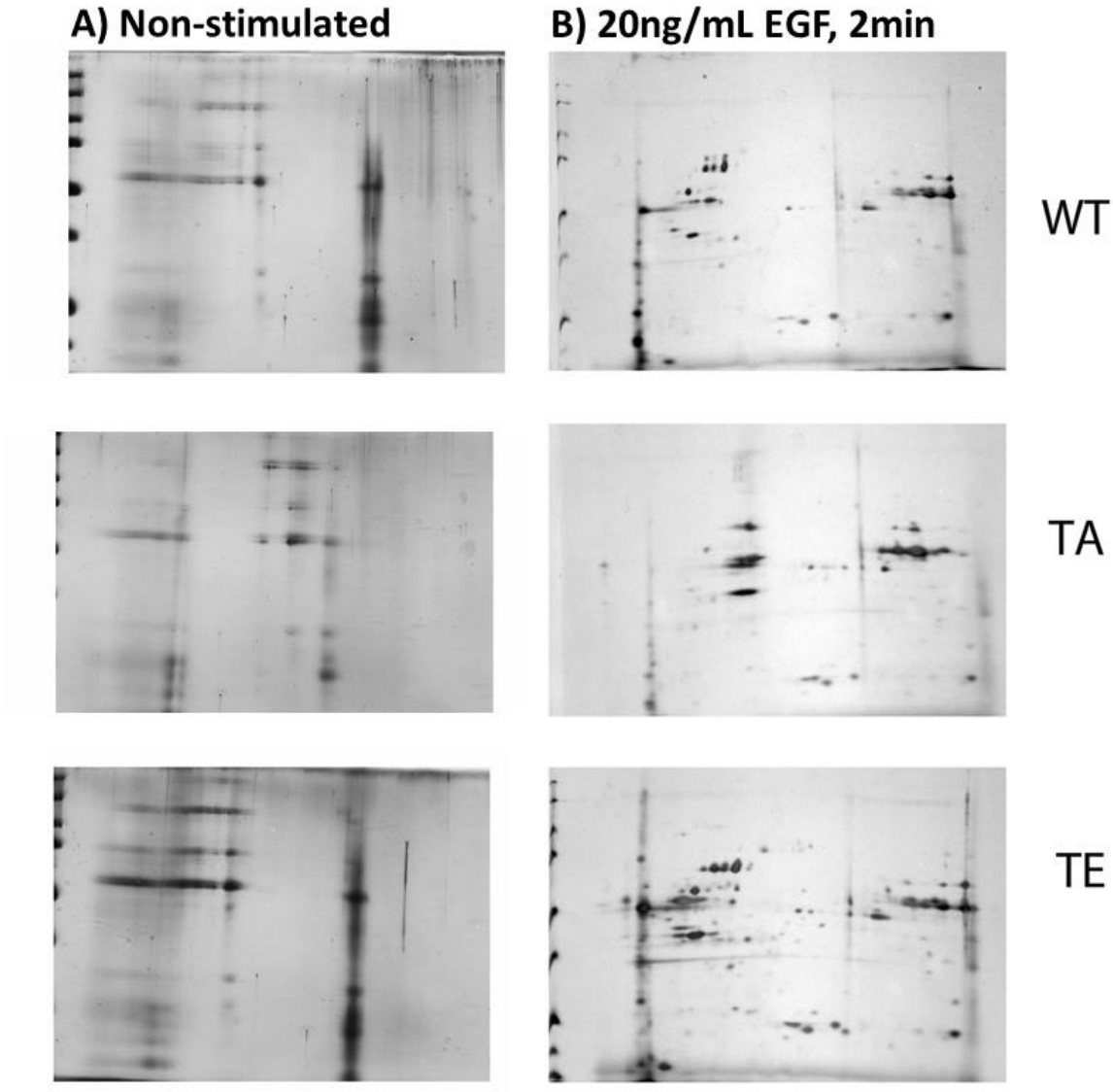

Figure 12. 2-dimensional electrophoresis gel analysis of Shc protein recruitment. HEK293T cells overexpressing ^{WT}Shc, ^{TA}Shc or ^{TE}Shc were (A) starved overnight or (B) stimulated with 20ng/ml EGF for 2 minutes after starvation period. Cells were lysed with lysis buffer and strep-tagged Shc was precipitated on strep-Tactin beads. Precipitants were separated by their isoelectric points and then by molecular weight. Protein spots were visualized by silver stain.

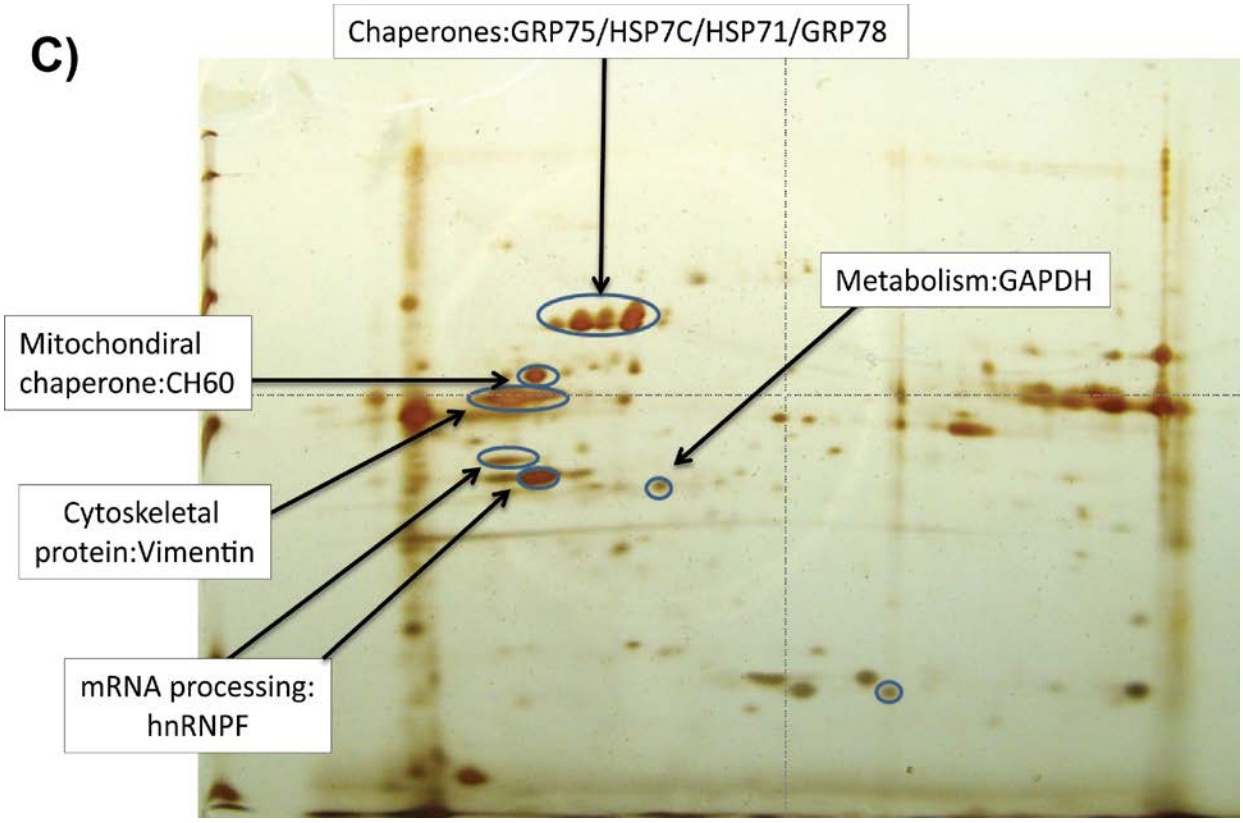

Figure 12. 2-dimensional electrophoresis gel analysis of Shc protein recruitment. . (C) Identification of proteins which preferentially interact with the threonine mimetic mutant Shc^{TE} using mass spectrometry. Mass spectrometry experiments and analysis were performed by the MDACC core.

We identified the proteins that are specifically recruited to ^{TE}Shc and not ^{TA}Shc as indicated in figure 12. A number of chaperones are preferentially recruited suggesting an unfolding of Shc protein upon threonine phosphorylation. Chaperonin 60 (CH60) is a mitochondria chaperone protein which is consistent with the observation that p46 Shc migrates into the mitochondria [161]. Both vimentin and heterogeneous nuclear ribonucleoprotein F (hnRNPF) have been identified in a screen for Grb2 binding partners (Zamal Ahmed, personal communication), which raises the possibility that Shc and Grb2

interact with these two proteins as a complex. Glyceraldehyde 3-phosphate dehydrogenase (GAPDH) is an enzyme that plays important roles in metabolism, a process that is critically linked to cancer development [162,163]. Given our observation that Shc is threonine phosphorylated in two metastatic breast cancer cell lines (MDA-MB-468 and MDA-MB-231; Figures 5 and 7) and that a direct role of p52 Shc in metabolism has not been described, we performed a pull-down experiment to confirm the interaction between Shc and GAPDH. As shown in figure 13, strep-tagged ^{WT}Shc interact with GAPDH upon EGF stimulation whereas ^{TE}Shc interacts with GAPDH constitutively. Moreover, ^{TA}Shc was unable to pull-down GAPDH regardless of EGF stimulation status. Hence, the interaction between GAPDH and Shc requires Shc threonine phosphorylation.

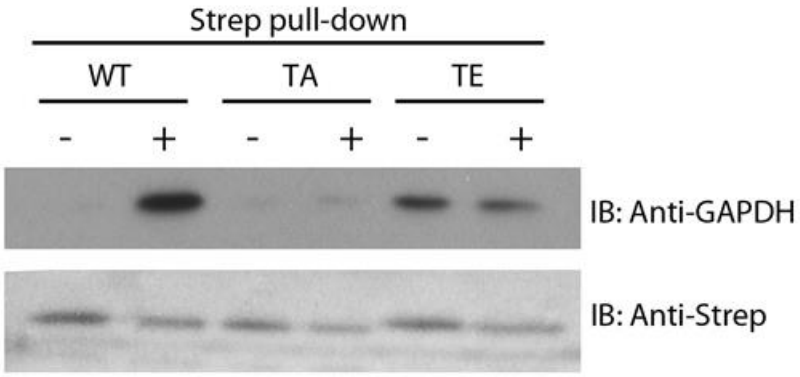

Figure 13. Threonine phosphorylated Shc associates with GAPDH. HEK293T cells overexpressing ^{WT}Shc, ^{TA}Shc or ^{TE}Shc were starved overnight and then stimulated with 20ng/ml EGF for 2 minutes. Cells were lysed with lysis buffer and strep-tagged Shc was precipitated on strep-Tactin beads. The precipitants were immunoblotted for GAPDH.

In addition to the 2D analysis of Shc protein recruitment, we performed a literature search for proteins whose binding to Shc might be affected by threonine phosphorylation.

We selected three isoforms of the scaffold 14-3-3 [164], the ubiquitin-protein ligase Nedd4 [165]and Pin1 [26,54,166]. As noted above, 14-3-3 proteins are known to binding to phosphorylated threonine and serine residues, while both Nedd4 and Pin1 contain WW domains that recognize either proline-rich or pThr/pSer motifs. These proteins were overexpressed, isolated and immobilized on agarose beads through their fusion tags, and used as bait for pull-down experiments. Since Shc is threonine phosphorylated upon EGF stimulation within 5 minutes in the MDA-MB-468 cell line, it was used as prey. MDA-MB-468 cells were starved overnight and then stimulated with EGF for 5 minutes. Erk activity was inhibited by the use of the Mek inhibitor U0126 to abolish Shc threonine phosphorylation. All proteins tested were able to pull-down Shc (Figure 14). Nedd4 binds to Shc constitutively which suggests that the interaction is driven by the proline-rich motifs within the CH1 domain of Shc rather than phosphorylation (Figure 14B). Interestingly, while all three 14-3-3 isoforms could bind to Shc in an EGF stimulation-dependent manner, they were differentially affected by Erk activity. When Erk activity is inhibited, the ζ isoform interaction with Shc is reduced, whereas the binding between Shc and 14-3-3 τ increased and its binding with 14-3-3 ε remain unchanged (Figure 14C and D). The sequences of the three 14-3-3 isoforms are highly conserved, it would therefore be interesting to find out how they are able to bind differently to Shc. Another notable feature is that the 14-3-3 proteins preferentially bind to the p52 rather than the p46 isoforms, even though the phosphothreonine sites are identical. This suggests that the N-terminal sequence on p52 play a role in stabilizing the interaction. 14-3-3 ζ has been previously reported to upregulate PI3K signaling when recruited to Shc, it is therefore likely that threonine-phosphorylated Shc augments Akt phosphorylation by interacting with 14-3-3 ζ [96,167]. Finally, Pin1 interacts with Shc when cells are stimulated with EGF

and the binding is abolished when Erk activity is inhibited. This is consistent with the fact that Pin1 binding and activity are pT/pS-dependent. As expected, C113A mutation in Pin1 did not affect its binding to Shc as this mutation has been shown to affect isomerase activity without altering its phosphothreonine binding ability [168].

Since Pin1 is critical in oncogenesis [169,170] and is overexpressed in the MDA-MB-468 cell line [171], we tested to see if binding between Shc and Pin1 is indeed direct. We purified both recombinant Shc and Pin1 from *E. coli*. and performed a pull-down experiment through the His-tag on Shc. Shc was also preincubated with Erk in the presence or absence of ATP and $MgCl_2$ to verify that threonine phosphorylation is critical to the interaction. To our surprise Erk-mediated phosphorylation is only partially responsible for Shc and Pin1 binding. One possible explanation is that the Pin1 WW domain can also interact with proline-rich motifs and ShcCH1 contains several such motifs. The inconsistent results obtained from the pull-down experiments using cell lysates and purified protein could be due to competing binding partners that exist in the cell lysates.

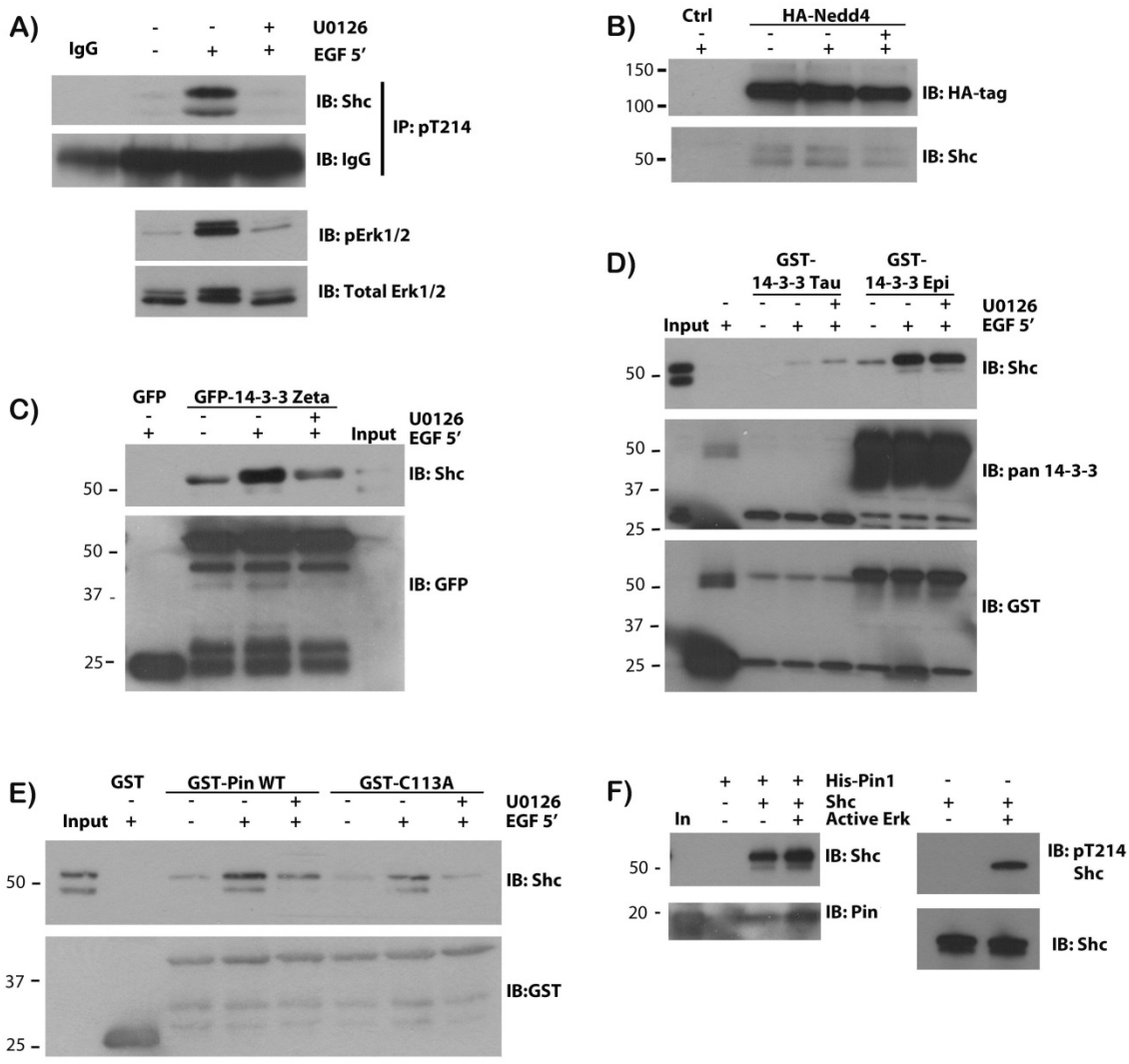

Figure 14. Pull-down experiments to identify Shc protein binding partners that are affected by Shc threonine phosphorylation. MDA-MB-468 cells were starved overnight and then stimulated with 20ng/ml EGF for 5 minutes with or without pre-incubation with 10μM of the Mek inhibitor U0126. (A) Erk was effectively inhibited by U0126 as shown by immunoblotting for phospho-Erk1/2. (B) to (E) Fusion proteins were purified and immobilized on agarose beads and incubated with MDA-MB-468 lysates overnight. Beads were washed with lysis buffer and the samples were analyzed by western blotting for the

presence of Shc. (B) HA-tagged Nedd4 (C) GFP-14-3-3 ζ (D) GST-14-3-3 τ and GST 14-3-3 ε (E) GST-Pin1 WT or C113A (F) Recombinant His-tagged p52 Shc and Pin1 were purified from *E. coli.* Shc was phosphorylated by active Erk2. After the removal of Erk2, immobilized Shc was incubated with Pin1. The direct binding of Shc and Pin1 was confirmed by western blotting (left panel). Shc is phosphorylated by Erk on threonine residues (right panel).

4.3 Discussion

Although it is clear that serine/threonine phosphorylation on scaffold molecules function as feedback events in RTK signaling, the molecular mechanism of how this occurs is less so. In this Chapter, we show upon activation of EGFR, Erk phosphorylates Shc on three residues which leads to elevated Erk and Akt phosphorylation in the HEK293T in an *in vitro* system. This suggests that phosphorylation of Shc on threonine residues mediates a positive feedback loop in Erk-signaling and crosstalk between the Erk and Akt pathways. Furthermore, we found that in two triple-negative breast cancer cell lines, MDA-MB-468 and MDA-MB-231, Shc exhibits a significant level of phosphorylation on T214 but not in the non-transformed MCF10A cell line. This suggests phosphorylation of Shc on threonine residues is involved in breast cancer oncogenesis, which is in line with the observation of the upregulation of Erk and Akt phosphorylation in the HEK293T *in vitro* system.

To understand how threonine phosphorylation augments downstream signaling, we explored two possibilities. First, we investigated whether threonine phosphorylation affects Shc overall conformation. This is because two of the phosphorylation sites reside in the disordered CH1 domain. Intrinsically disordered regions on proteins allow for

many transient conformations which are important for regulating dynamics in signaling by altering protein recruitment and affecting the accessibility for kinases and/or phosphatases. By changing the charges of these intrinsically disordered regions, phosphorylation is particularly important in shifting the equilibrium of conformations [172]. However, using a number of biochemical and biophysical techniques, we failed to detect any significant conformational changes in Shc.

Second, we examined whether the formation of these new phospho-motifs alters protein recruitment. Several domains are well-characterized for their abilities to bind to pS/pT residues, for example the WW-domain and 14-3-3 proteins [160]. We identified three proteins whose binding to Shc is pT-dependent: GAPDH, Pin1 and 14-3-3 ζ. Previous reports show that 14-3-3 ζ binding to the SH2 domain of Shc to be mediated by the phosphorylation of 14-3-3 ζ on tyrosine 179 which leads to upregulation in PI3K and subsequently AKT signaling [68,96]. Our data suggest an additional mechanism for this interaction whereby 14-3-3 ζ binds to threonine phosphorylated Shc. This is not surprising given that 14-3-3 proteins are known for their roles in binding to pS/pT. 14-3-3 ζ structure shows the pS residue lies within the binding pocket for pS/pT motifs in the protein (PDB: 4HKC). T407 also resides in the pY-binding pocket of ShcSH2 (PDB: 1TCE). Hence, there is a possibility that simultaneous phosphorylation on both 14-3-3 ζ and ShcSH2 enhance the interaction of the two proteins (Figure 15). As discussed in Chapter 1, recruitment of 14-3-3 ζ to Shc has been shown to increase PI3K signaling. Given that PI3K is an upstream activator of Akt, it seems likely that this interaction is at least partially responsible for the elevated pAkt level seen in ^{TE}Shc cells.

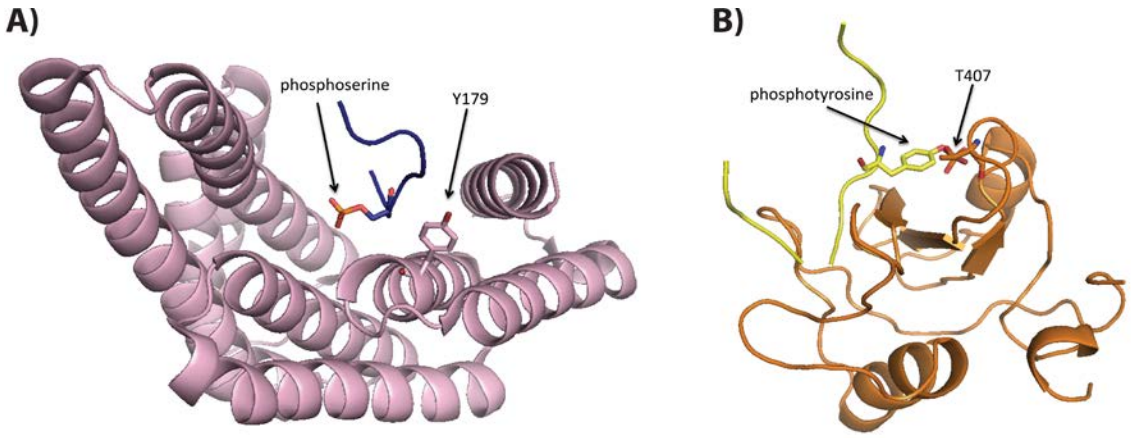

Figure 15. Structures of 14-3-3 ζ and ShcSH2. A) 14-3-3 ζ (purple) in complex with a phosphoserine-containing peptide (blue) derived from the integrin receptor (PDB: 4HKC). Phosphorylated serine on integrin peptide and tyrosine 179 on 14-3-3 ζ are highlighted as sticks models. Y179 is faces towards the phosphoserine-binding pocket in 14-3-3 ζ. B) ShcSH2 (orange) in complex with phosphotyrosine-containing peptide (yellow) derived from the T-cell receptor (PDB: 1TCE). T407 on ShcSH2 and phosphorylated tyrosine on T-cell peptide are highlighted as sticks models. T407 is in close proximity to the phosphotyrosine-binding pocket of ShcSH2.

Pin1 has previously been shown to recruit p66Shc to the mitochondria in a PKC-dependent manner, which is a process that leads to apoptosis [54]. Here we show that p52Shc can also bind to Pin1, albeit through different phospho-residues. However, the role for this interaction is unclear and requires further investigation. Some peptide prolyl cis-trans isomerases (PPIases), such as Pin1 specifically catalyzes proline residues preceded by pS/pT. PPIases catalyzes the conversion of cis-trans conformation of proline which can potentially switch local conformations from one to another [170] and adjust protein-recruitment profiles. In addition, because some phosphatases only act on certain phospho-isoforms, such as PP2A [173], proline-isomerization can also alter the rate of

phosphorylation/dephosphorylation [170]. We have previously identified another PPIase, cyclophilin A (CypA) as a direct binding partner for Shc [25]. Given that ShcCH1 is proline-rich, it is likely that Shc is regulated by proline isomerization. This would form an interesting direction for future investigation into Shc signaling in addition to the better characterized PTMs.

Finally, p66Shc has recently been reported to regulate glycolysis indirectly through the inhibition of mTOR signaling [70]. It would be interesting to see if p52Shc plays a direct role in glycolytic flux through the phosphothreonine-dependent recruitment of GAPDH.

Another important point that requires further investigation is the importance of the individual phosphorylation sites. While in the *in vitro* systems such as the 293T phospho-mutants cell lines and the recombinantly expressed and purified Shc proteins examine the effects of all three sites together, whether endogenous Shc is phosphorylated on all three sites in cellular environment and their individual contributions to downstream signaling require further characterization. We have been unable to examine the endogenous phosphorylation levels of Shc T276 and T407 due to the lack of specific antibodies.

Chapter 5

Discussion

Deciphering cellular signaling networks is vital to our understanding of how external inputs are translated into appropriate phenotypic outputs through the intracellular environment. At the protein level the combinatorial use of protein domains and post-translational modifications are important strategies in generating signaling networks. In this thesis, I examined the multifaceted role of the scaffold protein Shc in Erk signaling both prior to and post-growth factor stimulation via two strategies. First, I described a novel role for Shc in Erk inhibition prior to growth factor stimulation through the PTB domain of Shc in Chapter 3. Second, I investigated how Erk-mediated Shc phosphorylation after stimulation regulates signaling feedback and crosstalk in Chapter 4.

I demonstrate that in the absence of extracellular stimulation, Shc and Erk associate via a novel interface using the α2-β3 loop in ShcPTB and N-terminal lobe in Erk (Chapter 3, Figure 6). This association is inhibitory to Erk phosphorylation and restricts Erk in the cytoplasm. Upon EGF stimulation, Shc contributes towards an initial phase of Erk activation by 1) binding to activated RTKs which triggers the release of Erk through an allosteric mechanism and 2) the recruitment of Grb2-Sos complex to the plasma membrane, which is well established in previous research. Activated Erk in turn phosphorylates Shc on three threonine residues. These phosphothreonines subsequently mediate 1) a positive feed-forward loop in sustaining Erk activity and 2) crosstalk with Akt signaling, possibly through the recruitment of 14-3-3 ζ (Figure 1). In the following sections, I discuss the potential roles of these findings.

5.1 Signaling

Protein complexes can be generated by the specific binding between a folded domain on one protein and a short motif on another [10,15]. One such folded domain is the phosphotyrosine-binding (PTB) domain. The core PTB fold contains two orthogonal anti-parallel β-sheets capped by a C-terminal α-helix, which enables this class of protein domain to bind to NPXY motifs. While all PTB domains contain this core fold, the loop responsible for binding to Erk in ShcPTB is unique to Shc [174]. Hence, this mode of interaction with Erk could be unique to the Shc family among the PTB-containing proteins. This suggests the diversity that exists outside the conserved polypeptide fold within a single class of protein domain can also be used to mediate specific protein-protein interactions. Along the same line, another example for non-canonical binding in the PTB domain family is Frs2. In addition to the core PTB-fold which enables the domain to recognize the NPXY consensus sequence, it contains an extra β-sheet which allows it to bind to a VTVS sequence on FGF receptors [175].

Analysis of Erk interacting partners by von Kriegsheim *et. al.* [7] indicated that a number of proteins, such as RSK and NF1, associate with Erk prior to growth factor stimulation. Similar to Shc, these proteins also release Erk post-stimulation. It will be interesting to investigate whether conformational changes in these proteins also trigger the release of Erk, much as we identified with Shc in this work.

Both Shc and Erk have been shown to regulate the signaling initiated by numerous growth factors. While this study focuses on EGF stimulation, it will be interesting to find

out if other growth factors would lead to the dissociation of the Shc-Erk complex and phosphorylation of Shc by Erk. More importantly, can the interaction between Shc and Erk contribute towards the differences in signaling transmitted by different RTKs? For example, the NGF receptor TrkA contains only one binding site for ShcPTB [176], whereas EGFR contains two [177]. Would the difference in the number of Shc molecules recruited to a RTK be translated into the number of Erk molecules released and hence signal strength? Also, how would the duration of Erk activation, a property that is dependent on which RTK is stimulated and cell type, affect Shc threonine phosphorylation and Shc-mediated crosstalk with the Akt pathway?

5.2 Development

The role of Shc in Erk signaling through the recruitment of Grb2 (which is dependent on the phosphorylation on Y239/240/317 of Shc) was explored in the development of cardiovascular, muscles, immune and neuronal systems (Section 1.5). In all cases, there are differences in the phenotypic outcome between Shc-null and Shc Y239/240/317F mutants. This indicates that in addition to the recruitment of Grb2, Shc functions in these developmental systems via mechanisms that are independent of the Shc-Grb2 axis. It would therefore be interesting to investigate the importance of the novel interactions that we have identified in this thesis in developmental systems. For example, in the neuronal system, microencephaly was observed in both Shc-null and Y239/240/317F animals. However, the molecular basis for this phenotype mediated by the two genotypes is different. The subventricular zone of the brain in the Shc-null animals showed a reduction in cell proliferation, whereas Y239/240/317F animals exhibited an increased in apoptosis. Since cell proliferation and apoptosis are associated

with Erk and Akt signaling respectively, it seems likely that Y239/240/317 phosphorylation in the neuronal system mediates cell survival through binding to Grb2 and its subsequent recruitment of the p85 subunit of PI3K which then in turn activates Akt (Section 1.4.2). In contrast, since cell proliferation was not affected in the Y239/240/317F animals, cell proliferation as a result of Erk signaling would be mediated by a Grb2-independent mechanism in the Shc-null animals. The direct interaction between Shc and Erk, as well as Shc threonine phosphorylation by Erk regulates Erk activity independent of Grb2, hence we speculate that the novel mechanisms described in this thesis between Shc and Erk play important roles in Erk signaling in the development of the neuronal system. The same argument is true for the development of the cardiovascular system. Deleting ShcA in mice causes embryonic lethality due to abnormality in the heart. However, Y239/240/317F mutant animals are viable with grossly normal cardiovascular structures, suggesting that the cardiovascular defects seen in ShcA-null animals are not due to the phosphorylation of Y239/240/317. Interestingly, experiments in MEFs obtained from the Shc-null embryos suggest that Erk signaling is affected by the removal of Shc, as Shc was required for Erk phosphorylation when cells were exposed to a low level of growth factors. Again, this indicates that Shc regulates Erk signaling through a Grb2-independent mechanism. Both Shc-Erk direct binding and pT Shc are likely to be important in potentiating Erk activity. This is because at a low growth factor level, a relatively small number of RTK would be activated and subsequently phosphotyrosine-mediated signaling would be limited. The higher phospho-Erk level seen in WT compared with Shc-null MEFs under such condition is probably caused by 1) an increase in 'free' Erk available for activation driven by the dissociation of Shc-Erk complex and 2) the positive feedback in Erk activation mediated by threonine phosphorylated Shc.

Furthermore, even though we did not find a direct relationship between the phosphorylation of Y239/240/317 and T214/276/407 on Shc, the overall Erk activity would be a combined effect of both types of phosphorylation events. Hence, it would be interesting to delineate the effects of T214/276/407 phosphorylation from Y239/240/317 phosphorylation, such as by the use of Shc T214/276/407A mutant animals. Since T214/276/407 seems to be important in the temporal regulation of Erk phosphorylation, rather than function as an 'on' switch for Erk activity in the HEK293T *in vitro* system, investigating the role of T214/276/407 in developmental systems might shed light in the importance of temporal regulation of Erk in such systems.

5.3 Disease

As discussed in Section 1.6.2, even though Shc plays critical roles in the pathogenesis of breast cancer, it does not seem to function through the upregulation of Erk activity. Instead, Shc augments Akt signaling to mediate cell survival via the recruitment of 14-3-3 ζ using ShcSH2. Previous work shows that the interaction between 14-3-3 ζ and the Shc SH2 domain is mediated by the tyrosine phosphorylation of 14-3-3 ζ. Here, we show that Shc recruits 14-3-3 ζ when Shc is threonine phosphorylated and that Akt signaling is upregulated in the presence of the Shc phosphothreonine (^{TE}Shc) mutant. Taken together, our data suggests that Shc threonine phosphorylation augments Akt signaling through the recruitment of 14-3-3 ζ. This interaction would have important implications in oncogenesis.

This work presents two potential avenues for therapeutic intervention in diseases driven by Erk activity. First, we can exploit the knowledge of the Shc-Erk dissociation mechanism to obtain small molecules that would block the binding of RTK without

triggering a conformation change in Shc to stabilize the Shc-Erk complex. Such small molecules could be useful in diseases caused by over-active Erk cascade with Shc overexpression. In this scenario, the small molecule would serve two functions: 1) blockade of RTK-Shc interaction. This would lead to a lack of Shc tyrosine phosphorylation by RTK and hence Shc-Grb2/Sos interaction and the subsequent activation of the Erk cascade; 2) Shc would be trapped in a conformation that can 'mop-up' Erk by direct binding. The usefulness of such small molecules is supported by a recent mouse study which shows that disabling ShcPTB signaling can lead to delayed tumor onset [98].

Second, the Shc threonine phosphorylation sites could potentially serve as markers for erroneous Erk and Akt signaling in TNBC with EGF receptor overexpression. The two TNBC cell lines in which we found pT214 to be significantly phosphorylated both contain an overexpression of EGFR [178,179]. While TNBC describes a collection of disease with highly variable genotypes, some can be sub-grouped by their EGF receptor expression status [180,181]. To explore the role of Shc threonine phosphorylation in TNBC, we can perform IHC analysis for pT Shc level on patient tumor samples and correlate clinical outcome, such as stage of disease and disease-free survival. To investigate if our observations that threonine phosphorylation of Shc on T214/276/407 upregulates Erk and Akt signaling, we can also correlate pT Shc level with pErk and pAkt levels using IHC of cancer patient samples.

5.4 Summary

Using a quantitative proteomics approach, Zheng *et. al.* comprehensively described the temporal contribution of Shc in the EGFR pathway. Shc was found to associate with distinct sets of proteins and to be phosphorylated at multiple sites at specific time-points

post-EGF stimulation [26], revealing that versatility in Shc-mediated protein-protein interaction is required to regulate EGF signaling. The present study of the relationship between Shc and Erk illustrates the degree of complexity a single signaling axis can reach. A phenotypic output is thus the result of compounded effects of multiple relationships between any two signaling molecules. Combined with the recent advances in high-throughput screening of protein complexes [182,183,184] and computational analysis of protein interactome [185,186], the ability to elucidate finer details of how proteins interact as exemplified by the present work will lead to the development of therapeutic strategies that can target important nodes in signaling networks of human disease [187,188,189].

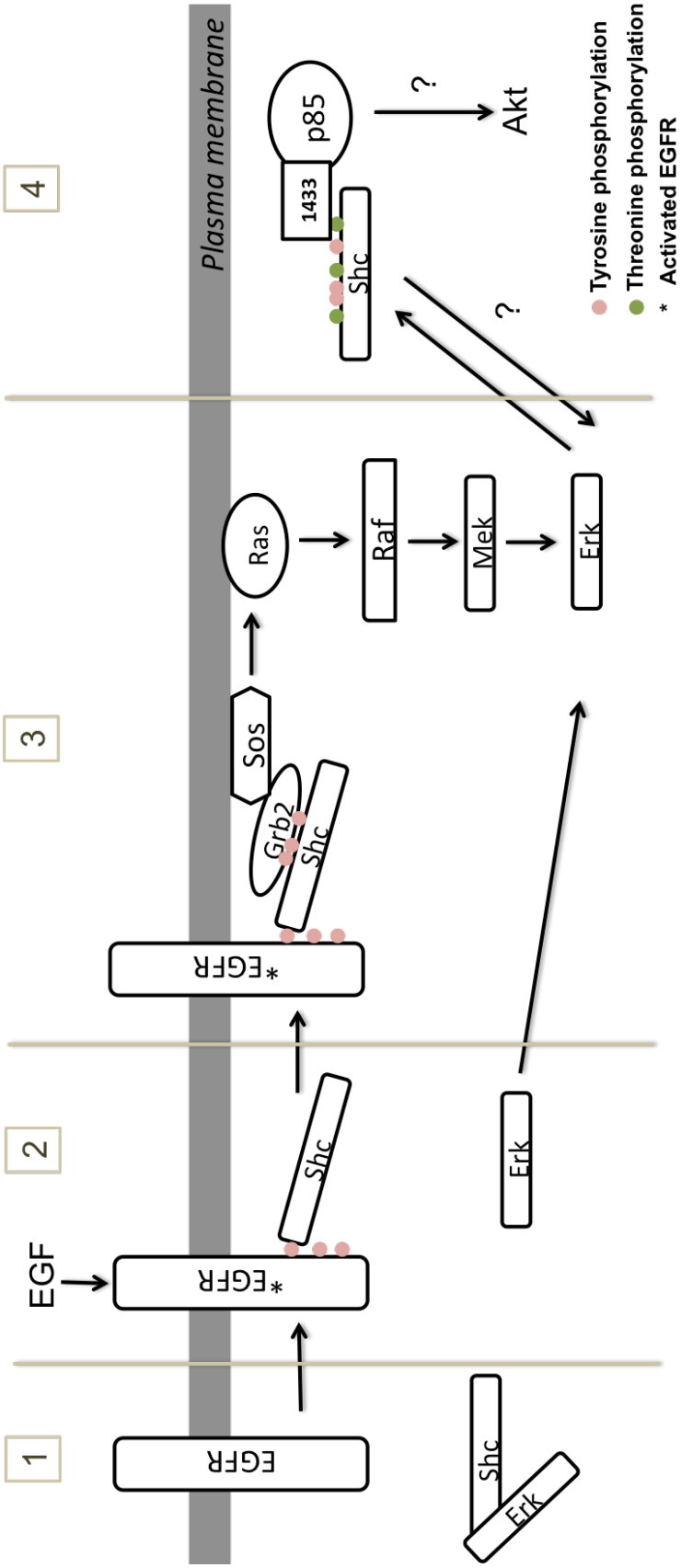

Figure 1 Summary of the mutual regulation between Shc and Erk. 1. In the absence of extracellular stimulation, Shc and Erk forms a complex via a novel binding interface. 2. Upon EGF stimulation, Shc binds to the activated EGF receptor, which triggers a conformational change in Shc and leads to Erk dissociation from the complex. 3. Shc is phosphorylated by the receptor on its tyrosine residues, which recruits the Grb2-Sos complex to the membrane. This activates Ras, which initiates the activation of the Erk cascade. 4. Activated Erk phosphorylates Shc on threonine residues, which further elevates the Erk phosphorylation and activate Akt, possibly through the recruitment of 14-3-3 zeta-p85 complex.

Bibliography

[1] M.A. Lemmon, J. Schlessinger, Cell Signaling by Receptor Tyrosine Kinases, Cell 141 (2010) 1117-1134.

[2] R.T. Dorsam, J.S. Gutkind, G-protein-coupled receptors and cancer, Nature Reviews Cancer 7 (2007) 79-94.

[3] G.R. Dubyak, Ion homeostasis, channels, and transporters: an update on cellular mechanisms, Advances in Physiology Education 28 (2004) 143-154.

[4] K. Muroya, S. Hattori, S. Nakamura, Nerve growth factor induces rapid accumulation of the GTP-bound form of p21ras in rat pheochromocytoma PC12 cells, Oncogene 7 (1992) 277-281.

[5] K. Huff, D. End, G. Guroff, Nerve growth factor-induced alteration in the response of PC12 pheochromocytoma cells to epidermal growth factor, J Cell Biol 88 (1981) 189-198.

[6] B.N. Kholodenko, J.F. Hancock, W. Kolch, Signalling ballet in space and time, Nature Reviews Molecular Cell Biology 11 (2010) 414-426.

[7] A. von Kriegsheim, D. Baiocchi, M. Birtwistle, D. Sumpton, W. Bienvenut, N. Morrice, K. Yamada, A. Lamond, G. Kalna, R. Orton, D. Gilbert, W. Kolch, Cell fate decisions are specified by the dynamic ERK interactome, Nat Cell Biol 11 (2009) 1458-1464.

[8] R. Avraham, Y. Yarden, Feedback regulation of EGFR signalling: decision making by early and delayed loops, Nature Reviews Molecular Cell Biology 12 (2011) 104-117.

[9] T. Kaneko, L. Li, S.S.C. Li, The SH3 domain - a family of versatile peptide- and protein-recognition module, Frontiers in Bioscience 13 (2008) 4938-4952.

[10] Y.L. Deribe, T. Pawson, I. Dikic, Post-translational modifications in signal integration, Nature Structural & Molecular Biology 17 (2010) 666-672.

[11] W.A. Lim, T. Pawson, Phosphotyrosine Signaling: Evolving a New Cellular Communication System, Cell 142 (2010) 661-667.

[12] T. Pawson, Specificity in signal transduction: From phosphotyrosine-SH2 domain interactions to complex cellular systems, Cell 116 (2004) 191-203.

[13] T. Pawson, G.D. Gish, P. Nash, SH2 domains, interaction modules and cellular wiring, Trends in Cell Biology 11 (2001) 504-511.

[14] T. Pawson, P. Nash, Protein-protein interactions define specificity in signal transduction, Genes & Development 14 (2000) 1027-1047.

[15] T. Pawson, Protein Modules and Signaling Networks, Nature 373 (1995) 573-580.

[16] J. Schlessinger, M.A. Lemmon, SH2 and PTB domains in tyrosine kinase signaling, Sci STKE 2003 (2003) RE12.

[17] L.N. Johnson, R.J. Lewis, Structural basis for control by phosphorylation, Chemical Reviews 101 (2001) 2209-2242.

[18] T. Pawson, P. Nash, Assembly of cell regulatory systems through protein interaction domains, Science 300 (2003) 445-452.

[19] L. O'Rourke, J.E. Ladbury, Specificity is complex and time consuming: Mutual exclusivity in tyrosine kinase-mediated signaling, Accounts of Chemical Research 36 (2003) 410-416.

[20] T. Pawson, J.D. Scott, Signaling through scaffold, anchoring, and adaptor proteins, Science 278 (1997) 2075-2080.

[21] D.N. Dhanasekaran, K. Kashef, C.M. Lee, H. Xu, E.P. Reddy, Scaffold proteins of MAP-kinase modules, Oncogene 26 (2007) 3185-3202.

[22] A.M. Cheng, T.M. Saxton, R. Sakai, S. Kulkarni, G. Mbamalu, W. Vogel, C.G. Tortorice, R.D. Cardiff, J.C. Cross, W.J. Muller, T. Pawson, Mammalian Grb2 regulates multiple steps in embryonic development and malignant transformation, Cell 95 (1998) 793-803.

[23] G.M. Findlay, M.J. Smith, F. Lanner, M.S. Hsiung, G.D. Gish, E. Petsalaki, K. Cockburn, T. Kaneko, H.M. Huang, R.D. Bagshaw, T. Ketela, M. Tucholska, L. Taylor, D.D. Bowtell, J. Moffat, M. Ikura, S.S.C. Li, S.S. Sidhu, J. Rossant, T. Pawson, Interaction Domains of Sos1/Grb2 Are Finely Tuned for Cooperative Control of Embryonic Stem Cell Fate, Cell 152 (2013) 1008-1020.

[24] M.C. Good, J.G. Zalatan, W.A. Lim, Scaffold Proteins: Hubs for Controlling the Flow of Cellular Information, Science 332 (2011) 680-686.

[25] R. George, H.L. Chan, Z. Ahmed, K.M. Suen, C.N. Stevens, J.A. Levitt, K. Suhling, J. Timms, J.E. Ladbury, A complex of Shc and Ran-GTPase localises to the cell nucleus, Cellular and Molecular Life Sciences 66 (2009) 711-720.

[26] Y. Zheng, C.J. Zhang, D.R. Croucher, M.A. Soliman, N. St-Denis, A. Pasculescu, L. Taylor, S.A. Tate, W.R. Hardy, K. Colwill, A.Y. Dai, R. Bagshaw, J.W. Dennis, A.C. Gingras, R.J. Daly, T. Pawson, Temporal regulation of EGF signalling networks by the scaffold protein Shc1, Nature 499 (2013) 166-+.

[27] M.K. Wills, N. Jones, Teaching an old dogma new tricks: twenty years of Shc adaptor signalling, Biochem J 447 (2012) 1-16.

[28] G. Pelicci, L. Lanfrancone, F. Grignani, J. McGlade, F. Cavallo, G. Forni, I. Nicoletti, F. Grignani, T. Pawson, P.G. Pelicci, A novel transforming protein (SHC) with an SH2 domain is implicated in mitogenic signal transduction, Cell 70 (1992) 93-104.

[29] G. Pelicci, L. Dente, A. De Giuseppe, B. Verducci-Galletti, S. Giuli, S. Mele, C. Vetriani, M. Giorgio, P.P. Pandolfi, G. Cesareni, P.G. Pelicci, A family of Shc related proteins with conserved PTB, CH1 and SH2 regions, Oncogene 13 (1996) 633-641.

[30] J.P. O'Bryan, Z. Songyang, L. Cantley, C.J. Der, T. Pawson, A mammalian adaptor protein with conserved Src homology 2 and phosphotyrosine-binding domains is related to Shc and is specifically expressed in the brain, Proc Natl Acad Sci U S A 93 (1996) 2729-2734.

[31] N. Jones, W.R. Hardy, M.B. Friese, C. Jorgensen, M.J. Smith, N.M. Woody, S.J. Burden, T. Pawson, Analysis of a Shc family adaptor protein, ShcD/Shc4, that associates with muscle-specific kinase, Molecular and Cellular Biology 27 (2007) 4759-4773.

[32] E. Fagiani, G. Giardina, L. Luzi, M. Cesaroni, M. Quarto, M. Capra, G. Germano, M. Bono, M. Capillo, P. Pelicci, L. Lanfrancone, RaLP, a new member of the Src homology and collagen family, regulates cell migration and tumor growth of metastatic melanomas, Cancer Research 67 (2007) 3064-3073.

[33] E. Migliaccio, S. Mele, A.E. Salcini, G. Pelicci, K.M. Lai, G. Superti-Furga, T. Pawson, P.P. Di Fiore, L. Lanfrancone, P.G. Pelicci, Opposite effects of the p52shc/p46shc and p66shc splicing isoforms on the EGF receptor-MAP kinase-fos signalling pathway, EMBO J 16 (1997) 706-716.

[34] A. Ventura, L. Luzi, S. Pacini, C.T. Baldari, P.G. Pelicci, The p66Shc longevity gene is silenced through epigenetic modifications of an alternative promoter, Journal of Biological Chemistry 277 (2002) 22370-22376.

[35] M.M. Zhou, K.S. Ravichandran, E.T. Olejniczak, A.M. Petros, R.P. Meadows, M. Sattler, J.E. Harlan, W.S. Wade, S.J. Burakoff, S.W. Fesik, Structure and Ligand Recognition of the Phosphotyrosine Binding Domain of Shc, Nature 378 (1995) 584-592.

[36] A. Farooq, L. Zeng, K.S. Yan, K.S. Ravichandran, M.M. Zhou, Coupling of folding and binding in the PTB domain of the signaling protein Shc, Structure 11 (2003) 905-913.

[37] T. Trub, W.E. Choi, G. Wolf, E. Ottinger, Y. Chen, M. Weiss, S.E. Shoelson, Specificity of the PTB domain of Shc for beta turn-forming pentapeptide motifs amino-terminal to phosphotyrosine, J Biol Chem 270 (1995) 18205-18208.

[38] P. vanderGeer, S. Wiley, G.D. Gish, V.K.M. Lai, R. Stephens, M.F. White, D. Kaplan, T. Pawson, Identification of residues that control specific binding of the Shc phosphotyrosine-binding domain to phosphotyrosine sites, Proceedings of the National Academy of Sciences of the United States of America 93 (1996) 963-968.

[39] M.J. Smith, W.R. Hardy, G.Y. Li, M. Goudreault, S. Hersch, P. Metalnikov, A. Starostine, T. Pawson, M. Ikura, The PTB domain of ShcA couples receptor activation to the cytoskeletal regulator IQGAP1, EMBO J 29 (2010) 884-896.

[40] A. Charest, J. Wagner, S. Jacob, C.J. McGlade, M.L. Tremblay, Phosphotyrosine-independent binding of SHC to the NPLH sequence of murine protein-tyrosine phosphatase-PEST. Evidence for extended phosphotyrosine binding/phosphotyrosine interaction domain recognition specificity, J Biol Chem 271 (1996) 8424-8429.

[41] S. Ugi, T. Imamura, W. Ricketts, J.M. Olefsky, Protein phosphatase 2A forms a molecular complex with Shc and regulates Shc tyrosine phosphorylation and downstream mitogenic signaling, Mol Cell Biol 22 (2002) 2375-2387.

[42] J. Kraut-Cohen, W.J. Muller, A. Elson, Protein-tyrosine phosphatase epsilon regulates Shc signaling in a kinase-specific manner - Increasing coherence in tyrosine phosphatase signaling, Journal of Biological Chemistry 283 (2008) 4612-4621.

[43] M.A. Lemmon, K.M. Ferguson, Signal-dependent membrane targeting by pleckstrin homology (PH) domains, Biochem J 350 Pt 1 (2000) 1-18.

[44] K.S. Ravichandran, M.M. Zhou, J.C. Pratt, J.E. Harlan, S.F. Walk, S.W. Fesik, S.J. Burakoff, Evidence for a requirement for both phospholipid and phosphotyrosine binding via the Shc phosphotyrosine-binding domain in vivo, Molecular and Cellular Biology 17 (1997) 5540-5549.

[45] M.D. Shoulders, R.T. Raines, Collagen Structure and Stability, Annual Review of Biochemistry 78 (2009) 929-958.

[46] P. vanderGeer, S. Wiley, G.D. Gish, T. Pawson, The Shc adaptor protein is highly phosphorylated at conserved, twin tyrosine residues (Y239/240) that mediate protein-protein interactions, Current Biology 6 (1996) 1435-1444.

[47] A.E. Salcini, J. Mcglade, G. Pelicci, I. Nicoletti, T. Pawson, P.G. Pelicci, Formation of Shc-Grb2 Complexes Is Necessary to Induce Neoplastic Transformation by Overexpression of Shc Proteins, Oncogene 9 (1994) 2827-2836.

[48] Z. Weng, S.M. Thomas, R.J. Rickles, J.A. Taylor, A.W. Brauer, C. Seidel-Dugan, W.M. Michael, G. Dreyfuss, J.S. Brugge, Identification of Src, Fyn, and Lyn SH3-binding proteins: implications for a function of SH3 domains, Mol Cell Biol 14 (1994) 4509-4521.

[49] M.M. Zhou, R.P. Meadows, T.M. Logan, H.S. Yoon, W.S. Wade, K.S. Ravichandran, S.J. Burakoff, S.W. Fesik, Solution Structure of the Shc Sh2 Domain Complexed with a Tyrosine-Phosphorylated Peptide from the T-Cell Receptor, Proceedings of the National Academy of Sciences of the United States of America 92 (1995) 7784-7788.

[50] Z. Songyang, S.E. Shoelson, J. McGlade, P. Olivier, T. Pawson, X.R. Bustelo, M. Barbacid, H. Sabe, H. Hanafusa, T. Yi, et al., Specific motifs recognized by the SH2 domains of Csk, 3BP2, fps/fes, GRB-2, HCP, SHC, Syk, and Vav, Mol Cell Biol 14 (1994) 2777-2785.

[51] K.S. Ravichandran, K.K. Lee, Z. Songyang, L.C. Cantley, P. Burn, S.J. Burakoff, Interaction of Shc with the zeta chain of the T cell receptor upon T cell activation, Science 262 (1993) 902-905.

[52] R. Schmandt, S.K. Liu, C.J. McGlade, Cloning and characterization of mPAL, a novel Shc SH2 domain-binding protein expressed in proliferating cells, Oncogene 18 (1999) 1867-1879.

[53] E. Migliaccio, M. Giorgio, S. Mele, G. Pelicci, P. Reboldi, P.P. Pandolfi, L. Lanfrancone, P.G. Pelicci, The p66shc adaptor protein controls oxidative stress response and life span in mammals, Nature 402 (1999) 309-313.

[54] P. Pinton, A. Rimessi, S. Marchi, F. Orsini, E. Migliaccio, M. Giorgio, C. Contursi, S. Minucci, F. Mantovani, M.R. Wieckowski, G. Del Sal, P.G. Pelicci, R. Rizzuto, Protein kinase C beta and prolyl isomerase 1 regulate mitochondrial effects of the life-span determinant p66Shc, Science 315 (2007) 659-663.

[55] M. Giorgio, E. Migliaccio, F. Orsini, D. Paolucci, M. Moroni, C. Contursi, G. Pelliccia, L. Luzi, S. Minucci, M. Marcaccio, P. Pinton, R. Rizzuto, P. Bernardi, F. Paolucci, P.G. Pelicci, Electron transfer between cytochrome c and p66Shc generates reactive oxygen species that trigger mitochondrial apoptosis, Cell 122 (2005) 221-233.

[56] K.S. Ravichandran, Signaling via Shc family adapter proteins, Oncogene 20 (2001) 6322-6330.

[57] N. Gotoh, M. Toyoda, M. Shibuya, Tyrosine phosphorylation sites at amino acids 239 and 240 of Shc are involved in epidermal growth factor-induced mitogenic signaling that is distinct from Ras/mitogen-activated protein kinase activation, Molecular and Cellular Biology 17 (1997) 1824-1831.

[58] P. Chardin, J.H. Camonis, N.W. Gale, L. Vanaelst, J. Schlessinger, M.H. Wigler, D. Barsagi, Human Sos1 - a Guanine-Nucleotide Exchange Factor for Ras That Binds to Grb2, Science 260 (1993) 1338-1343.

[59] M. Rozakisadcock, R. Fernley, J. Wade, T. Pawson, D. Bowtell, The Sh2 and Sh3 Domains of Mammalian Grb2 Couple the Egf Receptor to the Ras Activator Msos1, Nature 363 (1993) 83-85.

[60] J. Avruch, MAP kinase pathways: The first twenty years, Biochimica Et Biophysica Acta-Molecular Cell Research 1773 (2007) 1150-1160.

[61] S. Pacini, M. Pellegrini, E. Migliaccio, L. Patrussi, C. Ulivieri, A. Ventura, F. Carraro, A. Naldini, L. Lanfrancone, P. Pelicci, C.T. Baldari, p66SHC promotes apoptosis and antagonizes mitogenic signaling in T cells, Molecular and Cellular Biology 24 (2004) 1747-1757.

[62] S. Okada, A.W. Kao, B.P. Ceresa, P. Blaikie, B. Margolis, J.E. Pessin, The 66-kDa Shc isoform is a negative regulator of the epidermal growth factor-stimulated mitogen-activated protein kinase pathway, Journal of Biological Chemistry 272 (1997) 28042-28049.

[63] S.F. Walk, M.E. March, K.S. Ravichandran, Roles of Lck, Syk and ZAP-70 tyrosine kinases in TCR-mediated phosphorylation of the adapter protein Shc, Eur J Immunol 28 (1998) 2265-2275.

[64] T. Mizuno, K. Fujiki, A. Sasakawa, N. Hisamoto, K. Matsumoto, Role of the Caenorhabditis elegans Shc adaptor protein in the c-Jun N-terminal kinase signaling pathway, Mol Cell Biol 28 (2008) 7041-7049.

[65] E. Neumann-Haefelin, W. Qi, E. Finkbeiner, G. Walz, R. Baumeister, M. Hertweck, SHC-1/p52Shc targets the insulin/IGF-1 and JNK signaling pathways to modulate life span and stress response in C. elegans, Genes Dev 22 (2008) 2721-2735.

[66] L. Patrussi, M.T. Savino, M. Pellegrini, S.R. Paccani, E. Migliaccio, S. Plyte, L. Lanfrancone, P.G. Pelicci, C.T. Baldari, Cooperation and selectivity of the two Grb2 binding sites of p52Shc in T-cell antigen receptor signaling to Ras family GTPases and Myc-dependent survival, Oncogene 24 (2005) 2218-2228.

[67] Y. Radhakrishnan, L.A. Maile, Y. Ling, L.M. Graves, D.R. Clemmons, Insulin-like growth factor-I stimulates Shc-dependent phosphatidylinositol 3-kinase activation via Grb2-associated p85 in vascular smooth muscle cells, Journal of Biological Chemistry 283 (2008) 16320-16331.

[68] E.F. Barry, F.A. Felquer, J.A. Powell, L. Biggs, F.C. Stomski, A. Urbani, H. Ramshaw, P. Hoffmann, M.C. Wilce, M.A. Grimbaldeston, A.F. Lopez, M.A. Guthridge, 14-3-3:Shc Scaffolds Integrate Phosphoserine and Phosphotyrosine Signaling to Regulate Phosphatidylinositol 3-Kinase Activation and Cell Survival, Journal of Biological Chemistry 284 (2009) 12080-12090.

[69] H. Gu, H. Maeda, J.J. Moon, J.D. Lord, M. Yoakim, B.H. Nelson, B.G. Neel, New role for Shc in activation of the phosphatidylinositol 3-kinase/Akt pathway, Mol Cell Biol 20 (2000) 7109-7120.

[70] M.A. Soliman, A.M. Abdel Rahman, D.A. Lamming, K. Birsoy, J. Pawling, M.E. Frigolet, H. Lu, I.G. Fantus, A. Pasculescu, Y. Zheng, D.M. Sabatini, J.W. Dennis, T. Pawson, The adaptor protein p66Shc inhibits mTOR-dependent anabolic metabolism, Sci Signal 7 (2014) ra17.

[71] W.W. Smith, D.D. Norton, M. Gorospe, H. Jiang, S. Nemoto, N.J. Holbrook, T. Finkel, J.W. Kusiak, Phosphorylation of p66Shc and forkhead proteins mediates Abeta toxicity, Journal of Cell Biology 169 (2005) 331-339.

[72] S. Nemoto, T. Finkel, Redox regulation of forkhead proteins through a p66shc-dependent signaling pathway, Science 295 (2002) 2450-2452.

[73] M. Trinei, M. Giorgio, A. Cicalese, S. Barozzi, A. Ventura, E. Migliaccio, E. Milia, I.M. Padura, V.A. Raker, M. Maccarana, V. Petronilli, S. Minucci, P. Bernardi, L. Lanfrancone, P.G. Pelicci, A p53-p66Shc signalling pathway controls intracellular redox status, levels of oxidation-damaged DNA and oxidative stress-induced apoptosis, Oncogene 21 (2002) 3872-3878.

[74] F. Orsini, E. Migliaccio, M. Moroni, C. Contursi, V.A. Raker, D. Piccini, I. Martin-Padura, G. Pelliccia, M. Trinei, M. Bono, C. Puri, C. Tacchetti, M. Ferrini, R. Mannucci, I. Nicoletti, L. Lanfrancone, M. Giorgio, P.G. Pelicci, The life span determinant p66Shc localizes to mitochondria where it associates with mitochondrial heat shock protein 70 and regulates trans-membrane potential, Journal of Biological Chemistry 279 (2004) 25689-25695.

[75] K.M.V. Lai, T. Pawson, The ShcA phosphotyrosine docking protein sensitizes cardiovascular signaling in the mouse embryo, Genes & Development 14 (2000) 1132-1145.

[76] K.M.V. Lai, J.P. Olivier, G.D. Gish, M. Henkemeyer, J. Mcglade, T. Pawson, A Drosophila Shc Gene-Product Is Implicated in Signaling by the Der Receptor Tyrosine Kinase, Molecular and Cellular Biology 15 (1995) 4810-4818.

[77] S. Luschnig, J. Krauss, K. Bohmann, I. Desjeux, C. Nusslein-Volhard, The Drosophila SHC adaptor protein is required for signaling by a subset of receptor tyrosine kinases, Molecular Cell 5 (2000) 231-241.

[78] N. Altiok, S. Altiok, J.P. Changeux, Heregulin-stimulated acetylcholine receptor gene expression in muscle: requirement for MAP kinase and evidence for a parallel inhibitory pathway independent of electrical activity, Embo Journal 16 (1997) 717-725.

[79] W.R. Hardy, L.Y. Li, Z. Wang, J. Sedy, J. Fawcett, E. Frank, J. Kucera, T. Pawson, Combinatorial ShcA docking interactions support diversity in tissue morphogenesis, Science 317 (2007) 251-256.

[80] L. Zhang, V. Camerini, T.P. Bender, K.S. Ravichandran, A nonredundant role for the adapter protein Shc in thymic T cell development, Nature Immunology 3 (2002) 749-755.

[81] A.M. Fischer, C.D. Katayama, G. Pages, J. Pouyssegur, S.M. Hedrick, The role of erk1 and erk2 in multiple stages of T cell development, Immunity 23 (2005) 431-443.

[82] P. Trampont, L. Zhang, K.S. Ravichandran, ShcA mediates the dominant pathway to extracellular signal-regulated kinase activation during early thymic development, Mol Cell Biol 26 (2006) 9035-9044.

[83] L. Conti, C. DeFraja, M. Gulisano, E. Migliaccio, S. Govoni, E. Cattaneo, Expression and activation of SH2/PTB-containing ShcA adaptor protein reflects the pattern of neurogenesis in the mammalian brain, Proceedings of the National Academy of Sciences of the United States of America 94 (1997) 8185-8190.

[84] K.N. McFarland, S.R. Wilkes, S.E. Koss, K.S. Ravichandran, J.W. Mandell, Neural-specific inactivation of ShcA results in increased embryonic neural progenitor apoptosis and microencephaly, Journal of Neuroscience 26 (2006) 7885-7897.

[85] G. Ponti, E. Reitano, P. Aimar, E. Cattaneo, L. Conti, L. Bonfanti, NEURAL-SPECIFIC INACTIVATION OF ShcA FUNCTIONS RESULTS IN ANATOMICAL DISORGANIZATION OF SUBVENTRICULAR ZONE NEURAL STEM CELL NICHE IN THE ADULT BRAIN, Neuroscience 168 (2010) 314-322.

[86] C. Russo, S. Salis, V. Dolcini, V. Venezia, X.H. Song, J.K. Teller, G. Schettini, Amino-terminal modification and tyrosine phosphorylation of [corrected] carboxy-terminal fragments of the amyloid precursor protein in Alzheimer's disease and Down's syndrome brain, Neurobiol Dis 8 (2001) 173-180.

[87] C. Russo, V. Dolcini, S. Salis, V. Venezia, N. Zambrano, T. Russo, G. Schettini, Signal transduction through tyrosine-phosphorylated C-terminal fragments of amyloid precursor protein via an enhanced interaction with Shc/Grb2 adaptor proteins in reactive astrocytes of Alzheimer's disease brain, Journal of Biological Chemistry 277 (2002) 35282-35288.

[88] M. Rajendran, P. Thomes, L. Zhang, S. Veeramani, M.F. Lin, p66Shc-a longevity redox protein in human prostate cancer progression and metastasis, Cancer and Metastasis Reviews 29 (2010) 207-222.

[89] P.A. Davol, Shc proteins are strong, independent prognostic markers for both node-negative and node-positive primary breast cancer (vol 63, pg 6772, 2003), Cancer Research 63 (2003) 8562-8562.

[90] A.R. Frackelton, Jr., L. Lu, P.A. Davol, R. Bagdasaryan, L.J. Hafer, D.C. Sgroi, p66 Shc and tyrosine-phosphorylated Shc in primary breast tumors identify patients likely to relapse despite tamoxifen therapy, Breast Cancer Res 8 (2006) R73.

[91] J. Ursini-Siegel, W.R. Hardy, D.M. Zuo, S.H. Lam, V. Sanguin-Gendreau, R.D. Cardiff, T. Pawson, W.J. Muller, ShcA signalling is essential for tumour progression in mouse models of human breast cancer, Embo Journal 27 (2008) 910-920.

[92] M.A. Webster, J.N. Hutchinson, M.J. Rauh, S.K. Muthuswamy, M. Anton, C.G. Tortorice, R.D. Cardiff, F.L. Graham, J.A. Hassell, W.J. Muller, Requirement for both Shc and phosphatidylinositol 3 ' kinase signaling pathways in polyomavirus middle T-mediated mammary tumorigenesis, Molecular and Cellular Biology 18 (1998) 2344-2359.

[93] D. Dankort, B. Maslikowski, N. Warner, N. Kanno, H. Kim, Z.X. Wang, M.F. Moran, R.G. Oshima, R.D. Cardiff, W.J. Muller, Grb2 and Shc adapter proteins play distinct roles in Neu (ErbB-2)-induced mammary tumorigenesis: Implications for human breast cancer, Molecular and Cellular Biology 21 (2001) 1540-1551.

[94] C. Saucier, H. Khoury, K.M.V. Lai, P. Peschard, D. Dankort, M.A. Naujokas, J. Holash, G.D. Yancopoulos, W.J. Muller, T. Pawson, M. Park, The Shc adaptor protein is critical for VEGF induction by Met/HGF and ErbB2 receptors and for early onset of tumor angiogenesis, Proceedings of the National Academy of Sciences of the United States of America 101 (2004) 2345-2350.

[95] J.L. Jones, J.A. Shaw, J.H. Pringle, R.A. Walker, Primary breast myoepithelial cells exert an invasion-suppressor effect on breast cancer cells via paracrine down-regulation of MMP expression in fibroblasts and tumour cells, J Pathol 201 (2003) 562-572.

[96] J. Ursini-Siegel, W.R. Hardy, Y. Zheng, C. Ling, D. Zuo, C. Zhang, L. Podmore, T. Pawson, W.J. Muller, The ShcA SH2 domain engages a 14-3-3/PI3 ' K signaling complex and promotes breast cancer cell survival, Oncogene 31 (2012) 5038-5044.

[97] Y.K. Im, R. La Selva, V. Gandin, J.R. Ha, V. Sabourin, N. Sonenberg, T. Pawson, I. Topisirovic, J. Ursini-Siegel, The ShcA adaptor activates AKT signaling to potentiate

breast tumor angiogenesis by stimulating VEGF mRNA translation in a 4E-BP-dependent manner, Oncogene (2014).

[98] R. Ahn, V. Sabourin, J.R. Ha, S. Cory, G. Maric, Y.K. Im, W.R. Hardy, H. Zhao, M. Park, M. Hallett, P.M. Siegel, T. Pawson, J. Ursini-Siegel, The ShcA PTB Domain Functions as a Biological Sensor of Phosphotyrosine Signaling during Breast Cancer Progression, Cancer Research 73 (2013) 4521-4532.

[99] H. Towbin, T. Staehelin, J. Gordon, Electrophoretic Transfer of Proteins from Polyacrylamide Gels to Nitrocellulose Sheets - Procedure and Some Applications, Proceedings of the National Academy of Sciences of the United States of America 76 (1979) 4350-4354.

[100] S.M. Kelly, T.J. Jess, N.C. Price,

, Biochimica Et Biophysica Acta-Proteins and Proteomics 1751 (2005) 119-139.

[101] W.C. Johnson, Analyzing protein circular dichroism spectra for accurate secondary structures, Proteins-Structure Function and Genetics 35 (1999) 307-312.

[102] P.J. Roberts, C.J. Der, Targeting the Raf-MEK-ERK mitogen-activated protein kinase cascade for the treatment of cancer, Oncogene 26 (2007) 3291-3310.

[103] S. Arur, M. Ohmachi, S. Nayak, M. Hayes, A. Miranda, A. Hay, A. Golden, T. Schedl, Multiple ERK substrates execute single biological processes in Caenorhabditis elegans germ-line development, Proceedings of the National Academy of Sciences of the United States of America 106 (2009) 4776-4781.

[104] S.M. Carlson, C.R. Chouinard, A. Labadorf, C.J. Lam, K. Schmelzle, E. Fraenkel, F.M. White, Large-Scale Discovery of ERK2 Substrates Identifies ERK-Mediated Transcriptional Regulation by ETV3, Science Signaling 4 (2011).

[105] R.H. Chen, C. Sarnecki, J. Blenis, Nuclear-Localization and Regulation of Erk-Encoded and Rsk-Encoded Protein-Kinases, Molecular and Cellular Biology 12 (1992) 915-927.

[106] R. Marais, J. Wynne, R. Treisman, The Srf Accessory Protein Elk-1 Contains a Growth Factor-Regulated Transcriptional Activation Domain, Cell 73 (1993) 381-393.

[107] R. Treisman, The serum response element, Trends in Biochemical Sciences 17 (1992) 423-426.

[108] S. Meloche, J. Pouyssegur, The ERK1/2 mitogen-activated protein kinase pathway as a master regulator of the G1- to S-phase transition, Oncogene 26 (2007) 3227-3239.

[109] L.O. Murphy, J. Blenis, MAPK signal specificity: the right place at the right time, Trends in Biochemical Sciences 31 (2006) 268-275.

[110] B.J. Canagarajah, A. Khokhlatchev, M.H. Cobb, E.J. Goldsmith, Activation mechanism of the MAP kinase ERK2 by dual phosphorylation, Cell 90 (1997) 859-869.

[111] F.M. Zhang, A. Strand, D. Robbins, M.H. Cobb, E.J. Goldsmith, Atomic-Structure of the Map Kinase Erk2 at 2.3-Angstrom Resolution, Nature 367 (1994) 704-711.

[112] K.I. Patterson, T. Brummer, P.M. O'Brien, R.J. Daly, Dual-specificity phosphatases: critical regulators with diverse cellular targets, Biochem J 418 (2009) 475-489.

[113] W. Kolch, Coordinating ERK/MAPK signalling through scaffolds and inhibitors, Nature Reviews Molecular Cell Biology 6 (2005) 827-837.

[114] J.W. Ramos, E. Formstecher, H. Chneiweiss, M.H. Ginsberg, PEA-15 enforces cytoplasmic sequestration of ERK MAP kinase, Molecular Biology of the Cell 12 (2001) 402a-402a.

[115] E. Formstecher, J.W. Ramos, M. Fauquet, D.A. Calderwood, J.C. Hsieh, B. Canton, X.T. Nguyen, J.V. Barnier, J. Camonis, M.H. Ginsberg, H. Chneiweiss, PEA-15 mediates cytoplasmic sequestration of ERK MAP kinase, Developmental Cell 1 (2001) 239-250.

[116] C. Bartholomeusz, H. Itamochi, M. Nitta, H. Saya, M.H. Ginsberg, N.T. Ueno, Antitumor effect of E1A in ovarian cancer by cytoplasmic sequestration of activated ERK by PEA15, Oncogene 25 (2006) 79-90.

[117] A. Brunet, D. Roux, P. Lenormand, S. Dowd, S. Keyse, J. Pouyssegur, Nuclear translocation of p42/p44 mitogen-activated protein kinase is required for growth factor-induced gene expression and cell cycle entry, Embo Journal 18 (1999) 664-674.

[118] R. George, A.C. Schuller, R. Harris, J.E. Ladbury, A phosphorylation-dependent gating mechanism controls the SH2 domain interactions of the Shc adaptor protein, Journal of Molecular Biology 377 (2008) 740-747.

[119] A.C. Schuller, Z. Ahmed, J.A. Levitt, K.M. Suen, K. Suhling, J.E. Ladbury, Indirect recruitment of the signalling adaptor Shc to the fibroblast growth factor receptor 2 (FGFR2), Biochemical Journal 416 (2008) 189-199.

[120] K.M. Suen, C.C. Lin, R. George, F.A. Melo, E.R. Biggs, Z. Ahmed, M.N. Drake, S. Arur, S.T. Arold, J.E. Ladbury, Interaction with Shc prevents aberrant Erk activation in the absence of extracellular stimuli, Nat Struct Mol Biol 20 (2013) 620-627.

[121] C.D. Harvey, A.G. Ehrhardt, C. Cellurale, H.N. Zhong, R. Yasuda, R.J. Davis, K. Svoboda, A genetically encoded fluorescent sensor of ERK activity, Proceedings of the National Academy of Sciences of the United States of America 105 (2008) 19264-19269.

[122] M. Fukuda, Y. Gotoh, E. Nishida, Interaction of MAP kinase with MAP kinase kinase: Its possible role in the control of nucleocytoplasmic transport of MAP kinase, Embo Journal 16 (1997) 1901-1908.

[123] A. Farooq, M.M. Zhou, Structure and regulation of MAPK phosphatases, Cellular Signalling 16 (2004) 769-779.

[124] D.K. Morrison, R.J. Davis, Regulation of map kinase signaling modules by scaffold proteins in mammals, Annual Review of Cell and Developmental Biology 19 (2003) 91-118.

[125] Z. Timsah, Z. Ahmed, C.C. Lin, F.A. Melo, L.J. Stagg, P.G. Leonard, P. Jeyabal, J. Berrout, R.G. O'Neil, M. Bogdanov, J.E. Ladbury, Competition between Grb2 and Plc gamma 1 for FGFR2 regulates basal phospholipase activity and invasion, Nature Structural & Molecular Biology 21 (2014) 180-+.

[126] Z. Ahmed, C.C. Lin, K.M. Suen, F.A. Melo, J.A. Levitt, K. Suhling, J.E. Ladbury, Grb2 controls phosphorylation of FGFR2 by inhibiting receptor kinase and Shp2 phosphatase activity, Journal of Cell Biology 200 (2013) 493-504.

[127] C.C. Lin, F.A. Melo, R. Ghosh, K.M. Suen, L.J. Stagg, J. Kirkpatrick, S.T. Arold, Z. Ahmed, J.E. Ladbury, Inhibition of Basal FGF Receptor Signaling by Dimeric Grb2, Cell 149 (2012) 1514-1524.

[128] R. Akella, T.M. Moon, E.J. Goldsmith, Unique MAP kinase binding sites, Biochimica Et Biophysica Acta-Proteins and Proteomics 1784 (2008) 48-55.

[129] J.W. Ramos, The regulation of extracellular signal-regulated kinase (ERK) in mammalian cells, International Journal of Biochemistry & Cell Biology 40 (2008) 2707-2719.

[130] P.P. Roux, J. Blenis, ERK and p38 MAPK-activated protein kinases: a family of protein kinases with diverse biological functions, Microbiology and Molecular Biology Reviews 68 (2004) 320-+.

[131] M. Raman, W. Chen, M.H. Cobb, Differential regulation and properties of MAPKs, Oncogene 26 (2007) 3100-3112.

[132] R.P. Bhattacharyya, A. Remenyi, M.C. Good, C.J. Bashor, A.M. Falick, W.A. Lim, The Ste5 scaffold allosterically modulates signaling output of the yeast mating pathway, Science 311 (2006) 822-826.

[133] D. Jacobs, D. Glossip, H.M. Xing, A.J. Muslin, K. Kornfeld, Multiple docking sites on substrate proteins form a modular system that mediates recognition by ERK MAP kinase, Genes & Development 13 (1999) 163-175.

[134] S. Torii, M. Kusakabe, T. Yamamoto, M. Maekawa, E. Nishida, Sef is a spatial regulator for Ras/MAP kinase signaling, Developmental Cell 7 (2004) 33-44.

[135] B.T. Seet, I. Dikic, M.M. Zhou, T. Pawson, Reading protein modifications with interaction domains, Nat Rev Mol Cell Biol 7 (2006) 473-483.

[136] J.E. Ladbury, S.T. Arold, Energetics of Src homology domain interactions in receptor tyrosine kinase-mediated signaling, Methods Enzymol 488 (2011) 147-183.

[137] J.E. Ladbury, S. Arold, Searching for specificity in SH domains, Chem Biol 7 (2000) R3-8.

[138] M.J. Wagner, M.M. Stacey, B.A. Liu, T. Pawson, Molecular Mechanisms of SH2-and PTB-Domain-Containing Proteins in Receptor Tyrosine Kinase Signaling, Cold Spring Harbor Perspectives in Biology 5 (2013).

[139] B. Roshan, C. Kjelsberg, K. Spokes, A. Eldred, C.S. Crovello, L.G. Cantley, Activated ERK2 interacts with and phosphorylates the docking protein GAB1, Journal of Biological Chemistry 274 (1999) 36362-36368.

[140] S. Lehr, J. Kotzka, H. Avci, A. Sickmann, H.E. Meyer, A. Herkner, D. Muller-Wieland, Identification of major ERK-related phosphorylation sites in Gab1, Biochemistry 43 (2004) 12133-12140.

[141] H.H. Gu, B.G. Neel, The 'Gab' in signal transduction, Trends in Cell Biology 13 (2003) 122-130.

[142] C.F. Yu, Z.X. Liu, L.G. Cantley, ERK negatively regulates the epidermal growth factor-mediated interaction of Gab1 and the phosphatidylinositol 3-kinase, Journal of Biological Chemistry 277 (2002) 19382-19388.

[143] I. Lax, A. Wong, B. Lamothe, A. Lee, A. Frost, J. Hawes, J. Schlessinger, The docking protein FRS2 alpha controls a MAP kinase-mediated negative feedback mechanism for signaling by FGF receptors, Molecular Cell 10 (2002) 709-719.

[144] Y.J. Wu, Z.J. Chen, A. Ullrich, EGFR and FGFR signaling through FRS2 is subject to negative feedback control by ERK1/2, Biological Chemistry 384 (2003) 1215-1226.

[145] K. DeFea, R.A. Roth, Modulation of insulin receptor substrate-1 tyrosine phosphorylation and function by mitogen-activated protein kinase, Journal of Biological Chemistry 272 (1997) 31400-31406.

[146] C.F. Yu, B. Roshan, Z.X. Liu, L.G. Cantley, ERK regulates the hepatocyte growth factor-mediated interaction of Gab1 and the phosphatidylinositol 3-kinase, Journal of Biological Chemistry 276 (2001) 32552-32558.

[147] H.S. Jin, L.J. Liao, Y. Park, Y.C. Liu, Neddylation pathway regulates T-cell function by targeting an adaptor protein Shc and a protein kinase Erk signaling, Proceedings of the National Academy of Sciences of the United States of America 110 (2013) 624-629.

[148] B.D. Manning, L.C. Cantley, AKT/PKB signaling: Navigating downstream, Cell 129 (2007) 1261-1274.

[149] J. Ursini-Siegel, W.J. Muller, The ShcA adaptor protein is a critical regulator of breast cancer progression, Cell Cycle 7 (2008) 1936-1943.

[150] W.G. Mao, R. Irby, D. Coppola, L. Fu, M. Wloch, J. Turner, H. Yu, R. Garcia, R. Jove, T.J. Yeatman, Activation of c-Src by receptor tyrosine kinases in human colon cancer cells with high metastatic potential, Oncogene 15 (1997) 3083-3090.

[151] I.C. Northwood, F.A. Gonzalez, M. Wartmann, D.L. Raden, R.J. Davis, Isolation and Characterization of 2 Growth Factor-Stimulated Protein-Kinases That Phosphorylate the Epidermal Growth-Factor Receptor at Threonine 669, Journal of Biological Chemistry 266 (1991) 15266-15276.

[152] S.E. Winograd-Katz, A. Levitzki, Cisplatin induces PKB/Akt activation and p38(MAPK) phosphorylation of the EGF receptor (vol 25, pg 7381, 2006), Oncogene 26 (2007) 788-788.

[153] A. Suenaga, M. Hatakeyama, A.B. Kiyatkin, R. Radhakrishnan, M. Taiji, B.N. Kholodenko, Molecular Dynamics Simulations Reveal that Tyr-317 Phosphorylation Reduces Shc Binding Affinity for Phosphotyrosyl Residues of Epidermal Growth Factor Receptor, Biophysical Journal 96 (2009) 2278-2288.

[154] A. Suenaga, A.B. Kiyatkin, M. Hatakeyama, N. Futatsugi, N. Okimoto, Y. Hirano, T. Narumi, A. Kawai, R. Susukita, T. Koishi, H. Furusawa, K. Yasuoka, N. Takada, Y. Ohno, M. Taiji, T. Ebisuzaki, J.B. Hoek, A. Konagaya, B.N. Kholodenko, Tyr-317 phosphorylation increases shc structural rigidity and reduces coupling of domain motions remote from the phosphorylation site as revealed by molecular dynamics simulations, Journal of Biological Chemistry 279 (2004) 4657-4662.

[155] N. Sreerama, R.W. Woody, Estimation of protein secondary structure from circular dichroism spectra: Comparison of CONTIN, SELCON, and CDSSTR methods with an expanded reference set, Analytical Biochemistry 287 (2000) 252-260.

[156] G.L. Ellman, Tissue sulfhydryl groups, Arch Biochem Biophys 82 (1959) 70-77.

[157] R.R. Burgess, Refolding solubilized inclusion body proteins, Methods Enzymol 463 (2009) 259-282.

[158] F.H. Niesen, H. Berglund, M. Vedadi, The use of differential scanning fluorimetry to detect ligand interactions that promote protein stability, Nature Protocols 2 (2007) 2212-2221.

[159] A. Fontana, P.P. de Laureto, B. Spolaore, E. Frare, P. Picotti, M. Zambonin, Probing protein structure by limited proteolysis, Acta Biochimica Polonica 51 (2004) 299-321.

[160] M.B. Yaffe, A.E.H. Elia, Phosphoserine/threonine-binding domains, Current Opinion in Cell Biology 13 (2001) 131-138.

[161] A. Ventura, M. Maccarana, V.A. Raker, P.G. Pelicci, A cryptic targeting signal induces isoform-specific localization of p46Shc to mitochondria, Journal of Biological Chemistry 279 (2004) 2299-2306.

[162] R.A. Cairns, I.S. Harris, T.W. Mak, Regulation of cancer cell metabolism, Nat Rev Cancer 11 (2011) 85-95.

[163] C. Tristan, N. Shahani, T.W. Sedlak, A. Sawa, The diverse functions of GAPDH: views from different subcellular compartments, Cellular Signalling 23 (2011) 317-323.

[164] H.A. Fu, R.R. Subramanian, S.C. Masters, 14-3-3 proteins: Structure, function, and regulation, Annual Review of Pharmacology and Toxicology 40 (2000) 617-647.

[165] R.J. Ingham, G. Gish, T. Pawson, The Nedd4 family of E3 ubiquitin ligases: functional diversity within a common modular architecture, Oncogene 23 (2004) 1972-1984.

[166] K.P.Lu, G. Finn, T.H. Lee, L.K. Nicholson, Prolyl cis-trans isomerization as a molecular timer, Nature Chemical Biology 3 (2007) 619-629.

[167] C.L. Neal, J. Xu, P. Li, S. Mori, J. Yang, N.N. Neal, X. Zhou, S.L. Wyszomierski, D. Yu, Overexpression of 14-3-3zeta in cancer cells activates PI3K via binding the p85 regulatory subunit, Oncogene 31 (2012) 897-906.

[168] R. Ranganathan, K.P. Lu, T. Hunter, J.P. Noel, Structural and functional analysis of the mitotic rotamase Pin1 suggests substrate recognition is phosphorylation dependent, Cell 89 (1997) 875-886.

[169] J.E. Girardini, M. Napoli, S. Piazza, A. Rustighi, C. Marotta, E. Radaelli, V. Capaci, L. Jordan, P. Quinlan, A. Thompson, M. Mano, A. Rosato, T. Crook, E. Scanziani, A.R. Means, G. Lozano, C. Schneider, G. Del Sal, A Pin1/Mutant p53 Axis Promotes Aggressiveness in Breast Cancer, Cancer Cell 20 (2011) 79-91.

[170] K.P. Lu, X.Z. Zhou, The prolyl isomerase PIN 1: a pivotal new twist in phosphorylation signalling and disease, Nature Reviews Molecular Cell Biology 8 (2007) 904-916.

[171] A. Rustighi, L. Tiberi, A. Soldano, M. Napoli, P. Nuciforo, A. Rosato, F. Kaplan, A. Capobianco, S. Pece, P.P. Di Fiore, G. Del Sal, The prolyl-isomerase Pin1 is a Notch1 target that enhances Notch1 activation in cancer, Nature Cell Biology 11 (2009) 133-U162.

[172] J.D. Forman-Kay, T. Mittag, From Sequence and Forces to Structure, Function, and Evolution of Intrinsically Disordered Proteins, Structure 21 (2013) 1492-1499.

[173] X.Z. Zhou, O. Kops, A. Werner, P.J. Lu, M.H. Shen, G. Stoller, G. Kullertz, M. Stark, G. Fischer, K.P. Lu, Pin1-dependent prolyl isomerization regulates dephosphorylation of Cdc25C and tau proteins, Molecular Cell 6 (2000) 873-883.

[174] M.T. Uhlik, B. Temple, S. Bencharit, A.J. Kimple, D.P. Siderovski, G.L. Johnson, Structural and evolutionary division of phosphotyrosine binding (PTB) domains, Journal of Molecular Biology 345 (2005) 1-20.

[175] C. Dhalluin, K.S. Yan, O. Plotnikova, K.W. Lee, L. Zeng, M. Kuti, S. Mujtaba, M.M. Goldfarb, M.M. Zhou, Structural basis of SNT PTB domain interactions with distinct neurotrophic receptors, Molecular Cell 6 (2000) 921-929.

[176] I. Dikic, A.G. Batzer, P. Blaikie, A. Obermeier, A. Ullrich, J. Schlessinger, B. Margolis, Shc Binding to Nerve Growth-Factor Receptor Is Mediated by the Phosphotyrosine Interaction Domain, Journal of Biological Chemistry 270 (1995) 15125-15129.

[177] Y. Okabayashi, Y. Kido, T. Okutani, Y. Sugimoto, K. Sakaguchi, M. Kasuga, Tyrosines 1148 and 1173 of activated human epidermal growth factor receptors are binding sites of Shc in intact cells, J Biol Chem 269 (1994) 18674-18678.

[178] P.A. Kenny, G.Y. Lee, C.A. Myers, R.M. Neve, J.R. Semeiks, P.T. Spellman, K. Lorenz, E.H. Lee, M.H. Barcellos-Hoff, O.W. Petersen, J.W. Gray, M.J. Bissell, The morphologies of breast cancer cell lines in three-dimensional assays correlate with their profiles of gene expression, Molecular Oncology 1 (2007) 84-96.

[179] K.J. Chavez, S.V. Garimella, S. Lipkowitz, Triple negative breast cancer cell lines: one tool in the search for better treatment of triple negative breast cancer, Breast Dis 32 (2010) 35-48.

[180] H.S. Park, M.H. Jang, E.J. Kim, H.J. Kim, H.J. Lee, Y.J. Kim, J.J. Kim, E. Kang, S.W. Kim, I.A. Kim, S.Y. Park, High EGFR gene copy number predicts poor outcome in triple-negative breast cancer, Modern Pathology 27 (2014) 1212-1222.

[181] D.A. Ferraro, N. Gaborit, R. Maron, H. Cohen-Dvashi, Z. Porat, F. Pareja, S. Lavi, M. Lindzen, N. Ben-Chetrit, M. Sela, Y. Yarden, Inhibition of triple-negative breast cancer models by combinations of antibodies to EGFR, Proceedings of the National Academy of Sciences of the United States of America 110 (2013) 1815-1820.

[182] K. Venkatesan, J.F. Rual, A. Vazquez, U. Stelzl, I. Lemmens, T. Hirozane-Kishikawa, T. Hao, M. Zenkner, X.F. Xin, K.I. Goh, M.A. Yildirim, N. Simonis, K. Heinzmann, F. Gebreab, J.M. Sahalie, S. Cevik, C. Simon, A.S. de Smet, E. Dann, A. Smolyar, A. Vinayagam, H.Y. Yu, D. Szeto, H. Borick, A. Dricot, N. Klitgord, R.R. Murray, C. Lin, M. Lalowski, J. Timm, K. Rau, C. Boone, P. Braun, M.E. Cusick, F.P. Roth, D.E. Hill, J. Tavernier, E.E. Wanker, A.L. Barabasi, M. Vidal, An empirical framework for binary interactome mapping, Nature Methods 6 (2009) 83-90.

[183] R.M. Ewing, P. Chu, F. Elisma, H. Li, P. Taylor, S. Climie, L. McBroom-Cerajewski, M.D. Robinson, L. O'Connor, M. Li, R. Taylor, M. Dharsee, Y. Ho, A. Heilbut, L. Moore, S. Zhang, O. Ornatsky, Y.V. Bukhman, M. Ethier, Y. Sheng, J. Vasilescu, M. Abu-Farha, J.P. Lambert, H.S. Duewel, I.I. Stewart, B. Kuehl, K. Hogue, K. Colwill, K. Gladwish, B. Muskat, R. Kinach, S.L. Adams, M.F. Moran, G.B. Morin, T. Topaloglou, D. Figeys, Large-scale mapping of human protein-protein interactions by mass spectrometry, Molecular Systems Biology 3 (2007).

[184] J.F. Rual, K. Venkatesan, T. Hao, T. Hirozane-Kishikawa, A. Dricot, N. Li, G.F. Berriz, F.D. Gibbons, M. Dreze, N. Ayivi-Guedehoussou, N. Klitgord, C. Simon, M. Boxem, S. Milstein, J. Rosenberg, D.S. Goldberg, L.V. Zhang, S.L. Wong, G. Franklin, S.M. Li, J.S. Albala, J.H. Lim, C. Fraughton, E. Llamosas, S. Cevik, C. Bex, P. Lamesch, R.S. Sikorski, J. Vandenhaute, H.Y. Zoghbi, A. Smolyar, S. Bosak, R. Sequerra, L. Doucette-Stamm, M.E. Cusick, D.E. Hill, F.P. Roth, M. Vidal, Towards a proteome-scale map of the human protein-protein interaction network, Nature 437 (2005) 1173-1178.

[185] A.L. Barabasi, Z.N. Oltvai, Network biology: Understanding the cell's functional organization, Nature Reviews Genetics 5 (2004) 101-U115.

[186] X.W. Zhu, M. Gerstein, M. Snyder, Getting connected: analysis and principles of biological networks, Genes & Development 21 (2007) 1010-1024.

[187] J.T. Erler, R.N. Linding, Network Medicine Strikes a Blow against Breast Cancer, Cell 149 (2012) 731-733.

[188] K.I. Goh, I.G. Choi, Exploring the human diseasome: the human disease network, Briefings in Functional Genomics 11 (2012) 533-542.

[189] A.L. Barabasi, N. Gulbahce, J. Loscalzo, Network medicine: a network-based approach to human disease, Nature Reviews Genetics 12 (2011) 56-68.

Vita

Kin Man Suen was born in Hong Kong in 1982. She attended the Adcote School For Girls in the United Kingdom and graduated in 2001. She read Biochemistry at University College London. During her bachelor degree, she spent a year as a placement student in GlaxoSmithKline. This experience drew her to bench science. She joined Professor J. Ladbury's laboratory in 2006 as a research technician and moved to MD Anderson Cancer Center with him in 2009. She started her Ph.D. study in 2011 at the University of Texas Graduate School of Biomedical Sciences at Houston.

Email:

kinmansuen@yahoo.com